UNIVERSIDADE ESTADUAL DE CAMPINAS

INSTITUTO DE BIOLOGIA

Flavia Karina Delella

"Efeito da finasterida e da doxazosina sobre a próstata de rato: análise ultra-estrutural e da expressão dos colágenos tipo I e tipo III e do TGF-β 1"

Tese apresentada ao Instituto de Biologia para obtenção do Título de Doutor em Biologia Celular e Estrutural, na área de Biologia Celular.

Orientador: Prof. Dr. Sérgio Luis Felisbino

Campinas, 2010

FICHA CATALOGRÁFICA ELABORADA PELA BIBLIOTECA DO INSTITUTO DE BIOLOGIA – UNICAMP

Delella, Flávia Karina
D377e Efeito da finasterida e da doxazosina sobre a próstata de rato: análise ultra-estrutural e da expressão dos colágenos tipo I e tipo III e do TGF- β 1/ Flávia Karina Delella. – Campinas, SP: [s.n.], 2010.

Orientador: Sérgio Luis Felisbino.
Tese (doutorado) – Universidade Estadual de Campinas, Instituto de Biologia.

1. Próstata. 2. Matriz extracelular. 3. Finasterida. 4. Doxazossina. 5. Colágeno. 6. Elastina. I. Felisbino, Sérgio Luis. II. Universidade Estadual de Campinas. Instituto de Biologia. III. Título.

(rcdt/ib)

Título em inglês: Finasteride and doxazosin effects on rat prostate: ultrastructural and type I and type III and TGF- 1 expression analyses.
Palavras-chave em inglês: Prostate; Extracellular matrix; Finasteride; Doxazosin; Collagen; Elastin.
Área de concentração: Biologia Celular.
Titulação: Doutora em Biologia Celular e Estrutural.
Banca examinadora: Sérgio Luis Felisbino, Paulo Pinto Joazeiro, Fernanda Cristina Alcântara dos Santos, Raquel Fantin Domeniconi, Wagner José Fávaro.
Data da defesa: 22/07/2010.
Programa de Pós-Graduação: Biologia Celular e Estrutural.

Campinas, 22 de Julho de 2010.

BANCA EXAMINADORA

Prof. Dr. Sérgio Luis Felisbino (Orientador) _____
Assinatura

Prof. Dr. Paulo Pinto Joazeiro _____
Assinatura

Profa. Dra. Fernanda Cristina Alcântara dos Santos _____
Assinatura

Profa. Dra. Raquel Fantin Domeniconi _____
Assinatura

Prof. Dr. Wagner José Fávaro _____
Assinatura

Prof. Dr. Wellerson Rodrigo Scarano _____
Assinatura

Prof. Dr. Luis Fernando Barbisan _____
Assinatura

Prof. Dr. Robson Franscisco Carvalho _____
Assinatura

Agradecimentos

"O segredo é não correr atrás das borboletas... É cuidar do jardim para que elas venham até você." Mário Quintana

Ao meu orientador, Prof. Dr. Sérgio Luis Felisbino, pelos inúmeros ensinamentos desde o começo do meu mestrado, pela confiança e dedicação ao me orientar neste trabalho de doutorado e por todos os incentivos profissionais nesses anos em que fiz parte do seu grupo de pesquisa. Agradeço a você Sérgio pelo meu crescimento profissional, pela oportunidade do estágio no exterior, pelas orientações em sala de aula e pelo sagrado lazer com os momentos *gourmets* oferecidos. Obrigada professor!

Aos membros da pré-banca e da banca examinadora, Profa. Dra. Renée Laufer Amorim, Prof. Dr. Paulo Pinto Joazeiro, Profa. Dra. Raquel Fantin Domeniconi, Profa. Dra. Fernanda Cristina Alcântara dos Santos, Prof. Dr. Wagner José Fávaro. Obrigada pela avaliação minuciosa, contribuindo de maneira expressiva para o enriquecimento deste trabalho.

Aos professores Dr. Alexandre Leite Rodrigues de Oliveira, Dra. Cristina Pontes Vicente e Dr. Wagner José Fávaro, pela participação na fase de minha qualificação e pelas contribuições científicas que fortaleceram o meu projeto de pós doutorado.

À Profa. Dra. Laurecir Gomes, coordenadora do curso de pós-graduação em Biologia Celular e Estrutural da Unicamp, e a todos os docentes credenciados ao programa pelo execelente nível deste curso.

À querida secretária Líliam Alves Senne Panagio, pela atenção e dedicação dispensadas durante esses anos de pós-graduação e também pela amizade.

À todos os professores e funcionários do Departamento de Morfologia da UNESP de Botucatu pela disponibilidade dos laboratórios para a execução deste trabalho, assim como pela agradável convivência.

Aos amigos do Departamento de Morfologia da Unesp de Botucatu, Francis, Fernanda Losi, Fernanda Carani, Rodrigo, Eduardo, Ludimila, Marcos, Kelly, Lucas, Marcão, Dani, Juliana, Camila, Renan, Gisleine, Glaura pelos momentos vividos dentro do departamento e, principalmente, pelos momentos de descontração.

Ao Justulin, profissional que admiro e que me orientou em tantas técnicas laboratoriais desenvolvidas em minha dissertação e durante a realização desta tese. Obrigada Justo!

À Dra Ana Maria Galvan Custódio, por ser a grande amiga que sempre me incentivou nesses anos de pós-graduação e pelas contribuições científicas desde a época da iniciação.

Aos amigos do LabMEC, os atuais e também àqueles que passaram pelo laboratório deixando a sua contribuição: Justulin, Carol, Juliana, Olga, Fernando, Lívia, Alexandre, Larissa, Elaine, Andrei, Jaqueline, Eliza, Marcela, Heloísa, Henrique. Obrigada pelo crescimento sempre elaborado em grupo.

Aos meus "irmãos" da graduação: Marco, Xexéu, Otávio, Dani, Cris, Renato, Gustavo, Maricy, Barbara, Pipoca e Juliana. Obrigada pela renovação de energia que acontece em cada um dos nossos encontros.

À pesquisadora Jill Macoska, que me recebeu como estudante internacional de doutorado e em cujo laboratório fiz um importante estágio com células tumorais prostáticas. Agradeço também ao pesquisador Sathish Kasina e aos colegas que fiz no Centro de Estudos do Câncer da Universidade de Michigan.

Aos animais de experimentação, que contribuíram com excelência para a execução deste trabalho e aos quais sempre tratei com respeito e profissionalismo.

À FAPESP pela bolsa de estudos concedida.

Agradecimentos Especiais

"Amar é querer estar perto, se longe; e mais perto, se perto."
Vinicius de Moraes

A Deus. Por essa oportunidade de crescimento profissional e pessoal.

Aos meus pais, Sonia e Rubens, e aos meus irmãos, Luciana e Junior, por serem os principais motivadores desta consquista. Obrigada pelo respeito e por todo incentivo!

À minha cunhada Mónica e ao meu cunhado Luiz Claudio, dois irmãos que ganhei e pelos quais tenho admiração e carinho.

À minha sobrinha Barbara, que me conquista a cada nova molecagem com sua sensibilidade e inteligência!

À minha sobrinha Valentina, que com seu jeito doce e delicado faz de mim a tia mais feliz do mundo!

À família Felisbino, Sérgio, Silvia, Pedro e Luisa, pela amizade desde a minha chegada à Botucatu e pelos momentos de lazer convividos.

À Duda, minha companheira fiel!

À família Pinhal, pelo carinho e por terem me acolhido como a minha segunda família e ao querido Danillo Pinhal, por seu amor e companheirismo.

Dedicatória

O que vale na vida não é o ponto de partida e sim a caminhada.

Caminhando e semeando, no fim terás o que colher.

(Cora Coralina)

Dedico a minha tese de doutorado e todo esforço aqui empregado à maior paixão da minha vida, vó Marica (in memorian)!

SUMÁRIO

Resumo

A finasterida e a doxazosina são drogas usadas no tratamento da hiperplasia prostática benigna (HPB) e, mais recentemente, estão sendo também usadas na quimioprevenção do câncer de próstata (CaP), principalmente devido aos seus efeitos na indução de apoptose das células epiteliais prostáticas. Entretanto, pouca atenção tem sido dispensada aos efeitos destes fármacos sobre o estroma glandular. Assim, o objetivo deste estudo foi analisar os efeitos da finasterida e da doxazosina no arranjo estromal e em componentes específicos, como o colágeno do tipo I, colágeno do tipo III e o TGF-Beta 1. Para isso, foram empregadas técnicas morfológicas, bioquímicas e moleculares. O tratamento com finasterida promoveu apoptose epitelial, alterações na membrana basal epitelial e na membrana basal das células musculares lisas, além da diminuição na expressão dos colágenos I e III. O bloqueio α-adrenérgico com doxazosina aumentou a quantidade de fibras do sistema elástico, promoveu apoptose nas células epiteliais, além de alterar a expressão dos colágenos I e III. Os dois fármacos influenciaram o aumento da expressão do TGF-Beta 1, que parece estar mais relacionado com o evento da apoptose no tratamento com a finasterida e com as alterações das fibras colágenas e a ativação de fibroblastos no tratamento com a doxazosina. Conclui-se que as alterações estromais pós tratamento com finasterida e doxazosina podem contribuir para a regressão prostática esperada no tratamento da HPB e na ruptura de eventos parácrinos responsáveis pela evolução tumoral no CaP.

Abstract

Finasteride and doxazosin are drugs used in the benign prostatic hyperplasia (BPH) treatment and, more recently, they're have been used in the prostate cancer (PCa) chemoprevention, mainly because their apoptotic effect in the prostatic epithelial cells. However, few attentions have been given to the effects of these drugs in the glandular stroma. Thus, the objective of this study was to analyze the effects of the finasteride or doxazosin treatment on stroma arrangement and on specific components, like collagen type I, collagen type III and TGF-Beta 1. For this aim, we have used morphological, biochemical and molecular approaches. Finasteride treatment provoked epithelial apoptosis, epithelial basal membrane and smooth muscle cells basal membrane alterations, besides decrease the type I and type III collagen fibers expression. The alpha-adrenergic blockade increased the elastic fibers system, promoted apoptosis in epithelial cells, as well altered the type I and type III collagen fibers expression. Both drugs influenced the TGF-Beta 1 up-regulation that show to be related with apoptosis in finasteride treatment and with collagen fibers alterations and fibroblasts activation in doxazosin treatment. In conclusion, the stromal alterations promoted by finasteride and doxazosin treatments can contribute to the prostate regression expected in the BPH treatment and to the rupture of paracrine events responsible by tumoral evolution in the PCa.

LISTA DE ABREVIATURAS E SIGLAS

AP – *Anterior Prostate*

AR – *Androgen Receptor*

AUA *– American Urological Association*

CaP *– Câncer de Próstata*

CML – *Célula Muscular Lisa*

Col I – *Colágeno tipo I*

Col III – *Colágeno tipo III*

Ct *- Threshold Cycle*

CT – *Controle*

DHT *– Diidrotestosterona*

DOX *– Doxazosina*

DP *– Dorsal Prostate*

ECM – *Extracellular Matrix*

EGF *–Fator de Crescimento Epidermal*

Fb *– Fibroblastos*

FDA *– Food and Drug Administration*

FGF-b *– Fator de Crescimento Fibroblástico Beta*

Fin – *Finasterida/Finasteride*

HPB *– Hiperplasia Prostática Benigna*

IGF *– Fator de Crescimento semelhante à Insulina Tipo-1*

KDa *– Quilo Dalton*

LUTS *– Lower Urinary Tract Symptoms*

MEC – *Matriz Extracelular*

PA – *Próstata Anterior*

PBS – *Tampão Fosfato-Salina*

PCR *– Reação em Cadeia da Polimerase*

PCPT *– Prostate Cancer Prevention Trial*

PD – *Próstata Dorsal*

PIA *– Proliferative Intrapostatic Atrophy*

PIN *– Prostatic Intraepithelial Neoplasia*

PSA *– Prostatic Specific Antigen*

PV – *Próstata Ventral*

q-RT-PCR *- Real Time quantitative Reverse Transcription PCR*

RNAm *– Ácido Ribonucléico Mensageiro*

RT *– Transcrição Reversa*

SMC – *Smooth Muscle Cell*

T *- Testosterona*

TBS-T *– Tampão Salina-Tris com Tween-20*

TGF-α *– Fator de Crescimento Transformante Alfa*

TGF β-1 – *Transforming Growth Factor Beta 1*

VEGF *– Vascular Endothelial Growth Factor*

VP – *Ventral Prostate*

µg *- micrograma*

µL *- microlitro*

µM *- micromolar*

1. Introdução

1.1 Biologia da Glândula Prostática

A próstata é uma glândula anexa do sistema genital masculino, encontrada apenas em mamíferos, cuja principal função é produzir parte do fluido seminal (Cunha et al., 1987). Nos homens, um dos seus produtos de secreção é o PSA (do inglês: *Prostatic Specific Antigen*), uma protease que evita a coagulação do fluido seminal, facilitando o motilidade dos espermatozóides. Outras funções designadas para a próstata incluem a manutenção do pH ótimo do fluido seminal e o fornecimento de nutrientes para os espermatozóides (McNeal, 1969).

No organismo masculino, a próstata permanece rudimentar até a puberdade, fase em que ocorre considerável aumento da produção de andrógenos que estimulam o desenvolvimento da glândula, o crescimento dos brotos alveolares e contribuem para os processos de diferenciação celular e da função secretora (Isaacs, 1984; Nazian, 1986). O crescimento prostático envolve os processos de canalização, alongamento dos ductos e sucessiva arborização das extremidades dos ductos distais (Donjacour & Cunha, 1988). Ao final do desenvolvimento, os ductos prostáticos são compostos por uma parte epitelial e uma parte estromal, sendo a interação entre esses dois componentes responsável pelo crescimento e pela atividade funcional da glândula (Nemeth et al., 1996).

Na espécie humana, essa glândula possui estrutura compacta, sem lobos distintos, pesa aproximadamente 20g e situa-se inferiormente à bexiga urinária, envolvendo a parte prostática da uretra. Morfologicamente, a próstata humana é dividida em três conjuntos de glândulas túbulo-alveolares (Figura 1A): 1) glândulas da zona central; 2) glândulas da zona periférica; 3) glândulas da zona de transição (McNeal, 1981; Roy-Burman et al., 2004; De Marzo et al., 2007). As lesões malignas, que acometem homens de meia idade, iniciam-se principalmente na zona periférica, raramente ocorrendo na zona de transição e raramente se desenvolvem na zona central (Cunha et al., 1987). Já a Hiperplasia Prostática Benigna (HPB) ocorre com frequência na zona de transição (De Marzo et al., 2007).

A morfologia e a fisiologia prostática normal e patológica têm sido extensivamente estudadas em roedores, cuja glândula nos animais sexualmente maduros é multilobar e

organizada ao redor da parte prostática da uretra, na base da bexiga urinária (Figura 1B) (Roy-Burman et al., 2004). Nesses animais, a próstata é composta por um par de lobos ventrais (PV), um par de lobos dorsolaterais (PDL) e um par de lobos anteriores (PA) ou glândula de coagulação, que estão associados às glândulas seminais (Figura 1B). Devido às diferenças morfogenéticas lobo-específicas, a morfologia final de cada lobo é distinta. No aspecto histológico, a próstata anterior apresenta inúmeras dobras epiteliais, a próstata dorsolateral exibe algumas dobras no epitélio e a próstata ventral apresenta epitélio contínuo, contendo o mínimo de dobras (Marker et al., 2003). O crescimento prostático nos roedores extende-se da vida fetal tardia até o estágio de maturidade sexual no indivíduo adulto, quando a arquitetura glandular é estabelecida (Cunha et al., 1987).

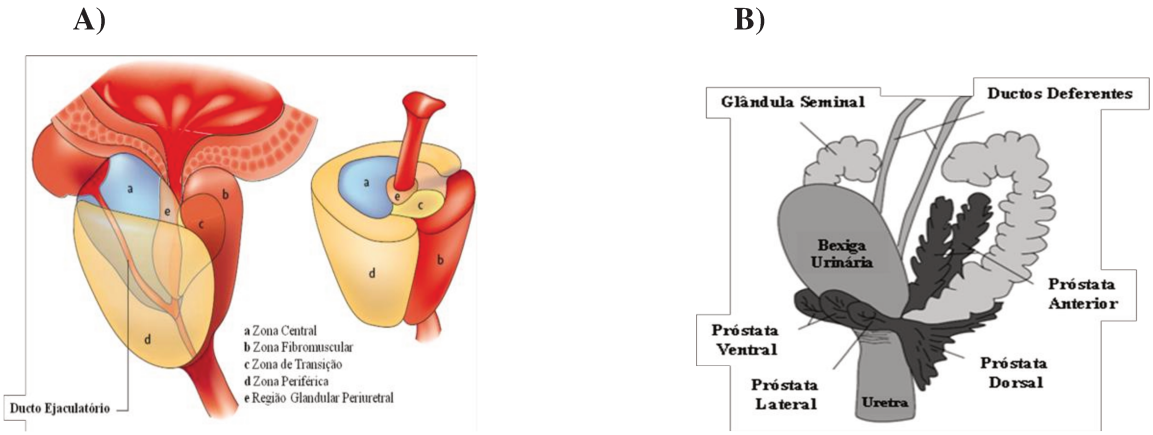

Figura 1: ***A)*** *Diagrama esquemático das zonas anatômicas da glândula prostática humana (adaptado de De Marzo et al., 2007) e* ***B)*** *do trato urogenital de roedores (adaptado de Abbott et al., 2003).*

Em termos de homologia com porções da próstata humana, os lobos anteriores são considerados análogos às glândulas da zona central (raramente acometido por neoplasias), enquanto os lobos dorsolaterais são considerados análogos às glândulas da zona periférica (zona onde surge a maioria dos carcinomas prostáticos). Os lobos ventrais do rato não têm um homólogo humano e a zona de transição humana não possui homologia com nenhuma estrutura na próstata do rato (Roy-Burman et al. 2004).

O epitélio prostático é composto por cinco tipos celulares: *células epiteliais secretoras* (revestem o lúmem dos alvéolos prostáticos, expressam altos níveis de receptores de andrógeno e são responsáveis pela produção e secreção do líquido prostático), *células epiteliais basais* (formam uma monocamada sobre a membrana basal, envolvendo o epitélio prostático e constituem a principal população de células proliferativas do epitélio da glândula prostática adulta), *células neuroendócrinas* (aparecem em menor quantidade e secretam uma variedade de fatores de crescimento que, possivelmente, afetam o desenvolvimento e a manutenção do tecido prostático), células do tipo *stem cells* (são raras e parecem localizar-se na camada de células basais) e *células transitórias amplificadoras* (expressam características entre células basais e secretoras e podem ser células progenitoras ainda não diferenciadas) (Peehl, 2005).

A próstata de ambas espécies possuem células epiteliais colunares secretoras que secretam proteínas prostáticas e fluidos da sua superfície apical em direção ao lúmen (Roy-Burman et al., 2004). Humanos possuem uma camada contínua de células basais entre as células secretoras e a membrana basal, enquanto os roedores possuem menos células basais que constituem uma camada descontínua ao redor da glândula (Marker et al., 2003). A próstata humana é composta por um estroma fibromuscular denso, com abundância em musculatura lisa, fibroblastos e colágeno, que circundam os elementos glandulares. O estroma prostático dos roedores é menos fibromuscular e é grandemente preenchido por tecido conjuntivo frouxo (Nemeth & Lee, 1996; Roy-Burman et al., 2004).

1.1.2 O Estroma Prostático e a Interação Epitélio-Estroma

O estroma prostático envolve os ductos e os alvéolos glandulares e é composto por três principais tipos celulares: células musculares lisas (CML), fibroblastos (Fb) e miofibroblastos, além de nervos, vasos sanguíneos e linfáticos (Marker et al., 2003). As células estromais são responsáveis por direcionar os processos de desenvolvimento, manutenção e diferenciação do epitélio, fornecendo nutrientes e fatores de crescimento, além de expressarem receptores esteroidais como o receptor androgênico (AR), receptores estrogênicos como ERα e ERβ e a enzima 5α redutase (Berry et al., 2008). Outros tipos

celulares presentes no estroma incluem as células endoteliais, os pericitos e as células inflamatórias (Marker et al., 2003, Taylor & Risbridger, 2008). Sustentando as células estromais, existe uma complexa matriz extracelular composta principalmente por fibras colágenas, fibras reticulares, fibras do sistema elástico, proteoglicanos e diversas glicoproteínas (de Carvalho et al., 1997; Vilamaior et al., 2000).

Interações entre o epitélio e o estroma são importantes em diversos estágios da morfogênese, na diferenciação celular e na função geral dos epitélios glandulares (Hall, 1978; Hay, 1981; Lin & Bissel, 1993). A comunicação entre as células do epitélio e as células estromais adjacentes é essencial para a manutenção da integridade normal e das funções da glândula (Taylor & Risbridger, 2008).

Na próstata, o estroma é responsável pelo desenvolvimento e manutenção da diferenciação do epitélio (Hall, 1978; Lin & Bissel, 1993; Vilamaior et al., 2000). A interação parácrina recíproca entre o epitélio e o estroma tem início durante as fases iniciais do desenvolvimento da glândula, no período fetal, e continua durante toda a vida pós natal, influenciando tanto a homeostasia como o desenvolvimento de lesões prostáticas (Cunha et al., 1996). No tecido embrionário, o mesênquima especifica a diferenciação funcional e a produção de proteínas epiteliais secretoras ou a expressão da especificidade de proteínas do citoesqueleto e de membrana (Cunha et al., 2004).

Experimentos com cultura de células epiteliais e estromais uterinas revelam que interações entre o mesênquima em desenvolvimento e o epitélio são recíprocas. Lejeune et al. (1981) mostraram que quando o epitélio uterino foi retirado, as células estromais não promoveram a decidualização uterina, mesmo em resposta aos hormônios estrógeno e progesterona. Esses resultados indicam que o epitélio é provido de sinais que induzem a resposta estromal ao tratamento hormonal. Assim como no útero, as interações entre o epitélio e o mesênquima durante o desenvolvimento prostático e entre o epitélio e o estroma na glândula adulta são mediadas por fatores de crescimento, de diferenciação e proteases, que modulam o micro ambiente local (Cunha et al., 2004).

Na próstata do indivíduo adulto, o estroma controla a homeostasia epitelial via regulação androgênica (Cunha et al., 1987; Hayward & Cunha, 2000). Essa interação parácrina é descrita em numerosos estudos que mostram que a resposta epitelial aos

andrógenos é mediada indiretamente através de fatores estromais solúveis (Cunha & Chung, 1981; Cunha et al., 1983). Porém, sabe-se que durante o processo de carcinogênese ocorre a diminuição ou a total ruptura da interação entre as céulas epiteliais e o estroma, resultando no crecimento descontrolado e nas transformações malignas do epitélio (Olumi et al., 1999).

Hayward e colaboradores (1996) mostraram que, durante o desenvolvimento do tecido prostático normal e sob a influência de andrógenos, células mesenquimais diferenciam-se em fibroblastos e em CML. Acredita-se que, durante a carcinogênese prostática, o músculo liso de-diferencia-se e converte ao fenótipo de Fb. Assim, a camada muscular diminui progressivamente em carcinomas prostáticos humanos durante a progressão de tumores de baixo para alto grau (Hayward et al., 1997). Além da diminuição das CML, esse estroma reativo é caracterizado por alterações fenotípicas nas células estromais e no arranjo dos componentes da MEC, tais como: deposição de componentes da MEC, como colágeno do tipo I e tenascina e aumento na densidade local de vasos sanguíneos (Tuxhorn et al., 2002; McAlhany et al., 2003). Com essas alterações, o estroma reativo fornece um micro ambiente apropriado para as células tumorais proliferarem e diferenciarem. Com isso, se faz necessário o entendimento do papel do estroma no CaP e das interações entre as células tumorais e o microambiente adjacente durante a iniciação e a progressão da doença, para o desenvolvimento e o sucesso de novas terapias (Taylor & Risbridger, 2008).

1.1.3 Colágeno I, Colágeno III e TGF-Beta 1

No estroma prostático, as CMLs e os Fbs desempenham importante função na produção de uma variedade de fatores autócrinos e parácrinos que contribuem para a homeostasia da glândula (Vilamaior et al., 2000). Os fatores de crescimento mais importantes para a regulação das funções da próstata normal são: EGF (*Fator de Crescimento Epidermal*), TGF-α (*Fator de Crescimento Transformante Alfa*), FGF-b (*Fator de Crescimento Fibroblástico básico*), IGF (*Fator de Crescimento Semelhante à*

Insulina Tipo-1) e a família TGF-β (*Fator de Crescimento Transformante beta*) (Russell et al., 1998).

O TGF-beta 1 é um importante regulador do tecido prostático normal e maligno. Na próstata integra, esse fator de crescimento estimula a diferenciação celular, inibe a proliferação das células epiteliais e induz a morte celular (Huang & Lee, 2003; Zhu & Kyprianou 2005; Fleisch et al., 2006). Quando secretado no sêmen, o TGF-beta 1 desenvolve importante papel como fator imunossupressor. As células do câncer prostático expressam altos níveis de TGF-beta 1, o que parece estar relacionado ao processo de metástase, por estimular a angiogênese e por inibir respostas imunes diretas às células tumorais. Essas células frequentemente perdem os receptores celulares para o TGF-beta 1, facilitando o processo de proliferação celular e dificultando a promoção de apoptose (para revisão Wikström et al., 2001).

A super expressão do TGF-Beta 1 é frequentemente observada durante a progressão do CaP (Gerdes et al., 2004). Esse fator de crescimento pode, transitoriamente, induzir a translocação do AR do núcleo para o citoplasma e induzir diferenciação de fibroblastos em miofibroblastos, principalmente no estroma reativo associado ao câncer (Gerdes et al., 2004). Além disso, o TGF-beta 1 estimula a secreção de FGF-b no estroma prostático e altos níveis de FGF-b circulante pode antagonizar os efeitos antiproliferativos do TGF-Beta-1 (Collins et al., 1996).

Afecções fibróticas também estão relacionadas com o aumento nos níveis de TGF-beta 1, que inicialmente recrutam células inflamatórias e fibroblastos para a área de injúria e estimulam estas células a produzirem citocinas e matriz extracelular (MEC). O TGF-beta 1 não só aumenta a síntese da MEC, como também inibe a sua degradação, regulando baixos níveis de expressão das metaloproteinases de matriz – MMPs (enzimas responsáveis por esse evento) e induz aumento na expressão dos inibidores dessas enzimas (inibidores teciduais de MMPs – TIMPs) (Verrecchia et al., 2007). A desregulação dessas funções está associada com a deposição excessiva de tecido conjuntivo, como o que ocorre nas cicatrizes e na fibrose em muitos órgãos (Ghahary et al., 1993).

O colágeno é uma das mais importantes macromoléculas da MEC e a razão entre a sua síntese e o seu acúmulo é fundamental para a estrutura e função do tecido ao qual faz parte

(Péterszegi et al., 2008). No estroma prostático, os principais tipos de colágeno existentes são: IV(constituinte da membrana basal), I (formam as fibras de colágeno mais numerosas do estroma prostático), III (formam as fibras reticulares) e VI (moléculas de ancoragem que associam-se ao colágeno do tipo I).

Vilamaior et al. (2000) demonstraram que o estroma da próstata ventral de ratos é composto por colágeno dos tipos I e III concentradas ao redor dos ductos e alvéolos prostáticos. Após a castração cirúrgica, essas fibras tornam-se onduladas e intimamente associadas às CMLs, sugerindo o papel dessas células na reorganização dos componentes fibrilares do estroma. Os autores concluíram que a reorganização estromal prostática promovida pela castração é de extrema importância para as discussões sobre os efeitos das terapias hormonais na fisiologia prostática.

O estroma reativo do CaP é composto por aproximadamente 50% de miofibroblastos, tipo celular cujo fenótipo ativo é pouco observado no tecido prostático normal, que sintetizam em excesso alguns componentes da MEC, como colágeno do tipo I, tenascina e MMPs (Tuxhorn et al., 2002). Sabe-se que a produção dessas proteínas no organismo humano adulto é específica a situações de remodelação tecidual, incluindo os processos de cicatrização e estroma reativo no câncer (para revisão: Tuxhorn et al., 2002).

1.2 Afecções Prostáticas

As lesões prostáticas surgem mais comumente em homens de meia idade e as chances de desenvolver lesões benignas ou malignas aumentam com o avanço da idade. O CaP e a HPB são as afecções prostáticas mais observadas e serão parcialmente discutidas nos itens a seguir.

1.2.1 Câncer de Próstata

O câncer prostático (CaP) é o câncer mais comum diagnosticado e o segundo que mais mata entre os homens na América e nos países da Europa Ocidental (Jemal et al., 2002; Rittmaster et al., 2009). As taxas de incidência desse tipo de câncer são cerca de seis

vezes maiores nos países desenvolvidos, comparados aos países em desenvolvimento (INCA, Estimativa 2010). No Brasil, o número de casos novos de câncer de próstata estimado para o ano de 2010 é de 52.350. Estes valores correspondem a um risco estimado de 54 casos novos a cada 100 mil homens. O aumento nas taxas de incidência no Brasil ao longo dos anos pode ser decorrente do aumento da expectativa de vida da população, da evolução dos métodos diagnósticos e da melhoria da qualidade dos sistemas de informação do país (INCA, Estimativa 2010).

Alguns fatores predispõem as chances de um homem desenvolver o CaP, tais como: a idade (homens mais velhos, com mais de 50 anos de idade, têm maiores chances de desenvolverem a doença); a raça (os descendentes africanos desenvolvem mais o CaP); histórico familiar (homens com casos de CaP na família têm o risco de desenvolver a doença aumentado em 2 a 3 vezes); dieta (homens obesos, com dieta rica em gordura animal apresentam maior pré disposição); além da influência dos componentes genéticos (Rittmaster et al., 2009).

Dados de autopsias feitas em homens jovens vítimas de traumas, com idade aproximada de 30 anos, revelaram que 1 em cada 3 próstatas analisadas apresentaram alterações histológicas compatíveis com os estágios iniciais do CaP (Sakr et al., 1994). Em contraste ao surgimento histológico da doença, os sinais clínicos geralmente não surgem antes dos 50 anos de idade. Esses resultados mostram que progressão entre o CaP pré clínico e a doença clínica é bastante lenta e silenciosa, assim métodos preventivos e o acompanhamento clínico são indicados principalmente aos homens com pré disposição ao desenvolvimento da doença (Rittmaster et al., 2009).

O desenvolvimento do CaP pode ser resultado do acúmulo de agressões locais promovidas durante décadas, tais como a exposição do epitélio prostático a agentes infecciosos, assim como a processos inflamatórios crônicos e carcinogênicos (Rittmaster, 2008). Estudos morfológicos descritos por De Marzo e colaboradores (2007) mostram que a progressão do CaP em muitos casos ocorre através da transição entre a atrofia inflamatória proliferativa (PIA – Proliferative Inflammatory Atrophy) e o adenocarcinoma e/ou pela transição entre PIA e a neoplasia intraepitelial prostática (PIN – Prostatic Intraepithelial Neoplasia) (De Marzo et al., 2007; Rittmaster, 2008) (Figura 2). Alguns

genes supressores tumorais (NKX3.1, CDKN1B e PTEN) que na próstata normal apresentam altos níveis de seus produtos protéicos, encontram-se diminuídos nas alterações PIA, NIP e CaP (De Marzo et al., 2007).

A continuidade entre o estágio de PIN e o estágio inicial do câncer invasivo é caracterizado pelo aumento das alterações nucleares e nucleolares, aumento da proliferação celular, variação no conteúdo de DNA, aumento da instabilidade genética e pela ruptura progressiva da membrana basal. Há também um aumento relativo da densidade de micro vasos na NIP e no carcinoma, quando comparado com o tecido prostático normal (Bostwick et al., 2004).

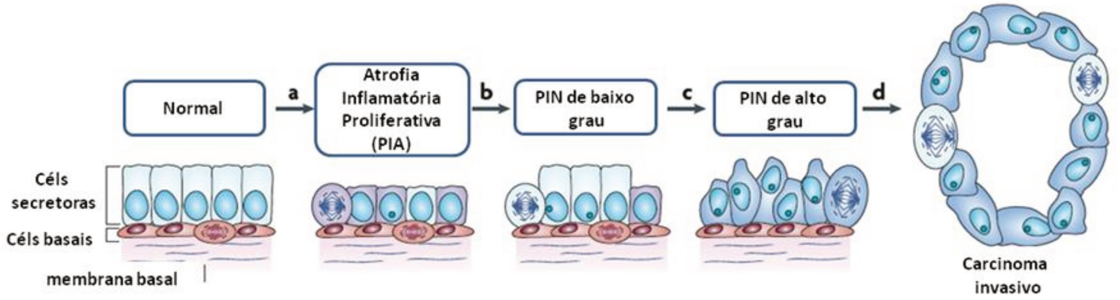

Figura 2: *Modelo celular e molecular da progressão do CaP.* ***a)*** *Estágio caracterizado pela infiltração de linfócitos, macrófagos e neutrófilos. Os fagócitos liberam O_2 reativo e N_2 causando danos no DNA, injúria e morte celular A manifestação morfológica se dá pela atrofia epitelial.* ***b)****Silenciamento do gene GSTP-1 através da metilação do seu promotor facilita o encurtamento dos telômeros.* ***c)*** *Células com telômeros deficientes sofrem instabilidade genética e acumulam alterações genéticas.* ***d)*** *A proliferação contínua das células epiteliais luminais com alterações genéticas levam à progressão do carcinoma invasivo. Esquema proposto por De Marzo et al., 2007.*

A sinalização do AR promove papel fundamental tanto no crescimento do CaP, como na resistência hormonal. A diidrotestosterona (DHT) liga-se ao AR, formando o complexo DHT-AR que atua no núcleo das células epiteliais prostáticas, ativando a transcrição de genes dependentes de andrógeno. Durante a progressão da doença, o tumor prostático pode progredir do estágio de dependência para o estado de independência androgênica (Tindall & Rittmaster, 2008), adquirindo comportamento invasivo e metastático.

Estudos imunohistoquímicos mostram que as células tumorais independentes de andrógeno continuam a expressar o AR (Ruizeveld de Winter et al., 1991), sugerindo que a via de sinalização do AR permanece intacta, mas a sua regulação pode estar alterada.

Alguns mecanismos podem contribuir para a ativação do AR mesmo em baixos níveis androgênicos, tais como: 1) Super expressão do AR; 2) Mutação do AR que requer baixos níveis de andrógeno ou outros ligantes esteróides para ser ativado; 3) Aumento da produção local de andrógeno pelas células prostáticas; 4) Ativação do AR por ligantes não esteroidais como fatores de crescimento e citocinas; 5) Alteração na expressão de coativadores e correpressores do AR; 6) Mecanismo recém descrito: processamento proteolítico do AR em uma isoforma independente de andrógeno (Feldman & Feldman, 2001; Meinbach & Lokeshwar, 2006; Wu et al., 2006; Devlin & Mudryj, 2009).

Apesar da maioria das neoplasias prostáticas serem originadas no compartimento epitelial, recentemente tem-se demonstrado que o estroma também é alvo das alterações morfológicas e bioquímicas induzidas pelas neoplasias. Estas alterações que, coletivamente são denominadas de reação ou ativação estromal, incluem aumento da proliferação celular, ativação de miofibroblastos adjacentes ao local da lesão epitelial, com aumento de síntese dos componentes da MEC e de enzimas que participam da remodelação estromal, além de citocinas que induzem migração celular e angiogênese. Estas alterações estromais criam um microambiente favorável à progressão dos carcinomas (Tuxhorn et al., 2002).

Olumi et al. (1999) demonstraram o potencial das células estromais em modular a progressão ou a supressão tumoral. Para tanto, estes autores realizaram experimentos utilizando sistema de co-cultura, com células epiteliais prostáticas imortalizadas, porém não tumorigênicas, cultivadas juntamente com fibroblastos normais. Neste modelo, os autores não observaram a completa transformação das células epiteliais prostáticas, nem o desenvolvimento de carcinomas. Em contrapartida, quando as mesmas células epiteliais foram cultivadas com fibroblastos isolados de áreas adjacentes a tumores, observou-se a completa transformação das células epiteliais e o desenvolvimento de carcinomas. Os mesmos resultados foram obtidos utilizando-se células epiteliais mamárias e fibroblastos senescentes transformados por radiação (Parrinello et al., 2005). Desta forma, o estroma parece ser um importante modulador da progressão ou da supressão tumoral (Tuxhorn et al., 2001; Parrinello et al., 2005).

1.2.2 Hiperplasia Prostática Benigna

A Hiperplasia Prostática Benigna (HPB) é o tumor benigno mais comum em homens de meia idade, caracterizada pelo processo proliferativo de células estromais e epiteliais, gerando o crescimento nodular do tecido prostático (McNeal, 1984). A prevalência dessa afecção é dependente da idade e evidências histológicas da HPB são raras em próstatas de homens com menos de 50 anos de idade, mas comummente encontradas em homens que atingem os 80 anos de idade (Berry et al., 1984). Está presente em, aproximadamente, 20% dos homens na faixa etária de 40 anos, com um aumento para 70% na faixa etária dos 60 anos (Isaacs, 1994).

A relação entre epitélio e estroma na prostata hiperplásica é altamente variável, mas aproximadamente 80% e 20% do volume hiperplásico é composto por elementos estromais e epiteliais, respectivamente (Bartsch et al., 1979). Metade da hiperplasia estromal é composta por células musculares lisas (Shapiro et al., 1992). Outras alterações histológicas que ocorrem na HPB são: aumento de síntese e deposição de matriz extracelular, principalmente colágeno do tipo I, redução de fibras elásticas, aparecimento de infiltrado inflamatório ao redor dos ductos e maior quantidade de corpos amiláceos no lúmen (Bostwick et al., 1992; Untergasser et al., 2005).

Embora ambos os componentes epiteliais e estromais estejam envolvidos no desenvolvimento da HPB, alguns estudos mostram que o estroma desenvolve papel fundamental na instalação da afecção e que a proliferação desordenada do epitélio glandular é um evento tardio que depende de sinais parácrinos enviados pelos nódulos estromais (McNeal, 1990; Deering et al., 1994; Ao et al., 2007).

Alguns fatores de crecimento participam do processo patológico da HPB, incluindo FGF, IGF e TGF-Beta. Estudos mostram que esses fatores podem ser secretados pelas células epiteliais e atuar em receptores localizados no estroma prostático e isso pode explicar a necessidade da interação epitélio-estroma no desenvolvimento dos nódulos prostáticos (Hieble & Ruffolo, 1996).

A manifestação clínica da HPB está associada com sintomas do sistema urinário baixo (do inglês *Lower Urinary Tract Symptoms* - LUTS), que incluem noctúria, frequência e urgência urinária (Boyle & Napalkov, 1995). Esses sintomas são causados pela

interferência da função da musculatura lisa com a obstrução do fluxo urinário através da parte prostática da uretra (Bostwick et al., 2004). Complicações mais sérias da HPB incluem: retenção urinária aguda, infecção do sistema urinário, insuficiência renal e hematúria (Untergasser et al., 2005). Na última década, a terapia médica tem substituído a cirurgia como tratamento inicial para homens que apresentem algum sintoma do LUTS associado à HPB (Seftel et al., 2008).

A Associação Urológica Americana (AUA) descreveu atualizações sobre a HPB em 2003, indicando que, embora para alguns casos clínicos as terapias médicas, como o uso de bloqueadores α-1 adrenérgicos e inibidores da enzima 5-alfa redutase, não sejam eficazes como a cirurgia, podem aliviar os sintomas do LUTS e oferecer bem estar aos pacientes, diminuindo alguns efeitos colaterais (Kramer et al., 2009).

1.3 Quimioprevenção do Câncer de Próstata: Finasterida e Doxazosina

Com o aumento no número de homens diagnosticados com CaP e com o contínuo aumento no número de óbitos a cada ano, é crescente a quantidade de novas alternativas terapêuticas sugeridas para reduzir as complicações causadas pela doença (Thompson et al., 1997).

Charles Huggins, na década de 50, descobriu que a privação androgênica era efetiva para o tratamento do CaP (Taylor & Risbridger, 2008). Desde então, os esforços de pesquisadores do mundo todo têm se resumido em estudos farmacêuticos *in vivo* e *in vitro* para a criação de novos compostos (análogos aos andrógenos ou bloqueadores), visando o sucesso da terapêutica ou a quimioprevenção do CaP. O avanço das ferramentas nas áreas de biologia celular e molecular favorece as pesquisas científicas, porém ainda existem muitas informações a serem descobertas sobre a progressão da doença.

A evolução no diagnóstico e nas técnicas de detecção prematura aumentam as chances de diagnóstico do CaP alojado apenas ao órgão, sem riscos de metástase. A proporção da doença e o prognóstico para os pacientes com CaP são determinados com base no escore de Gleason, nos níveis de PSA e na determinação do estágio clínico da doença (Devlin & Mudryj, 2009).

A preocupação atual da sociedade médico científica com a prevenção e com o diagnóstico precoce do CaP contribui para a escolha de tratamentos individuais para cada tipo de paciente e estágio do tumor, favorecendo a cura e diminuindo o sofrimento (Thompson et al., 2009). A prevenção é diferente do tratamento da doença. Para o tratamento, o paciente apresenta a doença e deve ser consultado para aceitar os possíveis efeitos colaterais e o custo do tratamento. Na prevenção, o indivíduo encontra-se bem e por isso o processo preventivo deve oferecer o mínimo de toxicidade e ser financeiramente acessível (Kramer et al., 2009; Thompson et al., 2009).

O fármaco Finasterida foi aprovado para ser indicado a pacientes na quimioprevenção do CaP nos EUA, além disso outros medicamentos, incluindo a dutasterida, as estatinas, os inibidores de cicloxigenase-2 (COX-2) e os moduladores de receptores de estrógeno estão sendo testados como possíveis quimiopreventivos em estudos clínicos e aguardam a aprovação para serem indicados e comercializados (Rittmaster et al., 2009).

Alguns estudos exploram a via de ativação da apoptose, como o uso da doxazosina, como possível terapia para pacientes com CaP dependente ou independente de andrógenos (Kyprianou, 1994). Atualmente, pesquisadores procuram por novos métodos terapêuticos, com efeitos colaterais reduzidos, para o tratamento do CaP, como por exemplo terapias que incluem a indução de apoptose nas células tumorais e a supressão da carcinogênese.

1.3.1 Finasterida

A finasterida (Fin, Figura 3), composto inibidor da enzima 5 α-redutase do tipo 2 (Prahalada et al., 1994; Griffiths et al., 1997; Prahalada et al., 1998), foi a primeira droga desenvolvida e aprovada pela agência americana *US Food and Drug Administration* (FDA) para o tratamento da HPB (Stoner, 1990). Essa droga é capaz de inibir de 80% a 90% a enzima 5 α-redutase do tipo 2, reduzindo o tamanho prostático para 30% a 40% (Prahalada et al., 1994). Além disso, a administração de Fin eleva os níveis séricos de T e diminui os níveis de DHT para 80% a 90% em relação aos níveis normais em homens e animais (Rittmaster, 1994). Assim, o tratamento da HPB com Fin alivia os sintomas em muitos

homens afetados por promover a diminuição da próstata e o consequente aumento do fluxo urinário (Marks et al., 1997).

Além de reduzir os sintomas urinários da HPB, a Fin tem sido administrada em pacientes com HPB previamente à cirurgia para diminuir a hematúria associada com a afecção, processo relacionado com a proliferação de microvasos e estimulado pela DHT (Marshall & Narayan, 1993). Pareek e colaboradores (2003) relataram que a Fin diminuiu a expressão do fator de crescimento de vasos sanguíneos (VEGF), inibindo a angiogênese e a densidade de microvasos na próstata de pacientes com HPB.

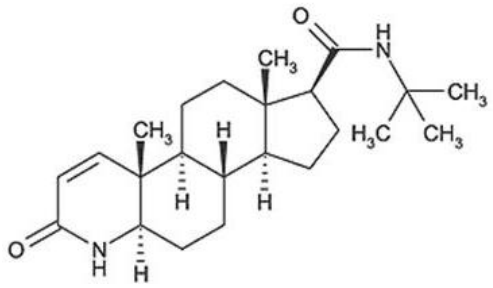

Figura 3: *Estrutura molecular da finasterida, composto inibidor da enzima* 5 α-redutase do tipo 2, *cuja fórmula empírica é* $C_{23}H_{36}N_2O_2$.

Estudos em roedores tratados com Fin mostram que, além de alterar os níves de T e de DHT, a inibição da enzima 5 α-redutase tipo 2 diminui o volume da glândula prostática, a altura das células epiteliais, a área ocupada pelo lúmen e promove morte celular por apoptose, sugerindo a diminuição da atividade secretória, além de promover a reorganização do estroma, principalmente pela alteração no arranjo das fibrilas colágenas (Rittmaster et al., 1995; Prahalada et al., 1998; Corradi et al., 2004).

Golbano et al. (2008) investigaram os efeitos da Fin no mecanismo de indução de apoptose em cultura de células tumorais prostáticas dependentes de andrógeno, LNCaP. O tratamento com Fin promoveu perda da viabilidade celular e acelerou o processo de apoptose de maneira dose-dependente, aumentando os níveis de Caspase-3, de Bax e diminuindo os níveis de Bcl-2 e Bcl-x_L.

Evidências sugerem que a DHT e os subtipos da enzima 5 α-redutase desempenham papel importante no desenvolvimento e na progressão do CaP. Comparado com os níveis encontrados na HPB, a 5 α-redutase do tipo 1 está aumentada na neoplasia intraepitelial (NIP) e no CaP primário e mais ainda no CaP recorrente (Tindall & Rittmaster, 2008). Um estudo recente de Thomas e colaboradores (2008) descreve que a enzima 5 α-redutase do tipo 1 é altamente expressa em muitos casos de CaP e que a expressão dos tipos 1 e 2 da isoenzima está aumentada nos casos de CaP de alta gradação quando comparado com os casos de CaP de baixa gradação. Os portadores de pseudohermafroditismo possuem deficiência congênita da enzima 5 α-redutase do tipo 2 e não existem relatos de casos de CaP ou de HPB nesses indivíduos, refletindo o possível papel dessa enzima no desenvolvimento do tumor (Imperato-McGinley & Zhu, 2002).

Alguns autores defendem a hipótese de que a inibição das enzimas 5 α-redutase pode reduzir o risco de desenvolvimento do CaP, diminuindo ou prevenindo a progressão da doença e/ou tratando a doença já existente (Tompson et al., 2003; Reddy, 2004). Assim, drogas inibidoras dos subtipos dessa enzima, como a Fin, estão sendo investigadas como possíveis ferramentas para a prevenção do desenvolvimento de CaP.

Apesar da aprovação recente para ser usada na quimioprevenção do CaP, testes realizados nos Estados Unidos com homens voluntários que ingeriram 5 mg de Fin/dia durante 7 anos, mostraram algumas dúvidas referentes à interpretação dos resultados das biopsias prostáticas (Thompson et al., 2003).

A instituição americana *Prostate Cancer Prevention Trial* (PCPT), apoiada por vários institutos americanos de estudos de prevenção e tratamento do CaP, foi escolhida para a realização desse estudo, cujo foco principal foi estabelecer a relação entre andrógenos e o risco de desenvolvimento do CaP. O estudo teve início em outubro de 1993, com a triagem de homens a partir de 55 anos de idade e com diagnóstico negativo para CaP. Após a triagem, 18882 homens com o PSA menor ou igual a 3.0 ng/ml foram randomizados para receber 5 mg de finasterida/dia ou placebo. Os participantes foram convocados a cada 6 meses para relatar sobre possíveis efeitos colaterais e a dosagem do PSA e o exame de toque retal foram feitos anualmente. Após 7 anos de estudo, a realização

de biópsia da glândula prostática foi recomendada a todos os participantes (Thompson et al., 2009).

Dentre os 4368 homens que receberam finasterida durante 7 anos, apenas 803 (18,4%) desenvolveram câncer, contra 1147 (24,4 %) entre 4692 pacientes que receberam placebo. Entretanto, uma maior incidência de tumores com gradação de Gleason 7, 8, 9 e 10 foi encontrada nos pacientes que receberam finasterida (37 %), contra 22,2% nos pacientes que receberam placebo (Thompson et al., 2003). O PCPT concluíu que, embora a finasterida previna ou atrase o aparecimento do câncer, ela aumenta o risco de CaP de alto-grau.

Essas considerações criaram polêmica sobre o uso e os benefícios da finasterida em pacientes com risco de desenvolvimento de CaP (Koltz & Clarke, 2008). Contudo, após a reavaliação dos resultados encontrados pelo PCPT, foi comprovado que a finasterida aumenta as chances de detecção do CaP de alto grau em biópsias por punção, por diminuir o volume da glândula prostática, e que a droga refina os resultados do PSA em pacientes com CaP (após o tratamento com a finasterida a maioria dos pacientes com CaP ainda apresentavam altos níveis de PSA, em contraste com os pacientes sem CaP) e que o tratamento não aumenta os riscos de desenvolver CaP de alto grau, pois este aspecto era artefatual. Assim, o uso da finasterida como quimiopreventivo do CaP foi aprovado e indicado para pacientes com pré-disposição ao desenvolvimento desse tipo de tumor (Thompson et al., 2009). Entretanto, nem todos urologistas ficaram convencidos do uso seguro da finasterida na prevenção do CaP. Os principais argumentos contra são o período curto do estudo, pois estes pacientes deveriam ser acompanhados por um período maior de tempo e que o tratamento com finasterida pode selecionar, ao longo do tempo, as células tumorais andrógeno-independentes, mais agressivas e metastáticas (Koltz & Clarke, 2008).

Em um estudo recente (Delella et al., 2009), o nosso grupo tratou ratos Wistar adultos durante 7 e 30 dias com finasterida e verificou aumento na expressão e na atividade da metaloproteinase de matriz -9 (MMP-9) e redução na atividade da MMP-2, concluindo que essas alterações podem afetar o comportamento e o destino de células prostáticas normais e tumorais durante o tratamento. Assim, mais estudos sobre os efeitos da finasterida sobre as células prostáticas são necessários para contribuir com esse debate.

1.3.2 Doxazosina

A doxazosina (DOX, Figura 4) é um bloqueador α-1 adrenérgico seletivo, seguro e aprovado pela FDA para o tratamento dos sintomas obstrutivos da HPB (Kyprianou et al., 1998) e são considerados a principal linha de fármacos para o tratamento de pacientes com *LUTS* associado à HPB (Tahmatzopoulos et al., 2004), por reduzir o tonus da musculatura lisa prostática e consequentemente inibir a dinâmica do componente que obstruía a parte prostática da uretra (Forray et al, 1994). A AUA (*American Urological Association*) recomenda o uso desses bloqueadores como drogas seguras e eficazes para pacientes que sofrem de HPB.

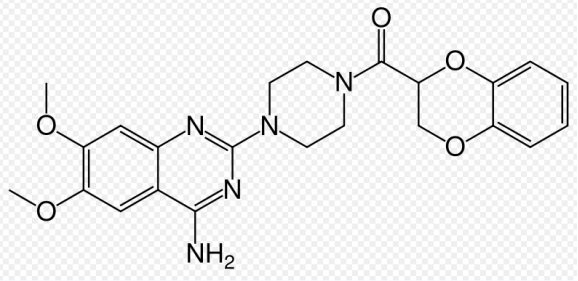

Figura 4: *Estrutura molecular do bloqueador α-1 adrenérgico, doxazosina, cuja fórmula estrutural é* $C_{23}H_{25}N_5O_5$*. Retirado do site http://www.drugs.com/pro/cardura-xl.html*

Além de contribuir na melhora do *LUTS,* estudos evidenciam que o tratamento com bloqueadores α-1 adrenérgicos tem efeitos na inibição da proliferação, indução de apoptose e supressão da vascularização tecidual (Kyprianou et al., 1998; Kyprianou et al., 2009). Essas alterações foram reportadas em estudos experimentais (Kyprianou & Benning, 2000; Benning & Kyprianou, 2002) e em humanos (Yang et al. 1997; Kyprianou et al., 1998), envolvendo apoptose de células epiteliais e estromais. A indução de apoptose nas células prostáticas normais e tumorais pela doxazosina mostrou-se independente da capacidade que essa droga tem em bloquear os receptores α-1 adrenérgicos e tem sido relacionada com um aumento na expressão do TGF-beta 1 (Yang et al., 1997; Glassman et al., 2001; Partin et al., 2003). Esses efeitos podem ocorrer pela indução da sinalização do TGF Beta-1 e

aumento na regulação dos reguladores de ciclo celular p21 e p27 e na expressão dos genes I Ba, inibidor de NF-kB (Yang et al., 1997). Assim, o TGF Beta-1 aumentado após o tratamento com DOX parece funcionar como um regulador inibitório da proliferação celular e indutor da apoptose prostáticas (Kyprianou et al., 1998).

Estudos posteriores mostraram que a doxazosina e outros bloqueadores α-adrenérgico induzem apoptose não apenas em células normais, como também em células tumorais (Kyprianou et al., 2009), além de induzir apoptose nas CMLs e degradação de outros componentes do estroma prostático, diminuindo a expressão da α-actina do músculo liso e melhorando os sintomas da HPB (Kyprianou et al., 1998).

Justulin Jr e colaboradores (2008) investigaram os efeitos da Dox (25mg/Kg/dia) no complexo prostático de ratos Wistar adultos, analisando parâmetros estruturais, o conteúdo das fibras de colágeno e os índices de proliferação celular e apoptose. O tratamento promoveu aumento do peso dos lobos próstaticos, aumento do lúmen alveolar, diminuição na altura das células epiteliais, redução das dobras epiteliais e células musculares lisas mais alongadas.

Os bloqueadores α-1 adrenérgicos, como a Dox, também são descritos como supressores da invasão e migração de células epiteliais do câncer prostático, por reduzirem a adesão dessas células com os componentes da matriz extracelular e por induzir apoptose nas células tumorais (Kyprianou & Benning, 2000; Benning & Kyprianou, 2002). Assim, a célula epitelial perde a associação com a membrana basal e sofre apoptose do tipo *anoikis,* com exceção das células tumorais que adquirem resistência a esse tipo de morte celular através da super expressão de fatores antiapoptóticos, como Bcl-2 (Tahmatzopoulos et al., 2004). Esses resultados sugerem os bloqueadores α-1 adrenérgicos como possíveis fármacos a serem usados no tratamento do CaP, apesar de mais estudos serem necessários para elucidar os mecanismos pelos quais esses compostos induzem a apoptose.

Keledjian & Kyprianou (2003) demonstraram que a doxazosina diminui a expressão do VEGF em células tumorais prostáticas humanas e em células endoteliais. No CaP ocorre aumento na expressão de VEGF (quando comparado à glândula normal) que relaciona-se diretamente com o estágio, gradação e densidade de microvasos sanguíneos do tumor (Strohmeyer et al., 2000). Esses estudos classificam os bloqueadores α-1 adrenérgicos,

como a doxazosina, como prováveis inibidores angiogênicos para pacientes com CaP (Tahmatzopoulos et al., 2004).

Novos e conclusivos estudos clínicos e experimentais sobre as propriedades apoptóticas dos bloqueadores α-1 adrenérgicos, como doxazosina e a terazosina, são necessários para assegurar a possibilidade do uso dessas drogas no tratamento de pacientes com CaP. Essas propriedades apontam para a significante estratégia terapêutica usando os bloqueadores α-1 adrenérgicos, tanto para a HPB como para o CaP, com a possibilidade de atuarem na prevenção do desenvolvimento de tumores (Kyprianou et al., 2009).

2. Objetivos

2.1 Objetivos Gerais

O objetivo do presente estudo foi investigar os efeitos da finasterida e da doxazosina sobre o estroma glandular, células e matriz extracelular, dos lobos prostáticos do rato Wistar adulto.

2.2 Objetivos Específicos

- Avaliar alterações em nível ultra-estrutural nas células e na matriz extracelular;
- Avaliar alterações nos níveis de expressão do RNAm dos colágenos tipo I e tipo III;
- Avaliar alterações na distribuição e organização dos colágenos fibrilares tipo I e tipo III;
- Avaliar alterações nos níveis de expressão do RNAm e da proteína do TGF beta-1.

3. Resultados

Os resultados obtidos nesta tese estão divididos em 3 capítulos apresentados na forma de artigos científicos:

Capítulo 1: *Doxazosin Treatment Alters Stromal Cell Behavior and Increases Elastic System Fibers Deposition in Rat Prostate. Microscopy Research and Technique, 2010, In Press.*

Capítulo 2: *Finasteride Effetcs On Type I Collagen, Type III Collagen And TGF-Beta 1 Expression In The Rat Ventral Prostate. A ser submetido ao periódico "Prostate".*

Capítulo 3: *Increased Type I Collagen and TGF-Beta 1 gene expression in doxazosin-treated rat ventral prostate. A ser submetido ao periódico "European Urology".*

Capítulo 1:

MICROSCOPY RESEARCH AND TECHNIQUE 00:000–000 (2010)

Doxazosin Treatment Alters Stromal Cell Behavior and Increases Elastic System Fibers Deposition in Rat Prostate

FLÁVIA KARINA DELELLA[1,2] AND SÉRGIO LUIS FELISBINO[1]*
[1]*Department of Cell Biology, Institute of Biology, UNICAMP—University of Campinas, Campinas, Sao Paulo, Brazil*
[2]*Department of Morphology, Institute of Biosciences, UNESP—Univ Estadual Paulista, Botucatu, Sao Paulo, Brazil*

KEY WORDS doxazosin; prostate; extracellular matrix; elastin; smooth muscle cell

ABSTRACT Doxazosin (DOX), an α-adrenoceptor antagonist, induces the relaxation of smooth muscle cell tonus and reduces the clinical symptoms of benign prostatic hyperplasia (BPH). However, the effects of DOX in the prostate stromal microenvironment are not fully known. In a previous study, we showed that DOX treatment for 30 days increased deposition of collagen fibers in the three rat prostatic lobes. Herein, we investigated the effects of DOX on stromal cell ultrastructure and elastic fiber deposition. Adult Wistar rats were treated with DOX (25 mg/kg/day); and the ventral, dorsal, and anterior prostates were excised at 30 days of treatment. The prostatic lobes were submitted to histochemical and stereological-morphometric analyze and transmission electron microscopy (TEM). Histochemical staining plus stereological analysis of the elastic fiber system showed that DOX-treated prostatic lobes presented more elaunin and elastic fibers than controls, mainly in the ventral lobe. Ultrastructural analysis showed that fibroblasts and smooth muscle cells from DOX-treated prostates presented active synthetic phenotypes, evidenced by enlarged rough endoplasmic reticulum and Golgi apparatus cisterns, and confirmed the observation of thickened elaunin fibers. Our findings suggest that, under α-adrenergic blockade by DOX, the fibroblasts become more active and smooth muscle cells shift from a predominantly contractile to a more synthetic phenotype. The deposition of collagen and elastic system fibers in the prostatic stroma may counterbalance the absence of smooth muscle tone during α-blockers treatment. *Microsc. Res. Tech. 00:000–000, 2010.*

INTRODUCTION

The prostate is a major male reproductive system accessory gland, whereas benign prostatic hyperplasia (BPH) and prostate cancer (PCa) are the most common proliferative disorders affecting older men (Crawford, 2009; Rittmaster, 2008; Thomson, 2008). Functionally, BPH consists of two components: static (generalized epithelial gland enlargement regulated by androgens) and dynamic (contraction of stromal smooth muscle cells, mediated predominantly by α1-adrenoceptors) (Lacey, 1996).

The α1-adrenoceptor antagonists, such as doxazosin (DOX) and terazosin, have been widely used to target the stromal smooth muscle cells in the treatment of BPH (Kirby, 1996). The competitive inhibition of catecholamine prevents contraction of smooth muscles and reduces their tone, thus alleviating the lower urinary tract symptoms (Smith et al., 1999).

Recently, DOX has also been demonstrated to inhibit prostate growth by inducing apoptosis in stromal and epithelial cells, showing additional effects on long-term BPH treatment and emerging as a potential drug for the prevention and treatment of androgen-independent PCa (Anglin et al., 2002; Chiang et al., 2005; Kyprianou, 2003; Kyprianou and Jacobs, 2000; Kyprianou et al., 1998; Yang et al., 1997).

In a previous work, our group demonstrated for the first time that DOX treatment also induces a reduction in the epithelial cell proliferation rate (Justulin et al., 2008). Furthermore, we also showed that DOX reduces both absolute and relative glandular weights with a significant increase of the collagen fiber deposition in the prostate stroma (Justulin et al., 2008). More recently, Imamura et al. (in press) using clinical specimens found that patients orally treated with α1-blockers often exhibit accumulation of collagen fibers in prostatic stroma and suggested that this structural change could be one of the factors responsible for the development of resistance to this treatment.

In addition to collagen fibers, elastic system fibers are also an important component of prostate stroma (Carvalho et al., 1997). The number and thickness of elastic system fibers increase in the rat ventral prostate (VP) stroma during castration-induced involution (Carvalho et al., 1997), and these fibers also appear to be altered in BPH (Chagas et al., 2002; Costa et al., 2004; Sugimoto et al., 2008).

Moreover, Smith et al. (1999), using culture of prostatic smooth muscle cells, found that contractility of

*Correspondence to: Sérgio L. Felisbino, Departamento de Morfologia, Instituto de Biociências, Universidade Estadual Paulista, CEP, 18.618-000, Botucatu, São Paulo, Brasil. E-mail: felisbin@ibb.unesp.br

Received 16 November 2009; accepted in revised form 2 January 2010

Contract grant sponsor: FAPESP; Contract grant numbers: 06/60114-6, 06/60115-2; Contract grant sponsors: CAPES of Brazil, CNPq, FUNDUNESP.

DOI 10.1002/jemt.20828

Published online in Wiley InterScience (www.interscience.wiley.com).

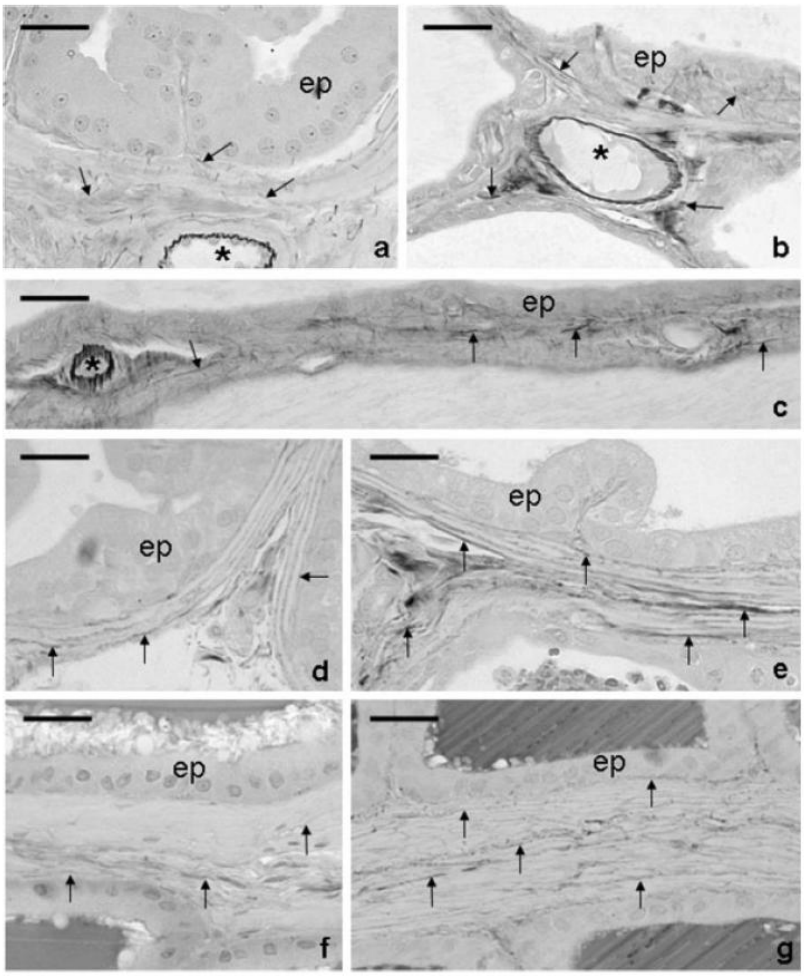

Fig. 1. Resin sections from rat prostatic lobes stained by Weigert's Resorcin–fuchsin. **a–c:** Ventral prostate; (**d**) and (**e**) dorsal prostate; (**f**) and (**g**) anterior prostate; (a, d, and f) control animals; (b, c, e, and g) doxazosin-treated animals. The elastin-containing elastic system fibers appear stained in dark (arrows). It can be observed that elaunin fibers are the main elastic system fibers in the control rat prostatic lobes and that 30 days of doxazosin treatment induced an increase in the number and thickness of these fibers in the three prostatic lobes. Epithelium (ep); blood vessels internal elastic laminae (*) were used as an internal positive control to the histochemical reaction. Bars = 20 μm.

smooth muscle cells decreased following DOX treatment. These authors also showed that DOX treatment reduced the expression of actin and myosin proteins, suggesting that α1-blockers induce dedifferentiation of smooth muscle into fibroblasts and myofibroblasts. A smooth muscle cell phenotype that is more synthetic than contractile also appears to play a major role in the process of depositing both collagen and elastic system fibers in the stroma during castration-induced prostate involution (Antonioli et al., 2004, 2007; Carvalho et al., 1997; Corradi et al., 2004; Vilamaior et al., 2000, 2005). Thus, in this study, we evaluated the effects of DOX treatment on stromal compartment of the ventral (VP), dorsal (DP), and anterior (AP) lobes, giving special attention to the phenotypes of the fibroblasts and smooth muscle cells and to elastic system fibers deposition.

MATERIALS AND METHODS

Animals

Adult male 3-month-old Wistar rats were maintained in a controlled environment with free access to food and water. The experiment was performed according to the *Guide for Care and Use of Laboratory Animals.* The animals were divided into two groups: control (CT) and the DOX-treated group. DOX-treated animals received daily doses of DOX (25 mg/kg of body weight)

(Doxazosin mesylate, Pfizer, Galena Pharmaceutical and Chemistry, SP, Brazil) dissolved in corn oil as vehicle, and administrated by oral gavage. The dosage and duration of treatments were based on consultation with Pfizer and in a previously published work (Yono et al., 2007). CT animals received only the vehicle. After 30 days of the DOX treatment, 10 animals from each group were killed by an overdose of pentobarbital. The VP, DP, and AP were excised, and alternate lobes were left and right assigned and processed for transmission electron microscopy (TEM) or for conventional microscopy. In our study, most of the lateral lobes presented acute prostatitis and, in this sense, it was excluded of the analysis.

Histochemistry and Stereological-Morphometric Analysis

Five lobe pairs of VP, DP, and AP from control and DOX-treated animals were immersed in 4% paraformaldehyde dissolved in phosphate buffer saline for 24 h. Fixed samples were washed in PBS for 24 h, dehydrated in a graded ethanol series, and embedded in glycol metacrylate resin (historesin embedding kit, Leica Heidelberg). Semiseriated resin (4 μm) sections were obtained and stained with Weigert's resorcin–fuchsin for elastic system fibers analysis (Carvalho et al., 1997).

The sections were analyzed with a Leica DMLB 80 microscope connected to a Leica C300FX camera. The digitalized images, obtained by using image analyzer Leica Q-win software Version 3 for Windows, were used for stereological-morphometric analysis.

The mean volume fraction of the elastic system fibers in the prostatic lobes was determined according to the Weibel system of point counting (Weibel et al., 1966) and using a 168-point grid test. Twenty-five microscopic fields were chosen at random from five different individual prostatic lobes from each experimental group. The volume fraction of elastic system fibers was expressed as percentage (%) after counting the number of points that coincided with elastic system fibers and the total number of points that coincided with the stromal area. All the measurements were taken from the intermediate regions, which represented the major portions of the prostatic lobe alveoli/tubules (Nemeth and Lee, 1996).

Transmission Electron Microscopy

Tissue fragments of five animals from each experimental group were immersed in 2.5% glutaraldehyde, plus 0.25% tannic acid solution in Millonig's buffer for 2 h (Cotta-Pereira et al., 1976), washed, and postfixed in 1% osmium tetroxide in the same buffer for 1 h, washed again, dehydrated in graded acetone, and embedded in Araldite. Semithin sections were stained with Toluidin Blue and analyzed under light microscopy. Ultrathin silver sections were obtained with a diamond knife and contrasted with 2% alcoholic uranyl acetate and then with 2% lead citrate in 1 N sodium hydroxide solution for 10 min. Grids were examined under a Phillips transmission electron microscope, operating at 80 kV.

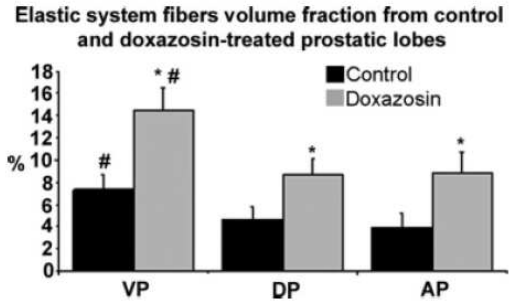

Fig. 2. Doxazosin effect on elastic system fibers volume fraction in the rat prostatic lobes. The values represent mean ± SD. In both control and treated groups, the ventral lobe (VP) had the highest elastic system fiber volume fraction among the prostatic lobes ($^{\#}P < 0.05$). Doxazosin treatment significantly increased the volume fraction of the elastic system fibers for all prostatic lobes ($^{*}P < 0.01$). Dorsal prostate (DP); anterior prostate (AP).

RESULTS

Histochemistry and Stereological-Morphometric Analysis

Histological analysis after Weigert's resorcin–fuchsin staining revealed a small number of delicate elaunin fibers in the control VP, DP, and AP lobes. These fibers were distributed mainly around smooth muscle cells, but also above the epithelium and in the interstitial space between the prostatic alveoli/tubules associated with collagen fibers (Figs. 1a, 1d, and 1f). DOX treatment promoted a visible increase of the elaunin fiber thickness and distribution in the three rat prostatic lobes (Figs. 1b, 1c, 1e, and 1g).

The measurement of Weigert's resorcin–fuchsin-stained areas by stereology showed that VP exhibited higher elastic system fiber volume fraction than dorsal and anterior lobes ($P < 0.05$) and confirmed the observation of increased elastic system fibers volume fraction in the three prostatic lobes after 30 days of DOX treatment, mainly in the VP ($P < 0.01$) (Fig. 2).

Transmission Electron Microscopy

The analysis of the control VP, by transmission electron microscopy (TEM), presented a thin layer of quiescent phenotype fibroblasts and smooth muscle cells that exhibited few protein synthesis-related organelles (Figs. 3a and 3b). Elaunin fibers, which were typically constituted by microfibril groups associated with an irregular elastin deposition and collagen fibrils were sparsely distributed between cells (Fig. 3a and 3b). DOX-treated VP stroma showed gross bundles of collagen fibrils and thickened elaunin fibers distributed among stromal cells (Figs. 3c–3e).

The stroma of control DP presented a dense and compact smooth muscle cell layer intermingled with thin bundles of collagen fibrils and thin elaunin fibers (Fig. 4a). DOX-treated DP presented less compact smooth muscle cells layer, thickened elaunin fibers, and an increased number of collagen fibrils (Figs. 4b and 4c).

The control AP presented a thick and compact smooth muscle cell layer intermingled with thin bundles of collagen fibrils and dispersed thin elaunin fibers

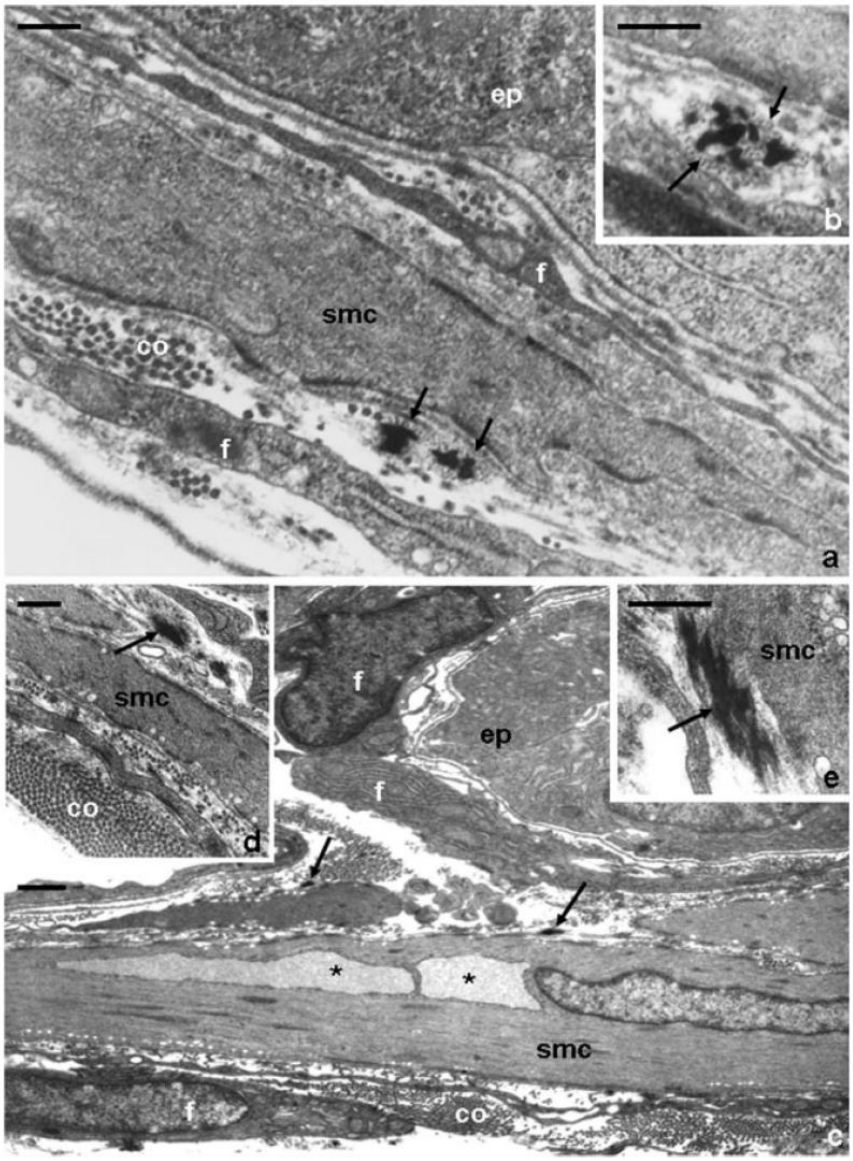

Fig. 3. Transmission electron microscopy of the control (**a** and **b**) and doxazosin-treated ventral prostate (**c**, **d**, and **e**): (a) ventral prostate stroma from control animals presents a thin layer of fibroblasts (f) and smooth muscle cells (smc) that exhibits few synthesis-related organelles. Collagen fibrils (co) are sparsely distributed between cells and elaunin fibers (arrows) are rare. b: Detail of an elaunin fiber, with groups of microfibrils (arrows) associated with an irregular elastin deposition. c, d, e: Doxazosin-treated ventral prostate stroma shows active smooth muscle cells and fibroblasts with visible rough endoplasmatic reticulum cisterns (asterisk). Gross bundles of collagen fibrils (co) and thickened elaunin fibers (arrows) can be observed among stromal cells. Epithelium (ep). Bars = 1 μm.

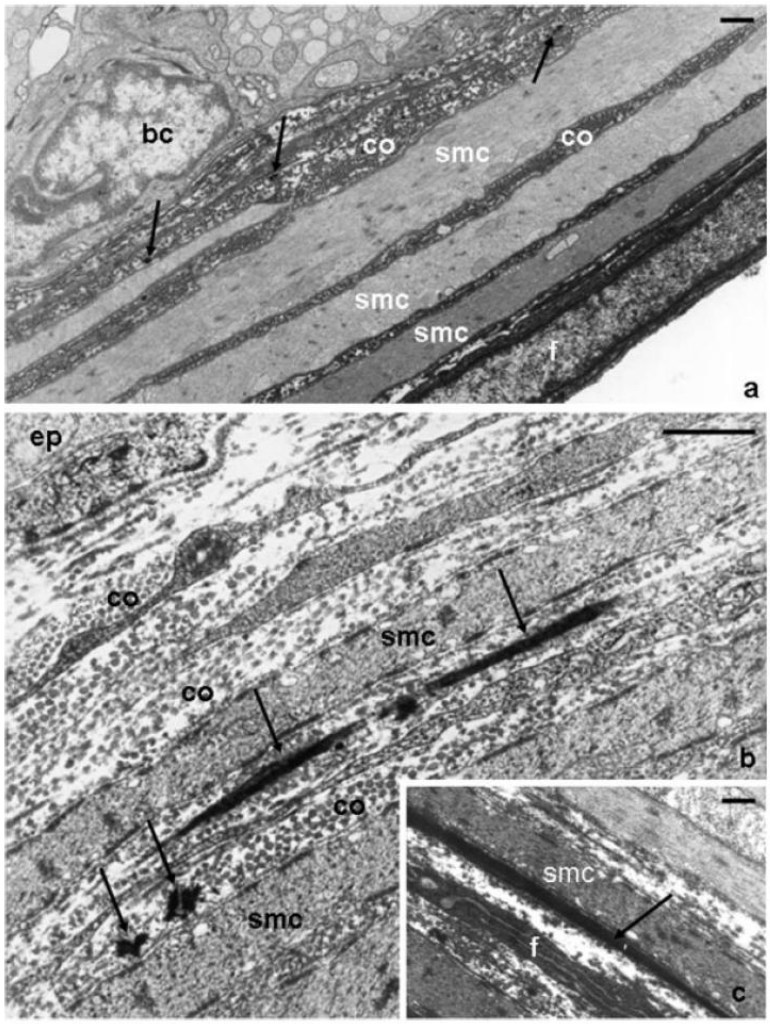

Fig. 4. Transmission electron microscopy of the control (**a**) and doxazosin-treated (**b** and **c**) dorsal prostate: (a) the stroma of control dorsal prostate presents a dense and compact layer of smooth muscle cells (smc) intermingled with thin bundles of collagen fibrils (co) and thin elaunin fibers (arrows). b, c: After doxazosin treatment, the smooth muscle cell layer appears less compact, whereas an increased amount of collagen fibrils (co) and thickened elaunin fibers (arrows) can be observed among these cells. Some fibroblasts (f) show enlarged rough endoplasmatic reticulum cisterns. Epithelium (ep); basal cell (bc). Bars = 1 μm.

(Fig. 5a). After Dox treatment, the distribution of collagen fibril bundles and elaunin fibers increased among stromal cells (Figs. 5b–5d).

The DOX-treated prostates exhibited smooth muscle cells and fibroblasts with active protein synthesis organelles, such as visible rough endoplasmic reticulum cisterns and well-developed Golgi apparatus cisterns (Figs. 3c, 4c, 5b, and 6a–6e).

DISCUSSION

In addition to androgen regulation, normal prostate physiology is maintained by a complex mechanism of epithelium-stroma crosstalk. Changes in the prostate stroma composition can alter epithelial homeostasis, leading to glandular dysfunction with possible emergence of diseases (Chung, 1995; Chung and Davies,

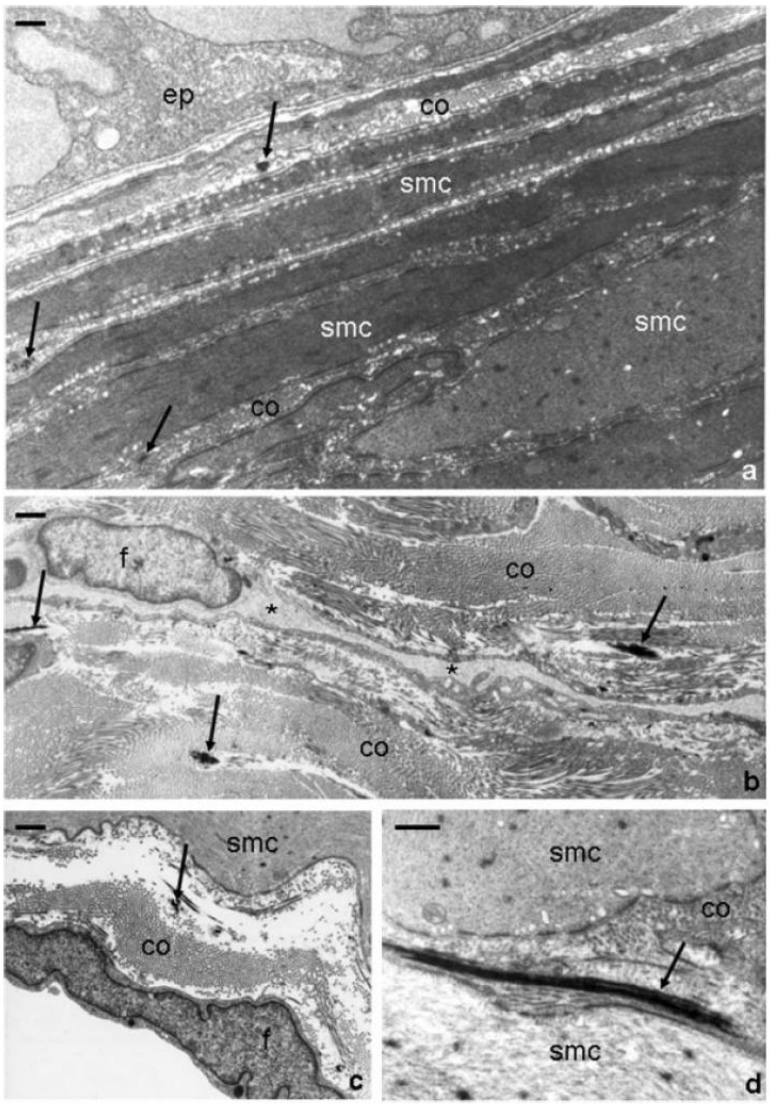

Fig. 5. Transmission electron microscopy of the control (**a**) and doxazosin-treated (**b**, **c**, and **d**) anterior prostate: (a) the stroma of control anterior prostate presents a thick and compact layer of smooth muscle cells (smc) intermingled with thin bundles of collagen fibrils (co) and dispersed thin elaunin fibers (arrows). b, c, d: Dox treatment promoted an increase in the quantity of collagen fibrils bundles (co) and elaunin fibers (arrows). Some fibroblasts (f) show enlarged rough endoplasmatic reticulum cisterns (asterisks). Epithelium (ep). Bars = 1 μm.

1996; Cunha et al., 2004; Wong and Tam, 2002). For example, the localized proliferation of the fibromuscular stroma is accepted to be the first step in BPH development (Pradhan and Chandra, 1975). Furthermore, alterations in the extracellular matrix components—collagen, elastic system fibers, and glycosaminoglycans—have also been observed in BPH (Cardoso et al., 2000; Chagas et al., 2002; Costa et al., 2004; Taboga and Vidal, 2003). However, little attention has been given to the effects of the drugs currently used in BPH treatment on prostate stromal cells and extracellular matrix.

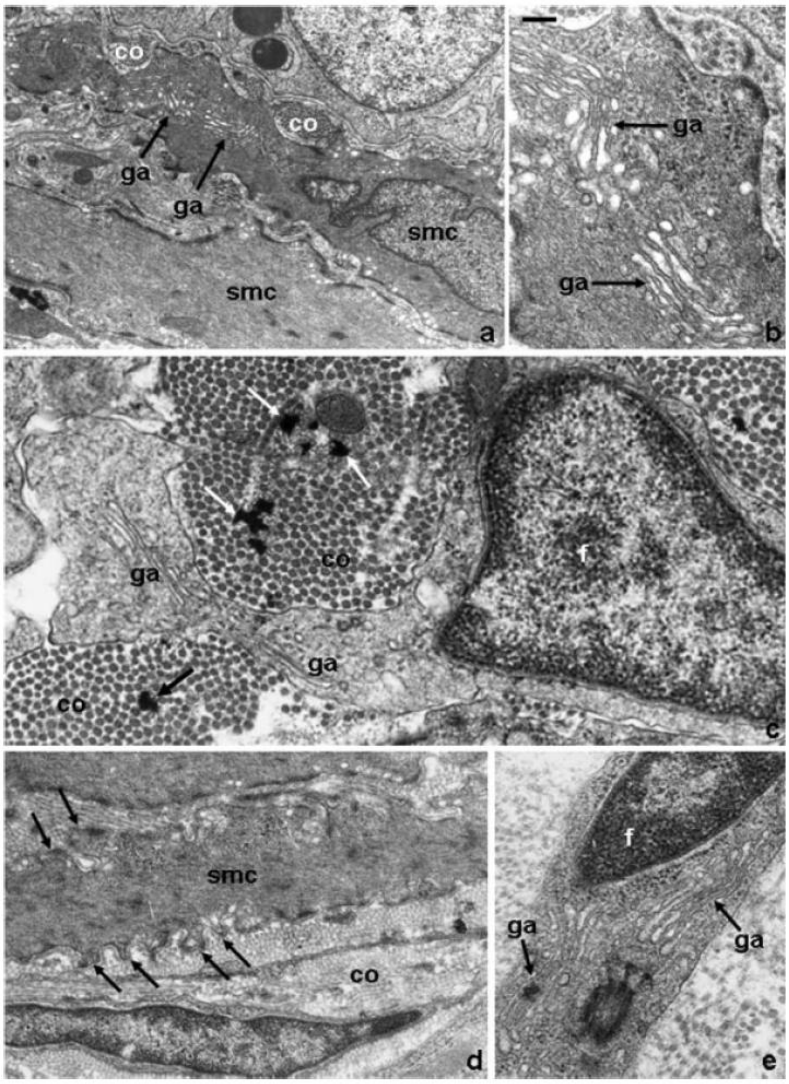

Fig. 6. Transmission electron microscopy of doxazosin-treated prostatic lobes. **a:** Ventral lobe showing smooth muscle cells (smc) with irregular outline associated with bundles of collagen fibrils (co) and well-developed Golgi aparatus (ga). **b:** Detail of (a) showing the Golgi aparatus cysterns and vesicles (ga). **c:** Dorsal lobe showing fibroblast (f) with loose chromatin and evident Golgi apparatus (ga). Note several elaunin fibers (arrows) intermingled with bundles of collagen fibrils (co). **d:** Anterior lobe showing smooth muscle cells with irregular outline (arrows) and associated with bundles of collagen fibrils (co). **e:** Anterior lobe showing a fibroblast (f) with well-developed Golgi apparatus (ga). Bars = 1 μm.

Changes in the prostate extracellular matrix induced by α-1 blockade were recently described. Terazosin treatment for 12 months altered glycosaminoglycan content and the activity of MMP-2, an enzyme involved in the degradation of extracellular matrix components, such as basement membrane, in the rat VP (Mitropoulos et al., 2007).

A previous work by our group demonstrated that DOX treatment increases the collagen fiber volume fraction in the stroma of rat prostatic complex, with a major enlargement of the anterior lobe and smaller augmentations of the ventral and dorsolateral lobes (Justulin et al., 2008). Recently, this effect was also observed in human prostates by Imamura et al. (2009).

In this study, we evaluated, histochemically and ultrastructurally, the changes in the prostate stroma induced by DOX treatment, with special attention to the content and distribution of elastic system fibers. Our results show that 30 days of DOX treatment elevated both the quantity and thickness of elastic system fibers in the three rat prostatic lobes, mainly in the VP. The VP also exhibited the highest values of elastic system volume fraction in both control and treated groups. This aspect may be related with the glandular structural differences found between the prostatic lobes, such as the number of smooth muscle cells layers around the tubules. The anterior lobe presents the thickest layer of smooth muscle cells, followed by DP and VPs (Roy-Burman et al., 2004). In this sense, as the muscular tonus of VP is maintained by a reduced number of smooth muscle cells, this lobe appears to be more affected by the α-adrenergic blockade requiring more intense stromal remodeling and elastic fiber system deposition.

The mechanism responsible for the increased deposition of elastic system fibers during DOX treatment remains to be determined. However, many studies have demonstrated that the apoptotic effect of DOX on prostate cells is mediated through the upregulation of TGF β-1 (Anglin et al., 2002; Glassman et al., 2001; Ilio et al., 2001; Justulin et al., in press; Kyprianou, 2003; Partin et al., 2003). Because TGF β-1 is known as a growth factor that augments the deposition of extracellular matrix proteins (Roberts et al., 1990) including elastin (Davidson et al., 1993; Kothapalli et al., 2009; Shanley et al., 1997), it is possible that this factor participates in the increase of elastic system fiber content observed in DOX-treated prostatic lobes.

Moreover, our ultrastructural analysis reveals that stromal cells from DOX-treated prostate exhibited a more secretory phenotype. This observation corroborates the study by Smith et al. (1999) who, using culture of prostatic smooth muscle cells, found that contractility of smooth muscle cells decreased following DOX treatment. These authors also showed that DOX treatment reduced the expression of actin and myosin proteins, suggesting that α1-blockers induce dedifferentiation of smooth muscle into fibroblasts and myofibroblasts.

Together, these observations suggest that smooth muscle cell relaxation induced by DOX promotes changes in the prostatic tissue biomechanical dynamic. The newly established tissue homeostasis, without the muscular tonus, may require stromal remodeling and reinforcement with consequent increase in deposition of collagen and elastic fibers by fibroblasts and smooth muscle cells.

In conclusion, this work demonstrated that stromal cells and elastic system fibers undergo modifications following DOX treatment and may contribute additional data on the effect of this drug during α-adrenergic blockade therapy.

ACKNOWLEDGMENTS

The authors thank the Electron Microscopy Center (Institute of Biosciences, UNESP, Botucatu) for the transmission electron microscopy protocol procedures and for the use of Phillips electron microscopy. This paper is part of the thesis presented by F.K.D. to the Institute of Biology, UNICAMP, in partial fulfillment of the requirement for her PhD degree. James Welsh's English language revision of this paper is acknowledged.

REFERENCES

Anglin IE, Glassman DT, Kyprianou N. 2002. Induction of prostate apoptosis by α1-adrenoceptor antagonists: Mechanistic significance of the quinazoline component. Prostate Cancer Prostatic Dis 5:88–95.

Antonioli E, Della-Colleta HH, Carvalho HF. 2004. Smooth muscle cell behavior in the ventral prostate of castrated rats. J Androl 25:50–56.

Antonioli E, Cardoso AB, Carvalho HF. 2007. Effects of long-term castration on the smooth muscle cell phenotype of the rat ventral prostate. J Androl 28:777–783.

Cardoso LEM, Costa WS, Sampaio FJ. 2000. Stromal modifications in benign prostatic hyperplasia as evidenced by glycosaminoglycan composition. Int Braz J Urol 26:630–634.

Carvalho HF, Vilamaior PSL, Taboga SR. 1997. Elastic system of the rat ventral prostate and its modifications following orchiectomy. Prostate 32:27–34.

Chagas MA, Babinski MA, Costa WS, Sampaio FJ. 2002. Stromal and acinar components of the transition zone in normal and hyperplastic human prostate. BJU Int 89:699–702.

Chiang CF, Son EL, Wu GJ. 2005. Oral treatment of the TRAMP mice with doxazosin suppresses prostate tumor growth and metastasis. Prostate 64:408–418.

Chung LW. 1995. The role of stromal-epithelial interaction in normal and malignant growth. Cancer Surv 23:33–42.

Chung LW, Davies R. 1996. Prostate epithelial differentiation is dictated by its surrounding stroma. Mol Biol Rep 23:13–19.

Corradi LS, Goes RM, Carvalho HF, Taboga SR. 2004. Inhibition of 5-α reductase activity induces stromal remodeling and smooth muscle cell de-differentiation in adult gerbil ventral prostate. Differentiation 72:198–208.

Cotta-Pereira G, Rodrigo FG, David-Ferreira JF. 1976. The use of tannic acid-glutaraldehyde in the study of elastic and elastic related fibers. Stain Technol 51:7–11.

Costa WS, de Carvalho AM, Babinski MA, Chagas MA, Sampaio FJ. 2004. Volumetric density of elastic and reticular fibers in transition zone of controls and patients with benign prostatic hyperplasia. Urology 64:693–697.

Crawford ED. 2009. Understanding the epidemiology, natural history, and key pathways involved in prostate cancer. Urology 73:4–10.

Cunha GR, Ricke W, Thomson A, Marker PC, Risbridger G, Hayward SW, Wang YZ, Donjacour AA, Kurita T. 2004. Hormonal, cellular, and molecular regulation of normal and neoplastic prostatic development. J Steroid Biochem Mol Biol 92:221–236.

Davidson JM, Zoia O, Liu JM. 1993. Modulation of transforming growth factor-β1 stimulated elastin and collagen production and proliferation in porcine vascular smooth muscle cells and skin fibroblasts by basic fibroblast growth factor, transforming growth factor-α, and insulin-like growth factor-I. J Cell Physiol 155:149–156.

Glassman DT, Chon JK, Borkowski A, Jacobs SC, Kyprianou N. 2001. Combined effect of terazosin and finasteride on apoptosis, cell proliferation, and transforming growth factor-β expression in benign prostatic hyperplasia. Prostate 46:45–51.

Imamura T, Ishii K, Kanda H, Arase S, Yoshio Y, Hori Y, Soga N, Kise H, Arima K, Sugimura Y. Structural changes in α1-adrenoceptor antagonist-treated human prostatic stroma. Clin Exp Med, in press.

Ilio KY, Park II, Pins MR, Kozlowski JM, Lee C. 2001. Apoptotic activity of doxazosin on prostate stroma in vitro is mediated through an autocrine expression of TGF-β1. Prostate 48:131–135.

Justulin LA Jr., Delella FK, Felisbino SL. 2008. Doxazosin reduces cell proliferation and increases collagen fibers in rat prostatic lobes. Cell Tissue Res 332:171–183.

Justulin LA Jr., Acquaro C, Carvalho RF, Silva MD, Felisbino SL. Combined effect of the finasteride and doxazosin on rat ventral prostate morphology and physiology. Int J Androl, in press.

Kirby RS. 1996. Doxazosin in treatment of the lower urinary tract. In: Kirby RS, McConnel JD, Fitzpatrick JM, Roeherborn CG, Boyle P, editors. Textbook of benign prostatic hyperplasia. Oxford: ISIS Medical Media. pp.287–293.

Kothapalli CR, Taylor PM, Smolenski RT, Yacoub MH, Ramamurthi A. 2009. Transforming growth factor β1 and hyaluronan oligomers

synergistically enhance elastin matrix regeneration by vascular smooth muscle cells. Tissue Eng A 15:501–511.
Kyprianou N. 2003. Doxazosin and terazosin suppress prostate growth by inducing apoptosis: Clinical significance. J Urol 169:1520–1525.
Kyprianou N, Jacobs SC. 2000. Induction of apoptosis in the prostate by α1-adrenoceptor antagonists: A novel effect of "old" drugs. Curr Urol Rep 1:89–96.
Kyprianou N, Litvak JP, Borkowski A, Alexander R, Jacobs SC. 1998. Induction of prostate apoptosis by doxazosin in benign prostatic hyperplasia. J Urol 159:1810–1815.
Lacey JP, Donatucci CF, Price DT, Page SO, Bennett SAL, Tenniswood MP, Schwinn DA. 1996. Effects of androcen deprivation on prostate α1-adrenergic receptors. Urology 48:335–341.
Mitropoulos D, Papakonstantinou E, Aletras AJ, Kalinderis N, Zervas A, Hatzichristou D, Karakiulakis G. 2007. Terazosin modifies the content of glycosaminoglycans and the activity of matrix metalloproteinase 2 in the rat ventral prostate. Eur Urol 51:447–456.
Nemeth HA, Lee C. 1996. Prostatic ductal system in rats: Regional variation in stromal organization. Prostate 28:124–128.
Partin JV, Anglin IE, Kyprianou N. 2003. Quinazoline-based α1-adrenoceptor antagonists induce prostate cancer cell apoptosis via TGF-β signalling and IκBα induction. Br J Cancer 88:1615–1621.
Pradhan BK, Chandra K. 1975. Morphogenesis of nodular hyperplasia prostate. J Urol 113:210–213.
Rittmaster RS. 2008. 5α-Reductase inhibitors in benign prostatic hyperplasia and prostate cancer risk reduction. Best Pract Res Clin Endocrinol Metab 22:389–402.
Roberts AB, Heine UI, Flanders KC, Sporn MB. 1990. Transforming growth factor-β. Major role in regulation of extracellular matrix. Ann NY Acad Sci 580:225–232.
Roy-Burman P, Wu H, Powell WC, Hagenkord J, Cohen MB. 2004. Genetically defined mouse models that mimic natural aspects of human prostate cancer development. Endocrinol Relat Cancer 11:225–254.
Shanley CJ, Gharaee-Kermani M, Sarkar R, Welling TH, Kriegel A, Ford JW, Stanley JC, Phan SH. 1997. Transforming growth factor-β 1 increases lysyl oxidase enzyme activity and mRNA in rat aortic smooth muscle cells. J Vasc Surg 25:446–452.
Shapiro E, Becich MJ, Hartanto V. 1992. The relative proportion of stromal and epithelial hyperplasia is related to the development of symptomatic benign prostatic hyperplasia. J Urol 147:1293–1297.
Smith P, Rhodes NP, Ke Y, Foster CS. 1999. Influence of the α1-adrenergic antagonist, doxazosin, on noradrenalin-induced modulation of cytoskeletal proteins in cultured hyperplastic prostatic stromal cells. Prostate 38:216–227.
Sugimoto K, Matsumoto S, Uemura H, Ito H. 2008. Distribution of elastic fiber on prostate. Hinyokika Kiyo 54:321–324.
Taboga SR, Vidal BC. 2003. Collagen fibers in human prostatic lesions: Histochemistry and anisotropies. J Submicrosc Cytol Pathol 35:11–16.
Thomson AA, Cunha GR, Marker PC. 2008. Prostate development and pathogenesis. Differentiation 76:559–564.
Vilamaior PS, Felisbino SL, Taboga SR, Carvalho HF. 2000. Collagen fiber reorganization in the rat ventral prostate following androgen deprivation: A possible role for smooth muscle cells. Prostate 45:253–258.
Vilamaior PS, Taboga SR, Carvalho HF. 2005. Modulation of smooth muscle cell function: Morphological evidence for a contractile to synthetic transition in the rat ventral prostate after castration. Cell Biol Int 29:809–816.
Weibel ER, Kistler GS, Scherle WF. 1966. Practical stereological methods for morphometric cytology. J Cell Biol 30:23–38.
Wong YC, Tam NNC. 2002. Dedifferentiation of stromal smooth muscle as a factor in prostate carcinogenesis. Differentiation 60:633–639.
Yang G, Timme TL, Park SH, Wu X, Wyllie MG, Thompson TC. 1997. Transforming growth factor β1 transduced mouse prostate reconstitutions. II. Induction of apoptosis by doxazosin. Prostate 33:157–163.
Yono M, Yamamoto Y, Yoshida M, Ueda S, Latifpour J. 2007. Effects of doxazosin on blood flow and mRNA expression of nitric oxide synthase in the spontaneously hypertensive rat genitourinary tract. Life Sci 81:218–222.

Capítulo 2:

FINASTERIDE EFFETCS ON TYPE I COLLAGEN, TYPE III COLLAGEN AND TGF-BETA 1 EXPRESSION IN THE RAT VENTRAL PROSTATE

Flávia Karina Delella[1,2], Fernanda Losi Alves de Almeida[1,2], Carolina Sarobo[2], Maeli Dal Pai Silva[2], Hernandes Faustino de Carvalho[1,3] and Sérgio Luis Felisbino[2]

[1]*Department of Cell Biology, Institute of Biology –University of Campinas (UNICAMP), Campinas, Sao Paulo, Brazil*

[2]*Department of Morphology, Institute of Biosciences – Sao Paulo State University (UNESP), Botucatu, Sao Paulo, Brazil*

[3]*National Institute of Photonics Applied to Cell Biology (INFABIC), State University of Campinas (UNICAMP), Campinas, Sao Paulo, Brazil*

Running title: Finasteride alters prostate collagen and TGF-Beta 1 expression

Key Words: finasteride, prostate, collagen, TGF-Beta 1, transmission electron microscopy, real time-PCR.

Grant Sponsor: FAPESP, Grant Numbers: 06/60114-6, 06/60115-2; CAPES do Brasil.

Correspondence to: Dr. Sérgio L. Felisbino, Department of Morphology, Institute of Biosciences, Sao Paulo State University 18618-000, Botucatu, SP, Brazil.

Telephone/fax: +55 0XX 14 3811 6264

E-mail: felisbin@ibb.unesp.br

ABSTRACT

BACKGROUND. Androgens and stromal-epithelial cell interactions are key regulators of prostate morphogenesis, growth and maintenance. These interactions are mediated by structural extracellular matrix components and also by a variety of paracrine factors secreted by stromal cells.

MATERIALS AND METHODS. Herein, we investigated the effects of the finasteride on type I and type III collagen and TGF Beta-1 gene expression by real-time PCR and protein content by immunohistochemical and western blotting of the rat ventral prostate, as well glandular morphological changes by transmission electron microscopy. Alpha actin was located by immunohistochemistry. Intact adult Wistar rats (n=15) and adult Wistar rats (n=15) treated with finasteride by subcutaneous injection (25mg/kg/day) during 7 and 30 days were killed by pentobarbital overdose.

RESULTS. Finasteride altered the epithelial and the stromal compartments and components. Apoptotic cells were mainly found at 30 day of the treatment in the epithelial cells and the epithelial basal membrane presented irregular folds at both periods of treatment. The collagen fibers were rearranged after the stromal volume gain, however COL1A1 and COL3A1 mRNA expression were decreased after 7 and 30 days of treatment. TGF Beta-1 mRNA expression and protein content were increased at both periods of treatment. The smooth muscle cells showed atrophic and had the basal membrane spined.

CONCLUSIONS. Our results suggest that finasteride-induced stromal changes involves type I and type III collagen remodeling without *de novo* synthesis and TGF Beta-1 mRNA and protein increase may be related with cell death pathway.

INTRODUCTION

Androgens are essential for prostatic development, growth and function (Cunha et al. 1987). The prostate androgen metabolism is regulated by a variety of androgen metabolism enzymes, like 5-α reductase that converts testosterone (T) into the most potent androgen dihidrotestosterone (DHT) (George and Wilson, 1994). Compared with DHT, T is less potent in activating androgen receptors (ARs) and maintaining the normal activity of epithelial cells (Li and Kim, 2009). However, later in life, these same hormones have a significant role in the development of prostatic diseases like benign prostate hyperplasia (BPH) and prostate cancer (PCa) (Tindall & Rittmaster, 2008).

Finasteride (Fin) is a 4-azasteroid testosterone analogue and inhibitor of 5-α reductase type 2 that use reduces DHT levels, increases T levels and diminishes prostatic size in men and in rodents (Stoner, 1992; Prahalada et al. 1994). This drug is used alone or in combination with other medications to treat benign prostatic hyperplasia (BPH), improving symptoms of prostate enlargement (Jimenez et al. 2003). It has been hypothesized that reducing the conversion of T to DHT in the prostate by the use of a 5alpha-reductase inhibitor, such as Fin, has the ability to reduce the incidence of biopsy-detectable prostate cancer in the Prostate Cancer Prevention Trial (PCPT) (Reddy, 2004; Canby-Hagino et al. 2006; Rittmaster, 2008).

The known effects of Fin in the prostate include reduction of the gland weight, glandular area size, epithelial cells height and the synthetic and proliferative cells activities (Prahalada et al. 1994; Lobaccaro et al. 1996; Huynh 2002). These effects are, in minor proportion, similar those obtained by androgen ablation by surgical castration (Vilamaior et al. 2000). Fin also increases the apoptotic index of rat epithelial prostatic cells (Rittmaster et al. 1995; Prahalada et al. 1998; Huynh 2002) and this process is closely associated with the downregulation of Bcl-2 and Bcl-x_L proteins (Huynh 2002). The changes of parenchyma components are less investigated and are followed by a major stromal remodeling, with changes in smooth muscle cells morphology and collagen fibers rearrangement (Corradi et al. 2004).

According to Corradi et al. (2004; 2009) Fin treatment promotes a denser layer accumulation of collagen surrounding the acini and this alteration are probably result of an

imbalance of the homeostatic interaction between the epithelium and the underlying stroma. Mariotti and Mawhinney (1981) analyzing the hormonal control of the seminal vesicle fibromuscular stroma concluded that castration of adult animals reduced 40% of the collagen below the epithelium, indicating that castration caused a much great decline in collagen synthesis. Analyzing the effects of androgen replacement on collagen synthesis, Thornton et al. (1985) administrated exogenous DHT for adult rats after two weeks of surgical castration that provided a significant increase of collagen content in the ventral prostate, such as also increased the DNA content and the prostate wet weight, concluding that collagenous components seem to be important in supporting the normal androgen-dependent proliferation and differentiation of prostatic epithelial cells.

The prostatic homeostasis is maintained by androgens that regulate the secretion of several growth factors, including epidermal growth factor (EGF), basic fibroblast growth factor (bFGF), insulin-like growth factor (IGF), and transforming growth factor β1 (TGF-β1) (Djakiew, 2000). Castration increases the prostatic levels of TGF- β 1 mRNAs, which return to normal after androgen replacement (Kyprianou & Isaacs, 1989). Glassman et al. (2001) observed higher level of TGF- β1 expression in the prostates of BPH patients on terazosin and finasteride combination therapy than with either terazosin or finasteride alone, but no data are related with the expression of TGF- β1 in rat prostate after finasteride treatment.

Even though some authors reported the collagen alterations in the prostatic stroma after androgen ablation, no information are known about collagen gene expression evaluation after Fin administration. Thus, in this work we investigated the effect of Fin on ventral rat prostatic lobe, with special attention to the type I collagen, type III collagen, TGF Beta-1, stromal cells and extracellular matrix remodeling.

MATERIALS AND METHODS

Animals and Finasteride Administration

Adult male 3-months-old Wistar rats were maintained in a controlled environment with free access to food and water. The experiment was performed according to the Guide for Care and Use of Laboratory Animals. The animals were divided into two groups: control rats (CT) and the finasteride-treated group (Fin). Fin animals received daily doses of finasteride (25 mg/kg of body weight) (Finasteride, Merck, Galena Pharmaceutical and Chemistry, SP, Brazil) dissolved in corn oil as vehicle, subcutaneously injected. Finasteride dosage and route of administration were chosen based on a previously published work of George (1997). CT animals received only the vehicle subcutaneously injected. After 7 and 30 days of the finasteride treatment, 15 animals from each group were killed by an overdose of pentobarbital. The ventral prostates (VP) were excised, immediately weighed and alternate lobes were left and right assigned and snap frozen or immersed in fixative.

Hormone assay

Blood samples from each animal were collected at the time of death. Plasma testosterone (T) and dihydrotestosterone (DHT) concentrations were determined using automatic equipment (VITROS ECi-Johnson and Johnson Ultra-Sensitive Chemiluminescence analysis, Johnson & Johnson Family of Companies, Langhorne, PA, USA). The sensitivity of this assay was 0.02 and 0.04 ng/mL for T and DHT respectively. The intra- and inter-assay variations for T assay were 5.36% and 5.10% and for DHT were 6.78% and 7.55% respectively.

Morphometric Analysis

The mean glandular and stromal area were performed in Hematoxylin/Eosin (H&E) sections and were analysed in a Leica DMLB 80 microscope connected to a Leica DC300FX camera and the digitalized images, using image analyzer Leica Q-win software Version 3 (Leica, Heidelberg, Germany) for WindowsTM, were used for morphometric analysis. The mean glandular and stromal area was determined in a total of 500 random

interactive measures at objective of 40X at 10 different points of 10 different fields from five different individual VP sections. All the measurements were made in the intermediate regions of the VP tubuloalveolar structure, which represent the major portions of the prostatic lobe.

Fin effects on collagen fibers area were measured using 10 automatic measures of 5 different animals (automatic detection of the red color by the software) in Picrossirius sections, coming down to 50 measures by experimental group.

Transmission Electron Microscopy

Tissue fragments of five animals from each experimental group were immersed in 2.5% glutaraldehyde, plus 0.25% tannic acid solution in Millonig's buffer for 2 h (Cotta-Pereira et al., 1976), washed, and post fixed in 1% osmium tetroxide in the same buffer for 1 h, washed again, dehydrated in graded acetone, and embedded in Araldite. Semithin sections were stained with Toluidin Blue and analyzed under light microscopy. Ultrathin silver sections were obtained with a diamond knife and contrasted with 2% alcoholic uranyl acetate and then with 2% lead citrate in 1 N sodium hydroxide solution for 10 min. Grids were examined under a Phillips transmission electron microscope, operating at 80 kV.

Immunohistochemistry

VP frozen sections (7 µm) fixed in cold methanol or VP Paraplast sections (5 µm) fixed in 4% paraformaldehyde dissolved in phosphate-buffered saline (PBS) for 24 hours, were collected in silanized glass slides, blocked first with 3% hydrogen peroxide in methanol for 15 minutes (to block endogenous peroxidase activity) and then blocked with 3% bovine serum albumin (BSA) in PBS for 1 hour at room temperature. Then, the sections were incubated with the primary monoclonal antibodies during 2 hours at room temperature: **Type I Collagen**, 1:300, Genetex, GTX 26308; **Type III Collagen**, 1:300, Abcam, ab 6310-100; **TGF-Beta 1**, 1:100, Santa Cruz, sc-146; **Alpha Actin**, 1:300, Santa Cruz, sc-32251. The primary antibody was detected using a secondary peroxidase-conjugated antibody (Santa Cruz Biotechnology, Santa Cruz, CA, USA), except TGF-Beta 1 that was detected using Mach 4 Universal HRP-Polymer Kit with DAB (Biocare Medical,

Concord, CA, USA). Chromogen color development was accomplished with 3.3'-diaminobenzidine tetrahydrochloride (Sigma, USA). Slides were counterstained with Harris's haematoxylin. The negative control was performed by abolishing the primary antibody incubation step.

Western blotting analysis for TGF-Beta 1

VP frozen samples of five different adult rat prostatic lobes from the control group and from days 7 and 30 of Fin treatment were mechanically homogenized in 50 mM TRIS-HCl buffer pH 7.5, 0.25% Triton X-100 plus EDTA by means of a Polytron for 30 s at 4°C. Following centrifugation of the homogenate, the protein was extracted from the supernatant and quantified as described by Bradford (1976). Protein samples (each 75 μg) were loaded onto 12% SDS-polyacrylamide gels for SDS-polyacrylamide gel electrophoresis under reducing conditions. After electrophoresis, the proteins were transblotted onto a nitrocellulose membrane (Sigma). The blot was blocked with 5% bovine serum albumin (BSA) in TBST (10 mM TRIS-HCl pH 7.5, 150 mM NaCl, 0.1% Tween-20) for 1 hour, incubated overnight at 4°C with 3% BSA in TBST containing a 1:1,000 dilution of the anti-Transforming growth factor beta 1 (TGF- Beta 1; MAB240; R&D Systems, Minneapolis, USA) or anti-β-actin (Actin; sc-1615; Santa Cruz Biotechnology, Santa Cruz, CA, USA) primary antibodies, washed (5× 5 minutes) in TBST, and incubated for 1 hour at room temperature with peroxidase-conjugated antibody, followed by five washes of 5 minutes in TBST. Antibody complexes were detected by means of chemiluminescence (Pierce® ECL Western Blotting Substrate). TGF- Beta 1 and β-actin protein expression was quantified by densitometric analysis of the bands as integrated optical density (IOD). The TGF- Beta 1 expression was normalized to the β-actin values. Normalized data are expressed as means±SD.

Second Harmonic Generation

The Second Harmonic Generation (SHG) was identified using an Olympus confocal system (IX-81 inverted microscope, the FV300 scan head, the FV-5 COMB2 laser combiner, and two Hamamatsu model 3896 PMTs). SHG was examined by excitation with

a Ti: Sapphire laser (Tsunami, Spectra Physics) at 800 nm and 800 MHz repetition rate, coupled to the scan head by and external port, and collected by the condenser in the forward direction with a bandpass filter at 400 nm (Oriel Corporation, Stanford, CT) and a blue shortpass filter to reject any fluorescence signal. The Fluoview software was used to reconstruct the images.

Type I Collagen, Type III Collagen and TGF-Beta 1 mRNA expression

Total RNA was isolated from VP samples using TRIzol Reagent (Invitrogen Life Technologies, Carlsbad, CA, USA), according to the manufacturer's protocol. Purified total RNA were reverse transcribed with random hexamer primers and a High-Capacity cDNA Archive Kit (Applied Biosystems). Collagen I, Collagen III and TGF-Beta 1 (Table 1) gene expression levels from each treatment were detected by quantitative real-time reverse transcription polymerase Chain Reaction (RT-qPCR) using an ABI 7300 Real Time PCR System (Applied Biosystems, Foster City, CA, USA). A sample without cDNA template (NTC) was used to verify that the master mix was free from contaminants. Real-time conditions were: 10 minutes at 95ºC, 40 cycles of denaturation at 95ºC for 15seconds, and annealing/extension at 60ºC for 1 minute. The Beta Actin RNA gene was used as a reference to normalize quantification of mRNA targets.

Table 1. GenBank accession numbers and primers used for Real-Time RT-PCR amplification analysis.

Gene	GenBank accession no.	Sequence (5'-3')
COL1A1	NM_053304.1	Forward TCT GAC TGG AAG AGC GGA GAG T Reverse ACA CGA GTC TGA CCT GTC TCC AT
COL3A1	M21354	Forward CGC AAT TGC AGA GAC CTG AA Reverse AAC CCA GTA TTC TCC GCT CTT G
TGF-Beta 1	NM_021578	Forward GAG GTG ACC TGG GCA CCA T Reverse GGC CAT GAG GAG CAG GAA
Beta Actin	NM_031144.2	Forward TCA GGT CAT CAC TAT CGG CAA TG Reverse TTT CAT GGA TGC CAC AGG ATT C

RT-qPCRs for target and reference genes were run in the same RT reaction using two replicates of each sample and reference gene. An amplification plot graphically

displayed the fluorescence detected over the number of cycles that were performed. Standard curves for both target genes and reference gene were obtained by using seven serial dilutions (1:10) of sample cDNA. Using the $2^{-\Delta\Delta Ct}$ method, data were recorded as the fold-change in gene expression normalized by the reference gene and relative to the calibrator sample (Livak and Schmittgen 2001). All samples then were normalized to the ΔCt value of a calibrator sample to obtain a ΔΔCt value (ΔCttarget – Δctcalibrator). Dissociation-melting curves confirmed the specific amplification of the cDNA target and the absence of nonspecific products.

Statistical analysis

One-way analysis of variance (anova) was performed to determine whether differences existed among all groups ($p < 0.05$), and then the Tukey–Kramer post-test was employed to determine the significance of the differences. A p-value of <0.05 was considered significant. The statistical tests were performed on Instat (version 3.0; Graph-Pad, Inc., San Diego, CA, USA).

RESULTS

VP Morphology and Morphometry-Stereology Analysis after Fin Treatment

Both periods of time of Fin treatment significantly increased the T plasma levels ($p<0.05$) and decreased the DHT plasma levels ($p < 0.05$) (Table 2). Fin also induced a significant and progressive reduction in the prostate absolute weight, with ~63 % at day 7 and ~54% at day 30 of treatment, and in the VP glandular area ($p<0.01$), compared with the control values (Table 2).

Control VP presented high columnar epithelial cells with countless polymorphics secretory vesicles, Golgi apparatus and rough endoplasmatic reticulum very developed, evidencing active secretory activity (Fig. 2a, b). The secretory epithelial cells exhibited predominantly basal nucleus occupying a large cytoplasmatic portion, composed by loose chromatin and evident nucleoli (Fig. 2a). A great amount of microvillous was found in the epithelial apical portion (Fig. 2b). The subepithelial stroma was composed by an organized

arrangement of stromal cells (smooth muscle cells and fibroblasts) wrapped up by thin elaunin fibers and bundles of collagen fibers. Collagen fibers were also distributed adjacent to the basal membrane (Fig. 2c, d). The smooth muscle cells showed regular basal membrane border, without irregular projections (Fig. 2c). These results are in agreement with the results found in the immunohistochemical reaction for alpha-actin (Fig. 4a, b), in which the smooth muscle cells showed large size and regular outline.

Fin altered VP morphology after both periods of treatment, but the alterations were preeminent at day-30. At day-7, the ultrastructure analysis showed reduction of the secretory epithelial cell height, decrease of secretory-related organelles amount and secretory vesicles number (Fig. 3a). The basal membrane lost that regular and straight phenotype found in the untreated VP and presented irregular shape and folds at day-7 (Fig. 3b) and at day-30 (Fig. 3c, d, e, f). Apoptotic cells were found in the VP epithelium treated (Fig. 3c), mainly at day-30 of treatment. Besides the epithelial components changes, the stromal components showed structural rearrangement. Collagen fibers were found combined in irregular bundles concentrated adjacent to the irregular course of the basal membrane and adjacent to basal lamina (Fig. 3b, d, e, f). The smooth muscle cells and the fibroblasts became retracted, with irregular border (Fig. 3b, c, d). As well the immunohistochemical reaction for alpha-actin showed smooth muscle cells presenting smaller diameter, with irregular outline (Fig. 4c, d), the ultrastructure confirmed these results and showed the basal membrane outline shaping numerous spine-like cytoplasmatic projections (Fig. 3b, c, d). Fibroblasts were found with a more activate phenotype, presenting loose chromatin and great amount of organelles synthesis-related (Fig. 3b, d). Furthermore, points of adhesion were frequently found between fibroblasts and the irregular course areas of the epithelial basal membrane (Fig. 3e).

Type I and Type III collagen analysis

The collagen evaluation were performed using morphometry-stereology analyze for collagen total area detection, immunohistochemical detection for the protein analysis and real time quantitative PCR for the mRNA analysis, mainly to verify if the 5-α reductase

inhibition promotes increase of the collagen synthesis or if occurs only a stromal fibers remodelment after the prostate regression.

Fin promoted an increase in the total area performed by collagen fibers ($p<0.01$) (Table 2). The Fig. 1 show VP sections stained with Picrossirius and used to measure the total collagen area, where collagen fibers were detected in red. Type I collagen became less dense in the interstitial stroma and accumulated below the glandular epithelium at day-7 (Fig. 5d), when compared with control VP (Fig. 5a). The distribution of type I collagen at day-30 (Fig. 5f) showed similar location to the VP control. Interestingly, collagen type I mRNA gene expression decreased after both periods of Fin treatment (Fig. 8).

In the normal VP, collagen type III were found distributed in the interstitial stroma and also found filling epithelial-infoldings and strongly involving blood vessels (Fig. 5c). The 5-α reductase inhibition caused apparent reduction in the collagen III content after 7 (Fig. 5e) and after 30 (Fig. 5g) days of treatment. Such as the collagen type I, the collagen type III mRNA gene expression also decreased at day-7 of treatment and kept the low level at day-30 (Fig. 8).

The total amount and density of collagen fibers in the stroma were also evaluated by the physic approach Second Harmonic Generation (SHG). Using hematoxylin and eosin stained sections, the eosin fluorescence was included in the images for allowing identification of the tissue structure, specially the epithelium. Collagen fibers appear highlight below epithelium and in the interstitial stroma. Control VP presented low collagen fibers concentration (Fig. 6a), otherwise the amount of collagen fibers increased progressively at day-7 (Fig. 6b) and at day-30 (Fig. 6c) in response to Fin treatment.

TGF-Beta 1 analysis

To evaluate the TGF-Beta 1 location, protein and mRNA quantification in the control VP and after Fin treatment, we used immunohistochemistry technique, western blotting and real time quantitative PCR, respectively. The immohistochemistry reaction for TGF-Beta 1 was weakly detected in the epithelium and in the stroma from the control group (Fig. 7a). After 7 days of Fin treatment, the TGF-Beta 1 immunostaining was also

found at both epithelial and stromal compartments, with a stronger reaction (Fig. 7b) than in control group. A similar pattern was observed at day-30 (Fig. 7c).

The figure 7d presents a representative Western Blotting for TGF-Beta 1 in the VP of control and Fin-treated animals. The densitometric quantification of the data (Fig. 7e) revealed an increase in the TGF-Beta 1 quantity ($p<0.05$), comparing the treated values with the control ones.

The results of the q-RT-PCR for TGF-Beta 1 are shown in Fig. 8. Fin treatment increased significantly TGF-Beta 1 mRNA expression after 30 days ($p<0.01$).Taken together, these results demonstrated that Fin treatment increased both TGF-Beta 1 mRNA and protein.

DISCUSSION

The 5-α reductase inhibition by Fin has been shown to induce involution of human and rat prostate through a reduction in ductal luminal fluid and apoptotic cell loss, resulting in prostate shrinkage (Prahalada et al., 1994; Rittmaster et al., 1995; Prahalada et al., 1998). Although many works have shown Fin effects on prostatic epithelial compartment, few data are known about the influence of this 5-α reductase inhibitor on the prostatic stromal fibers and stromal cells.

In a previous work our group demonstrated, by gelatin zymography, that Fin alters the stromal proteins matrix metalloproteinases (MMPs), increasing MMP-9 and reducing MMP-2 activities (Delella et al., 2009). These results directed us to analyze others finasteride influences in the prostate stroma. Thus, in the present study, we evaluated, using ultrastructural, biochemical and molecular approaches, Fin influence in the fibromuscular components, specifically on type I and type III collagen fibers, smooth muscle cells, fibroblasts and TGF-Beta 1.

The prostate gland has a fibromuscular stroma composed by smooth muscle cells, fibroblasts, collagen and elaunin fibers, which surround the glandular elements (Roy-Burman et al., 2004). It's known that reciprocal interactions between prostate stromal cells and prostate epithelial cells are central mechanisms of the prostate gland development and maintenance (Cunha et al., 1996). Thus, any alteration in the prostate stroma compartment

after prostate diseases treatment or chemoprevention should be evaluated. The results presented here suggest that Fin's effects on prostate stroma involve changes in the stromal cells organization and morphology, collagen fibers distribution, gene expression and content, besides alter the growth factor TGF-Beta 1.

It's well known the importance of adequate level of circulating androgen in the growth and maintenance of the prostate structural and functional integrity (Isaacs, 1984). Depletion of this androgen support results in drastic chemical and cellular changes in the gland (Lee, 1981). Here, we have demonstrated, by ultrastructural microscopy, an increase in the points of adhesion between fibroblast and epithelial basal membrane in the VP from rats treated with Fin at 25 mg/kg at day-30 of the treatment, compared with VP control. Prostatic regression promoted by Fin is less intense than that regression promoted by surgical castration, but the effects provoked are very similar (Vilamaior et al., 2000). In an anterior project our group described the same alterations in VP of Wistar rats after 21 days of castration (data submitted). In this manner, we believe that these alterations are related with the attempt to maintenance the glandular integrity by the stromal cells after prostatic shrinkage.

As far as we are aware, no previous study has investigated the effect of Fin in the stromal cells behavior of Wistar adult prostate. The smooth muscle cells and fibroblasts play important roles in producing a number of autocrine and paracrine factors that contribute to the epithelium cells functions and organ homeostasis (Müntzing, 1981; Izumiya and Nakada, 1997). Our results showed that Fin altered both fibroblast and SMC morphology. The treatment promoted major regression in the SMC that became minor and with the basal membrane irregular and sinuous, compared with SMC in control VP. On the other hand, fibroblasts showed synthesis-related stage, with voluminous nucleus, loose chromatin and innumerous synthesis-related organelles, like Golgi complex. These differential Fin effect can be explained by the differential presence of AR in the prostatic stromal cells. In a previous study, Prins et al. (1991) characterized the presence or absence of AR in the various cell populations within the intact adult rat prostate and showed that periacinar SMC stained strongly positive for AR, and this staining did not vary with the thickness of the muscle layer. The same study presented that the majority of stromal

fibroblasts were AR negative. So, in our study, the differential response of the stromal cells to the treatment can be due the drop of DHT levels promoted by Fin. In this manner, the stromal cells that are more androgen dependent, like SMC, withdraw, whereas fibroblasts, less androgen responsive, remained active.

Cellular and molecular evidences suggest that Fin is associated with atrophy and apoptosis in the prostate (Rittmaster et al., 1996; Sutton et al., 2006), similar effects to those saw after castration, but less dramatic. Our results show that Fin promoted apoptosis in VP epithelial cells, mainly at day 30 of the treatment, together with shrinkage of both glandular and stromal compartment. Golbano and co-workers (2008) showed that Fin treatment of the LNCaP hormone-dependent human prostate cancer cell line caused the loss of cell viability and accelerated apoptosis in a concentration-dependent manner, suggesting that Fin induces apoptosis in cancer cells via proteins of the Bcl-2 and caspase family. In a previous publication, our group showed that Fin promoted and increase in the apoptosis of epithelial cells (Delella et al., 2009) and these results are in concordance with the studies of others authors (Rittmaster et al., 1995; Yamashita et al., 1996; Prahalada et al., 1998). Herein, we observed again VP epithelial apoptosis at ultrastructure level, emphasizing this important property of Fin in the prevention and in the treatment of CaP.

Corradi and co-workers (2004; 2009) showed that the inhibition of 5α-reductase activity by Fin in gerbil ventral prostates caused a reorganization and morphological modification of the collagen fibers, which became denser, undulated and below the basal lamina and interspersed in between the loosely packed SMC. Similar collagen accumulation is suggested to occur in the prostate after castration-induced regression (Muntzing, 1981; Izumyia and Nakada, 1997). Thornton and co-workers (1985) showed that collagen seem to be important in supporting the normal androgen-dependent proliferation and differentiation of prostatic epithelial cells and that during androgen ablation both collagen synthesis and degradation activity are reduced. We have shown and confirm that the DHT withdraw by Fin promoted collagen accumulation. However RT-PCR results confirmed the hypothesis of collagen accumulation by the already existent collagen fibers remodeling in the larger stroma compartment after Fin treatment, without de novo synthesis.

TGF Beta-1 is a multifunctional cytokine that regulates extracellular matrix production and degradation, cell differentiation, proliferation and apoptosis (Schuster and Krieglstein 2002; Huang and Lee 2003; Zhu and Kyprianou 2005; Fleisch et al. 2006). The increased mRNA gene expression and the increase of TGF-beta 1 protein synthesis by VP epithelial and stromal in both periods of Fin administration is in agreement with some authors. In a previous study using benign prostate hyperplasia human specimens, Glassman et al. (2001) showed that prostates from patients treated with Fin and terazosin, administrated alone or in combination, presented higher levels of TGF-beta 1 protein expression in both epithelial and stromal cells, compared with the controls. The finding also is in accordance with the study of Sáez et al. (1998) that also demonstrated an increase in prostate TGF-beta1 expression after Fin administration. Additionally, we suggest that epithelial apoptosis in Fin-treated VP (Huang and Lee 2003; Zhu and Kyprianou, 2005) may also result from a known pro-Apoptotic TGF-beta- 1 effect.

In conclusion, the treatment with Fin interferes with epithelial cell behaviour and also induces changes in the stromal cells, in which TGF-beta 1 signaling is involved. However, the condensed stroma observed after Fin administration is more a consequence of pre-existent collagen fiber redistribution around a small parenchyma than a *de novo* collagen synthesis.

ACKNOWLEDGMENTS

This paper is part of the thesis presented by F.K.D. to the Institute of Biology, UNICAMP, in partial fulfillment of the requirement for her PhD degree. We are thankful to the Sao Paulo State Funding Agency (FAPESP; grant number 06/60114-6) for the PhD fellowship. The present work was done with support from CAPES-Brazil, CNPq, FUNDUNESP. INFABIC is co-funded by CNPq and FAPESP.

REFERENCES

Bradford MM. A rapid and sensitive method for the quantitation of microgram quantities of protein utilizing the principle of protein-dye binding. Anal Biochem 1976;72:248-254.

Canby-Hagino E.D., Brand T.C., Hernandez J., Thompson I.M. Chemoprevention of prostate cancer with finasteride. Expert Opin Pharmacother 2006;7:899-905.

Corradi L.S., Góes R.M., Carvalho H.F., Taboga S.R. Inhibition of 5a-reductase activity induces stromal remodeling and smooth muscle de-differentiation in adult gerbil ventral prostate. Differentiation 2004;72:198–208.

Corradi LS, Campos SGP, Santos FCA, Vilamaior PSL, Góes RM, Taboga SR. Long-term inhibition of 5-alpha reductase and aromatase changes the cellular and extracellular compartments in gerbil ventral prostate at different postnatal ages. Int J Exp Path 2009; 90:79–94.

Cotta–Pereira G, Rodrigo FG, David-Ferreira JF. The use of tanic acid-glutaraldehyde in the study of elastic related fibers. Stain Technol 1976;51:7-11.

Cunha GR, Donjacour AA. Stromal-epithelial interactions in normal and abnormal prostatic development. Prog Clin Biol Res 1987;239:251-272.

Cunha GR, Hayward SW, Dahiya R, Foster BA. Smooth muscle-epithelial interactions in normal and neoplastic prostatic development. Acta Anat 1996;155:63-72.

Delella FK, Justulin Jr LA, Felisbino SL. Finasteride treatment alters MMP-2 and -9 gene expression and activity in the rat ventral prostate. Int J Androl, 33: E114-E122.

Djakiew D. Dysregulated expression of growth factors and their receptors in the development of prostate cancer: review article. Prostate 2000;42:150-160.

Fleisch MC, Maxwell CA, Barcellos-Hoff MH. The pleiotropic roles of transforming growth factor beta in homeostasis and carcinogenesis of endocrine organs. Endocr Relat Cancer 2006;13:379–400.

George F.W. Androgen metabolism in the prostate of the finasteride-treated, adult rat: a possible explanation for the differential action of testosterone and 5a-dihydrotestosterone during development of the male urogenital tract. Endocrinology 1997;138:871–877.

George FW, Wilson JD. In: Knobil E, Neill JD, editors. Sex determination and differentiation. The Physiology of Reproduction. Raven Press, New York; 1994. p 3-28.

Glassman DT, Chon JK, Borkowski A, Jacobs SC, Kyprianou N. Combined effect of terazosin and finasteride on apoptosis, cell proliferation and transforming growth factor-beta expression in benign prostatic hyperplasia. Prostate 2001;46:45–51.

Golbano JM, López-Aparicio P, Recio MN, Pérez-Albarsanz MA (2008) Finasteride induces apoptosis via bcl-2, bcl-xl, bax and caspase-3 proteins in LNCaP human prostate cancer cell line. International Journal of Oncology 32: 919-924.

Huang X, Lee C. Regulation of stromal proliferation, growth arrest, differentiation and apoptosis in benign prostatic hyperplasia by TGF-beta. Front Biosci 2003;8:740–749.

Huynh H. Induction of apoptosis in rat ventral prostate by finasteride is associated with alteration in MAP kinase pathways and Bcl-2 related family of proteins. Int J Oncol 2002;20:1297-1303.

Isaacs JT. Antagonistic effect of androgen on prostatic cell death. The Prostate 1984; 5: 545-557.

Izumiya K, Nakada T. Inhibitors of collagen synthesis and hypophysectomy: effects on androgen induced growth of ventral prostate in rats. Arch Androl 1997;38:231-241.

Jimenez Cruz J.F., Quecedo Gutierrez L., Del Llano Senaris J. Finasteride: 10 years of clinical use. Systematic review of the literature. Actas Urol Esp 2003;27:202-215.

Kyprianou N, Isaacs JT: Expression of transforming growth factor-b in the rat ventral prostate during castration-induced programmed cell death. Mol Endocrinol 1989;3:1515–1522.

Lee C. Physiology of castration-induced regression in rat prostate. In MurphyG, Sandberg AA, Karr JP eds: “The prostatic cell: structure and function”. New York: Alan R. Liss, 1981. p 231-246.

Li J, Kim J. Molecular Profiles of Finasteride Effects on Prostate Carcinogenesis. Cancer Prev Res 2009;2:518-524.

Livak KJ, Schmittgen TD. Analysis of relative gene expression data using real-time quantitative PCR and the 2(-Delta Delta C(T)) Method. Methods 2001;25:402-408.

Lobaccaro JM, Boundon C, Lechevallier E, Mottet N, Rebillard X, Lumbroso S, Gibelin B, Sultan C. Effect of finasteride (Proscar) on the proliferation of cultured epithelial and stromal cells from normal and hyperplastic human prostates. Cell Mol Biol 1996;42:511-518.

Mariotti A, Mawhinney M. Hormonal control of accessory sex organ fibromuscular stroma. Prostate 1981;2:397-408.

Marker PC, Donjacour AA, Dahiya R, Cunha GR. Hormonal, cellular, and molecular control of prostatic development. Dev Biol 2003;253:165-174.

Müntzing J. Collagen synthesis and breakdown in the rat ventral prostate. Prog Clin Biol Res 1981;75A:137-144.

Prahalada S.R., Keenan K.P., Hertzog P.R., Gordon L.R., Peter C.P., Soper K.A., Zwieten M.J., Bokelman D.L. Qualitative and quantitative evaluation of prostatic histomophology in rats following chronic treatment with Finasterida, a 5-alpha reductase inhibitor. Urology 1994;43:680-685.

Prahalada S.R., Rhodes L., Grossman S.J., Heggan D., Keenan K.P., Cukierski M.A., Hoe C.M., Berman C., van Zwieten M.J. Morphological and hormonal changes in the ventral and dorsolateral prostatic lobes of rats treated with Finasterida, a 5-alpha reductase inhibitor. Prostate 1998;35:157–164.

Prins GS, Birch L, Greene GL. Androgen receptor localization in different cell types of the adult rat prostate. Endocrinology 1991;129:3187-3199.

Reddy G.K. Finasteride, a selective 5-alpha-reductase inhibitor, in the prevention and treatment of human prostate cancer. Clin Prostate Cancer 2004;2:206-208.

Rittmaster RS, Manning AP, Wright AS, Thomas LN, Whitefield S, Norman RW, Lazier CB, Rowden G. Evidence for atrophy and apoptosis in the ventral prostate of rats given the 5α-reductase inhibitor finasteride. Endocrinology 1995;136:741-748.

Rittmaster RS,Norman RW, Thomas LN, Rowden G. Evidence for atrophy and apoptosis in the prostates of men given finasteride. J Clin Endocrinol Metab 1996;81:814–819.

Roy-Burman P, Wu H, Powell WC, Hagenkord J, Cohen MB. Genetically defined mouse models that mimic natural aspects of human prostate cancer development. Endocr Relat Cancer 2004; 11:225-254.

Sáez C, González-Baena AC, Japón MA, Giráldez J, Segura DI, Miranda G, Rodríguez-Vallejo JM, González-Esteban J, Torrubia F. Regressive changes in finasteride-treated human hyperplastic prostates correlate with an upregulation of TGF-beta receptor expression. Prostate 1998;37:84-90.

Schuster N, Krieglstein K. Mechanisms of TGF-beta-mediated apoptosis. Cell Tissue Res 2002;307:1–14

Stoner E. The clinical development of a 5-alpha-reductase inhibitor, finasteride. J Steroid Biochem 1992;37:375-378.

Sutton MT, Yingling M, Vyas A, Atiemo H, Borkowski A, Jacobs SC, Kyprianou N. Finasteride targets prostate vascularity by inducing apoptosis and inhibiting cell adhesion of benign and malignant prostate cells. Prostate 2006;66:1194–1202.

Roberts AB, Sporn MB. The transforming growth factor beta. New York, Springer-Verlag, 1990.

Thornton M, Frederickson R, Mata L, Mawhinney M. Collagen and the proliferation and differentiation of rat ventral prostate epithelial cells. Biol Reprod 1985;33:213-227.

Tindall DJ, Rittmaster RS. The rationale for inhibiting 5-reductase isoenzymes in the prevention and treatment of prostate cancer. J Urol 2008;179:1235-1242.

Thornton M, Frederickson M, Mata L, Mawhinney M. Collagen and the proliferation and differentiation of rat ventral prostate epithelial cells. Biology of Reproduction 1985;33:213-227.

Vilamaior PSL, Felisbino SL, Taboga SR, Carvalho HF. Collagen fiber reorganization in the rat ventral prostate following androgen deprivation: A possible role for the smooth muscle cells. Prostate 2000;45:253-258.

Yamashita A, Hayashi N, Sugimura Y, Cunha GR, Kawamura J. Influence of diethylstilbestrol, Leuprolelin (a luteinizing hormone-releasing hormone analog), Finasteride (a 5 alpha-reductase inhibitor), and castration on the lobar subdivisions of the rat prostate. Prostate 1996;29:1-14.

Zhu B, Kyprianou N. Transforming growth factor beta and prostate cancer. Cancer Treat Res 2005;126:157–173.

LEGENDS OF FIGURES:

Fig. 1. VP sections stained by Picrossirius Red, elucidating collagen fibers in red. These sections were used to did the collagen area morphometry showed in the table 2. **a)** Control VP; **b)** Fin treated at day-7; **c)** Fin treated at day-30. Epithelium (EP), Lumen (L). Bars: 20 μm.

FIGURE 1:

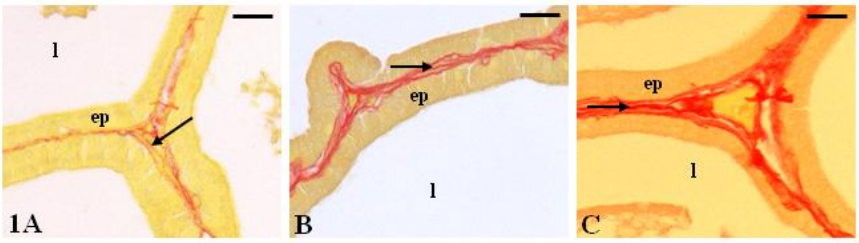

TABLE 2: Values of the morphometric-stereological data from control and finasteride-treated ventral prostates. Values represent mean±SD.

Parameters (n=5)	Control	Fin 7 Days	Fin 30 Days
Body Weigth (g)	406.1±57.9^{A}	403.9±56.7^{A}	475.7±49.1^{B}
Plasma T levels (ng/ml)	2.74±0.43^{A}	3.94±0.43^{B}	3.98±0.51^{B}
Plasma DHT levels (ng/ml)	0.82±0.09^{A}	0.15±0.013^{B}	0.27±0.02^{C}
VP Absolute weight (mg)	466.6±70.4^{A}	294±94.5^{B}	252.7±69.3^{B}
VP Glandular area (%)	93.67±1.08^{A}	83.73±1.93^{B}	79.28±3.0^{C}
VP Stromal area (%)	6.33±1.08^{A}	16.27±1.93^{B}	20.72±3.0^{C}
VP Collagen fibers area (%)	3.25±1.25^{A}	7.98±1.12^{B}	9.86±2.64^{C}

Statistically significant differences between control and treatments ($p \leq 0.05$).

A-C superscript letters represent statistically significant differences between the experimental groups; values with the same letter are not statistically different.

Fig. 2. Transmission electron microscopy of the control ventral prostate. **a)** Secretory epithelial cells with accumulation of secretory vesicles (arrow-heads) and a large amount of synthesis-related organelles, like rough endoplasmatic reticulum (*). Stroma (s), Lumen (l), Nucleus (n), Nucleoli (arrow). Bar: 3 µm. **b)** Details of apical portion of a secretory epithelial cell, with inumerous microvillous (arrows) and secretory vesicles (*). Lumen (l). Bar: 0,5 µm. **c)** Subepithelial stroma composed by a linear layer containing smooth muscle cell (smc), collagen fibers (co) and fibroblast (fb). Epithelium (ep). Bar: 0,5 µm. **d)** Intimate arrangement of the mainly prostatic stromal cells, smooth muscle cells (smc) and fibroblasts (fb) wrapped up by collagen (co) and elaunin fibers (arrow). Bar: 1 µm.

FIGURE 2:

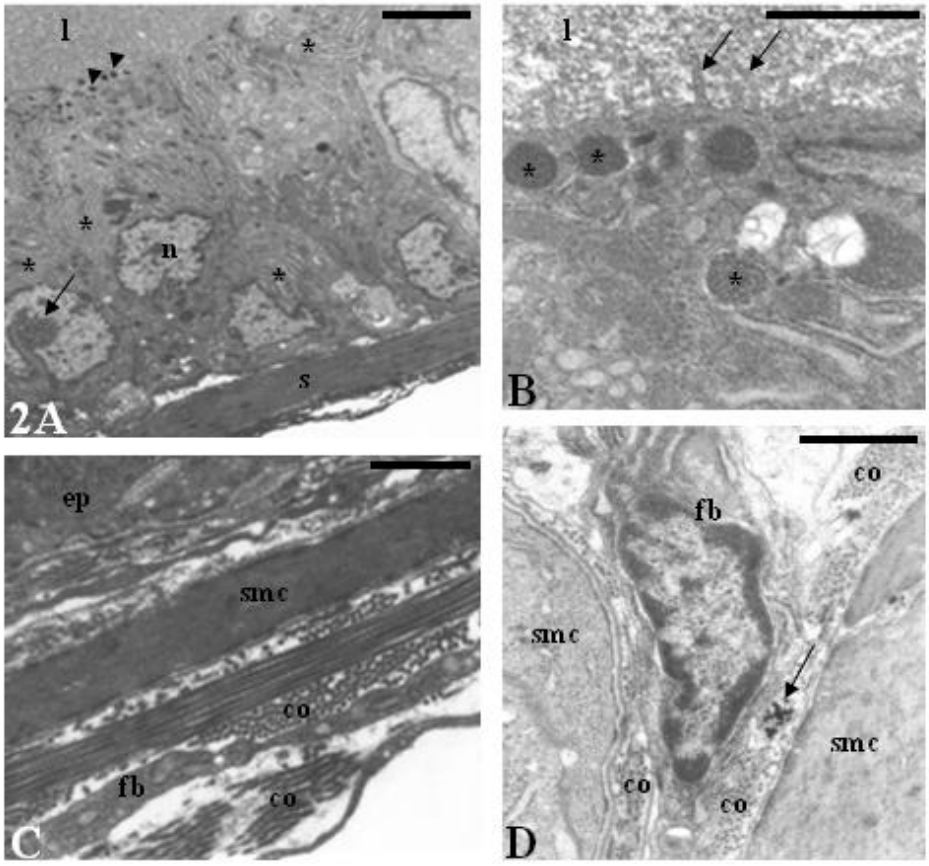

Fig. 3. Ultrastructure of treated ventral prostate after 7 days (**a** and **b**) and after 30 days (**c**, **d**, **e** and **f**) of Fin treatment. **a)** Glandular epithelium composed by cells with less secretory phenotype and subepithelial stroma. Epithelium (ep), Smooth Muscle Cell (smc), Fibroblast (fb). Bar: 3 µm. **b)** Detail of the subepithelial stroma, showing irregular epithelial basal membrane (arrows), active fibroblast (fb) with volumous nucleus (**) and evident Golgi apparatus (*), subepithelial concentration of collagen fibers (co), smooth muscle cell with irregular basal membrane (arrow-heads). Bar: 1 µm. **c)** Apoptotic body observed in Fin treated VP (traced black lines). Irregular Basal Membrane (arrows), Spiny Outline of the Smooth Muscle Cells (arrow-heads), Epithelium (ep). Bar: 2 µm. **d)** Active fibroblast (fb) with organelles synthesis-related (*) and irregular outline. Subepithelial deposition of collagen fibers (co). Spiny Outline of the Smooth Muscle Cells (arrow-heads). Bar: 2 µm. **e)** and **f)** Adherence (traced black lines) between fibroblast (fb) and tortuous epithelial basal membrane (arrows). Collagen fibers (co). Epithelium (ep), Smooth Muscle Cell (smc), Mitochondria (*). Bars: 0,5 µm.

FIGURE 3:

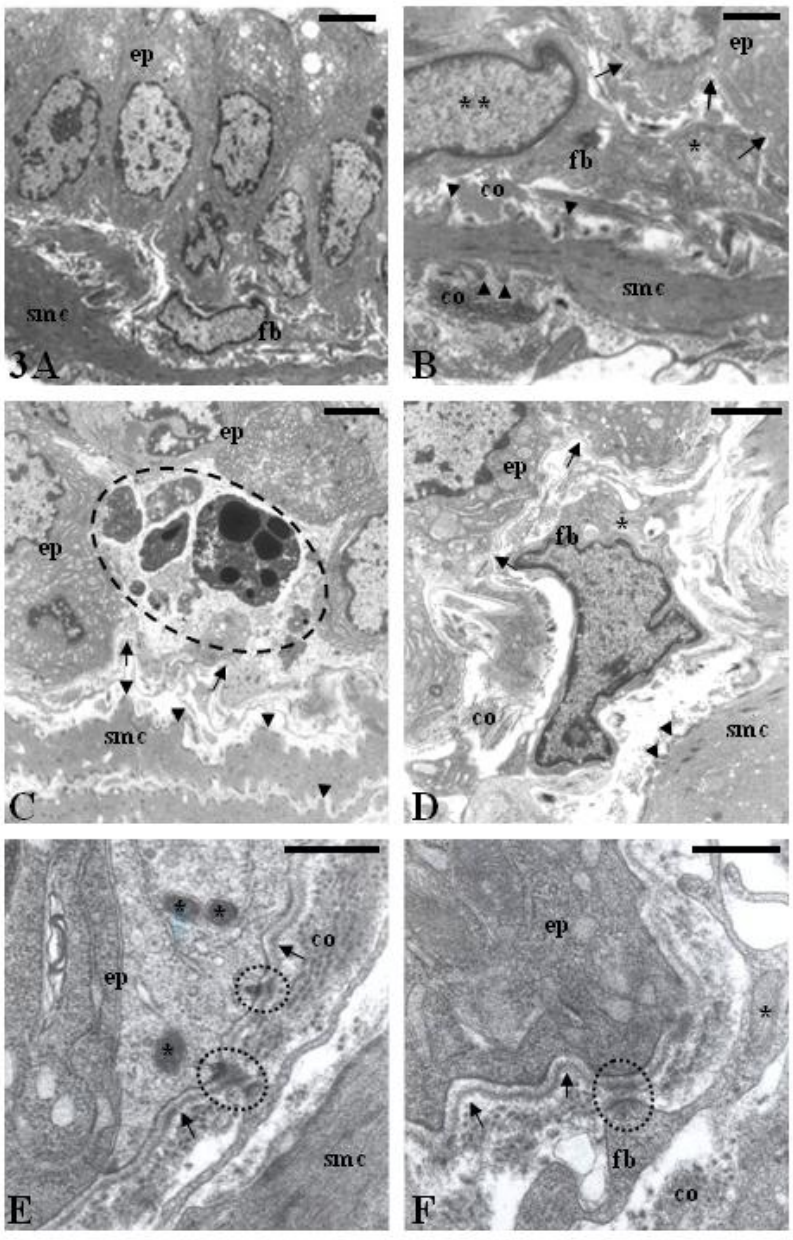
ep
smc
fb
3A
ep
**
fb
*
co
co
smc
B
ep
ep
smc
C
ep
fb
*
co
smc
D
*
*
co
ep
smc
E
ep
*
fb
co
F

Fig. 4. Immunohistochemical location of smooth muscle cells alpha actin (arrows) in the ventral prostate stroma of control animals (**a** and **b**) and in the ventral prostate stroma of the Fin-treated animals at day 30 (**c** and **d**). The smooth muscle cells layer (arrows) remained sinuous and thinner after the treatment. Epithelial (ep), Stroma (s), Lumen (*). Bars: 20 µm.

FIGURE 4:

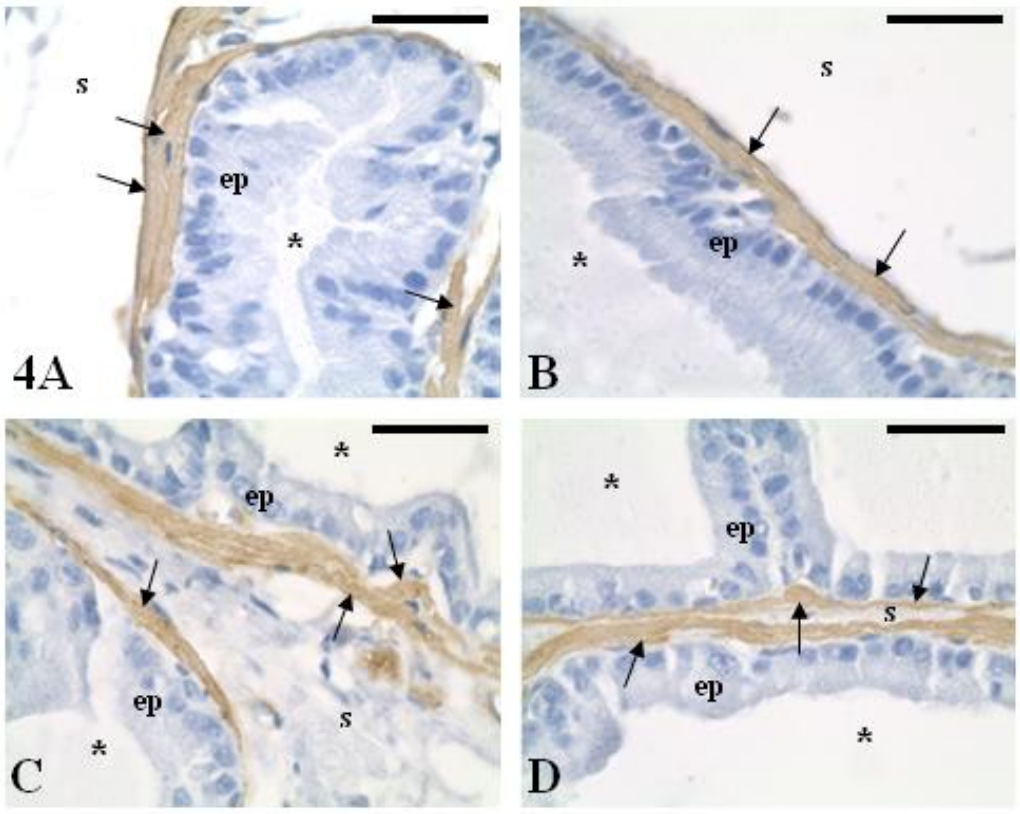

Fig. 5. Fin effect on type I collagen and type III collagen immunohistochemical detection on ventral prostate (VP). **b**: negative control. Bar = 10 µm. **a**, **d** and **f**: type I collagen (**a**: control VP; **d**: Fin day 7; **f**: Fin day 30). **c**, **e** and **g**: type III collagen (**c**: control VP; **e**: Fin day 7; **g**: Fin day 30). Epithelium (ep), Blood Vessel (Ve), Lumen (*). Bars = 20 µm.

Fig. 6. Imaging of collagen fibers (arrows) in the VP stroma by second harmonic generation (SHG) from the hematoxilin and eosin stained sections (data not show). **a)** Control VP; **b)** Fin treated at day-7; **c)** Fin treated at day-30. Epithelium (ep), Stroma (s). Bars = 20 µm.

FIGURES 5 and 6:

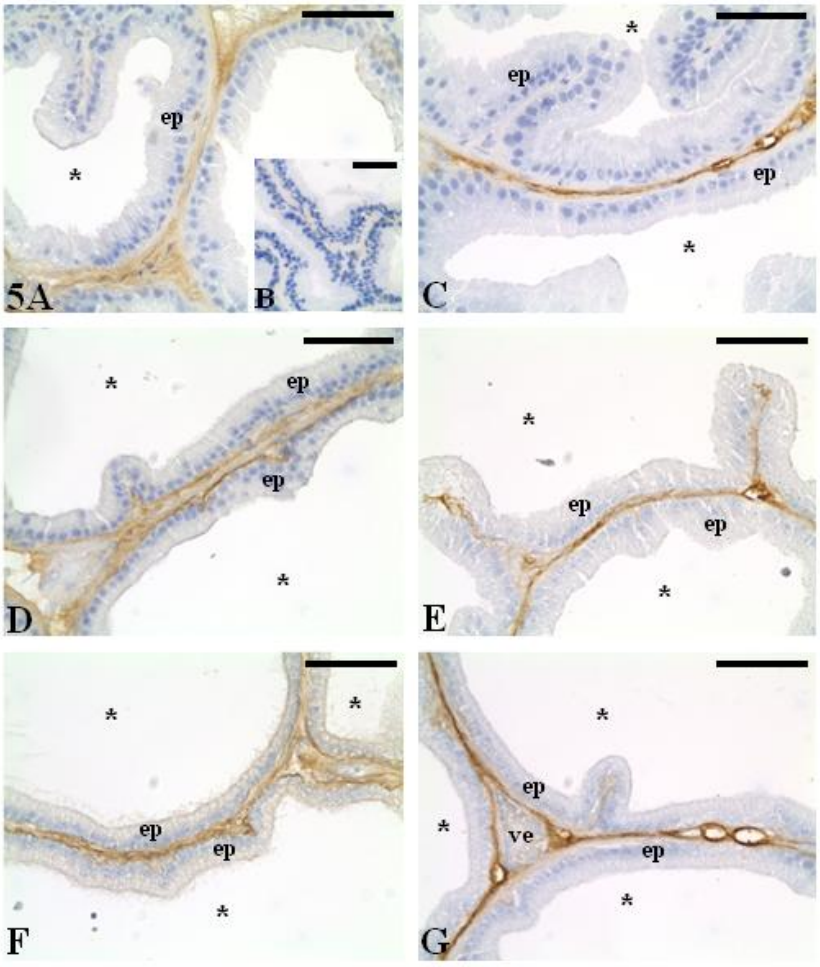

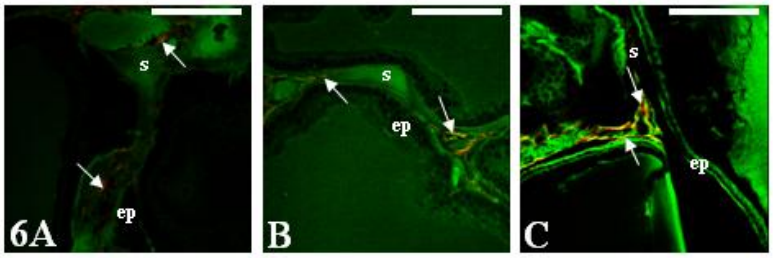

Fig. 7. Expression of transforming growth factor beta 1 (TGF-Beta 1) protein in the rat ventral prostate (VP). Immunohistochemistry study: **a)** Control VP; **b)** Fin day 7; **c)** Fin day 30. Bars = 10 μm. **d)** Western blot analysis of the Fin effects on TGF-Beta 1 and β-actin (Actin) in VP extracts (lane 1 control, lane 2 Fin day 7, lane 3 Fin day 30). Each lane represents a pool of 75 μg protein (15 μg from each of five individual extractions). **e)** Relative expression (IOD integrated optical density) of TGF-Beta 1 from ventral prostates in comparison with the constitutive control β-actin. Fin treatment altered the TGF-Beta 1 protein quantity. *Data are significantly different from CT group at $p<0.05$.

FIGURE 7:

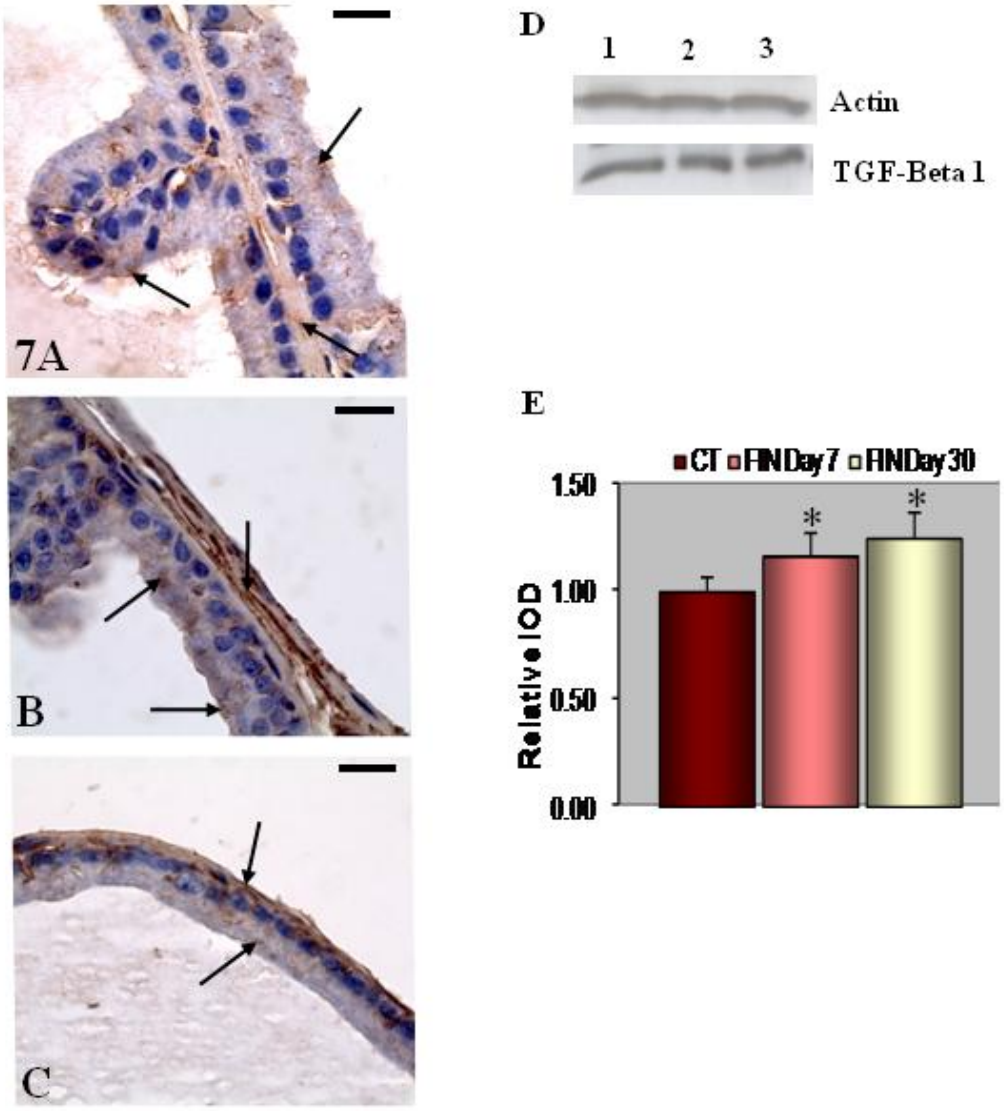
7A
B
C
D
1
2
3
Actin
TGF-Beta 1
E
CT
FINDay7
FINDay30
1.50
1.00
0.50
0.00
Relative IOD
*
*

Fig. 8. Quantification of type I and III Collagen and TGF Beta-1 mRNA expression by q-RT-PCR after 7 and 30 days of Fin treatment in the ventral rat prostate. Both Collagen I and III mRNA expression were significantly downregulation after both periods of treatment. TGF Beta-1 mRNA was upregulated after 7 and 30 days of Fin administration. Data are significantly different from CT group at $p < 0.01$. A-C superscript letters represent statistically significant differences between the experimental groups; values with the same letter are not statistically different.

FIGURE 8:

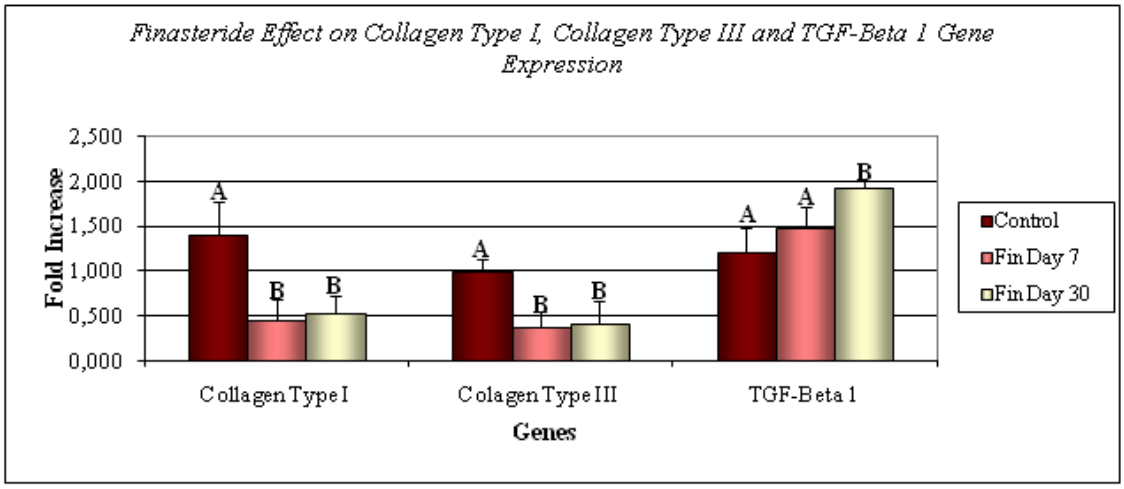
Finasteride Effect on Collagen Type I, Collagen Type III and TGF-Beta 1 Gene Expression
Fold Increase
2,500
2,000
1,500
1,000
0,500
0,000
A
B
B
A
B
B
A
A
B
Collagen Type I
Colagen Type III
TGF-Beta 1
Genes
Control
Fin Day 7
Fin Day 30

Capítulo 3:

Increased type I collagen and TGF beta-1 gene expression in doxazosin-treated rat ventral prostate

Flávia Karina Delella[a,b], Sérgio Luis Felisbino[b]

[a]*Department of Cell Biology, Institute of Biology –University of Campinas (UNICAMP), Campinas, Sao Paulo, Brazil*

[b]*Department of Morphology, Institute of Biosciences – Univ Estadual Paulista (UNESP), Botucatu, Sao Paulo, Brazil*

Running title: Doxazosin treatment alters prostate stroma.

Key words: alpha blockade, stroma, collagen fiber, fibrosis, hyperplasia, gene expression

Grant Sponsor: FAPESP, Grant Numbers: 06/60114-6, 06/60115-2; CAPES do Brasil.

Correspondence to: Dr. Sérgio L. Felisbino, Departamento de Morfologia, Instituto de Biosciencias, Univ Estadual Paulista (UNESP), 18618-970, Botucatu, SP, Brasil.

Telephone/fax: +55 0XX 14 3811 6264

E-mail: felisbin@ibb.unesp.br

Abstract

Background: The prostate smooth muscle cells relaxation induced by doxazosin, an alpha-adrenergic blocker, improves the clinical symptoms of benign prostatic hyperplasia (BPH). In a previous study, we showed that doxazosin treatment for 30 days increased the area occupied by collagen fibers in the rat prostate stroma.

Objective: Herein, we investigated the effects of doxazosin treatment on type I and type III collagen and TGF-beta1 gene expression.

Design, setting, and participants: For this aim, adult Wistar rats were treated with Doxazosin (25 mg/kg per day) and the ventral prostate were excised at 7 and 30 days after treatment. The ventral prostates were submitted to ultrastructural, immunohistochemical, biochemical and molecular analyze.

Results and limitations: Doxazosin treated prostates presented increased immunostaining for type I and type III collagen in the stromal space and also exhibited thickened bundles of collagen fibrils at transmission electron microscope than untreated prostates. Seven days after doxazosin treatment, COL1A1 and TGF-Beta 1 gene expression were transiently increased, while both COL1A1 and COL3A1 gene expression were reduced after 30 days.

Conclusions: Our data suggest that relaxation of smooth muscle cells by alpha-blockers can exerts a profibrotic effect in the prostatic stroma via TGF-beta1 pathway signaling. Our results contribute to a better understanding of the clinical data and also of the molecular mechanisms behind doxazosin treatment.

1. Introduction

Benign prostatic hyperplasia (BPH) is one of the most frequent age dependent diseases of men with a prevalence of approximately 50% in those aged 51–60 years [1]. Both glandular and stromal elements of the prostate grow during the development of BPH, although there is a significant increase in the volumetric amount of the fibromuscular tissue and a decrease in the glandular area compared to the normal prostate [2].

The most common BPH symptoms include urinary frequency, urgency, nocturia, decreased urine flow rates, hesitancy and incomplete bladder emptying [3]. Recently, to treat and decrease these symptoms, medical therapy has replaced surgery as the initial management [4].

In this way, α-adrenoceptor blockade represents an alternative method of treating the symptoms of BPH that involves the reduction of the dynamic component of urethral obstruction [5], mainly by the smooth muscle tonus reduction and consequent inhibition of the prostatic urethra obstruction [6]. In this manner, the American Urological Association (AUA) [7] advises the use of α-adrenoceptor blockade as a safe and effective drug for the treatment of patients with BPH [8].

Besides relaxation of prostate smooth muscle cells, some quilinazole-based class of α-adrenoceptor blockers, such as doxazosin (DOX), has also been demonstrated to inhibit prostate growth by inducing apoptosis in stromal and epithelial cells, showing additional effects on long-term BPH treatment [9, 10, 11, 12, 13]. However, the mechanism by which these drugs induce apoptosis is not clear. Some evidence suggests that apoptosis may result from activation of the transforming growth factor beta 1(TGF-beta1) signal transduction pathway [14].

In a previous work, our group demonstrated for the first time that DOX treatment also induces a significant increase of the collagen fibers deposition in the prostate stroma [15]. More recently, Imamura et al. [16] using clinical specimens found that patients orally treated with a1-blockers often exhibit accumulation of collagen fibers in prostatic stroma and suggested that this structural change could be one of the factors responsible for the development of resistance to this treatment.

In this sense, to gain new insights into the molecular mechanisms of action of DOX on prostatic stroma, we decided to better investigate the gene expression of collagen types involved with fibrosis and also of TGF-beta1, a well known pro-fibrotic growth factor.

2. Materials and methods

2.1 Animals and Doxazosin Administration

Adult male 3-month-old Wistar rats were maintained in a controlled environment with free access to food and water. The experiment was performed according to the Guide for Care and Use of Laboratory Animals. The animals were divided into two groups: control rats (CT) and the doxazosin-treated group (DOX). Doxazosin-treated animals received daily doses of doxazosin (25mg/kg of body weight) (Doxazosin mesylate, Pfizer, Galena Pharmaceutical and Chemistry, SP, Brazil) dissolved in corn oil as vehicle, administrated by oral gavage. The dosage and duration of treatments were based on consultation with Pfizer and in a previously published work [17]. CT animals received only the vehicle. After 7 and 30 days of the doxazosin treatment, 15 animals from each group were killed by an overdose of pentobarbital. The ventral prostates (VP) were excised, immediately weighed and alternate lobes were left and right assigned and snap frozen or immersed in fixative.

2.2 Transmission Electron Microscopy

Tissue fragments of five animals from each experimental group were immersed in 2.5% glutaraldehyde, plus 0.25% tannic acid solution in Millonig's buffer for 2 hours [18], washed, and postfixed in 1% osmium tetroxide in the same buffer for 1 hour, washed again, dehydrated in graded acetone, and embedded in Araldite. Semithin sections were stained with Toluidin Blue and analyzed under light microscopy. Ultrathin silver sections were obtained with a diamond knife and contrasted with 2% alcoholic uranyl acetate and then with 2% lead citrate in 1 N sodium hydroxide solution for 10 minutes. Grids were examined under a Phillips transmission electron microscope, operating at 80 kV.

2.3 Immunohistochemistry

VP frozen sections (7 µm) fixed in cold methanol or VP Paraplast sections (5 µm) fixed in 4% paraformaldehyde dissolved in phosphate-buffered saline (PBS) for 24 hours, were collected in silanized glass slides, blocked first with 3% hydrogen peroxide in methanol for 15 minutes (to block endogenous peroxidase activity) and then blocked with 3% bovine serum albumin (BSA) in PBS for 1 hour at room temperature. Then, the sections were incubated with the primary monoclonal antibodies during 2 hours at room temperature: **Type I Collagen**, 1:300, Genetex, GTX 26308; **Type III Collagen**, 1:300, Abcam, ab 6310-100; **TGF-Beta 1**, 1:100, Santa Cruz, sc-146; **Alpha Actin**, 1:300, Santa Cruz, sc-32251. The primary antibody was detected using a secondary peroxidase-conjugated antibody (Santa Cruz Biotechnology, Santa Cruz, CA, USA), except TGF-Beta 1 that was detected using Mach 4 Universal HRP-Polymer Kit with DAB (Biocare Medical, Concord, CA, USA). Chromogen color development was accomplished with 3.3'-diaminobenzidine tetrahydrochloride (Sigma, USA). Slides were counterstained with Harris's haematoxylin. The negative control was performed by abolishing the primary antibody incubation step.

2.4 Western blotting analysis for TGF-Beta 1

VP frozen samples of five different adult rat prostatic lobes from the control group and from days 7 and 30 of Dox treatment were mechanically homogenized in 50 mM TRIS-HCl buffer pH 7.5, 0.25% Triton X-100 plus EDTA by means of a Polytron for 30 s at 4°C. Following centrifugation of the homogenate, the protein was extracted from the supernatant and quantified as described by Bradford (1976). Protein samples (each 75 µg) were loaded onto 12% SDS-polyacrylamide gels for SDS-polyacrylamide gel electrophoresis under reducing conditions. After electrophoresis, the proteins were transblotted onto a nitrocellulose membrane (Sigma). The blot was blocked with 3% bovine serum albumin (BSA) in TBST (10 mM TRIS-HCl pH 7.5, 150 mM NaCl, 0.1% Tween-20) for 1 hour, incubated overnight at 4°C with 3% BSA in TBST containing a 1:1,000 dilution of the anti-Transforming growth factor beta 1 (TGF- Beta 1; MAB240; R&D Systems, Minneapolis, USA) or anti-β-actin (Actin; sc-1615; Santa Cruz Biotechnology,

Santa Cruz, CA, USA) primary antibodies, washed (5 × 5 minutes) in TBST, and incubated for 1 hour at room temperature with peroxidase-conjugated antibody, followed by five washes (5 minutes) in TBST. Antibody complexes were detected by means of chemiluminescence (Pierce® ECL Western Blotting Substrate). TGF- Beta 1 and β-actin protein expression was quantified by densitometric analysis of the bands as integrated optical density (IOD). The TGF- Beta 1 expression was normalized to the β-actin values. Normalized data are expressed as means±SD.

2.5 Collagen I, Collagen III and TGF-Beta 1 mRNA expression

Total RNA was isolated from ventral prostate samples using TRIzol Reagent (Invitrogen Life Technologies, Carlsbad, CA, USA), according to the manufacturer's protocol. Purified total RNA were reverse transcribed with random hexamer primers and a High-Capacity cDNA Archive Kit (Applied Biosystems). Collagen I, Collagen III and TGF-Beta 1 (Table 1) gene expression levels from each treatment were detected by quantitative real-time reverse transcription polymerase Chain Reaction (RT-qPCR) using an ABI 7300 Real Time PCR System (Applied Biosystems, Foster City, CA, USA). A sample without cDNA template (NTC) was used to verify that the master mix was free from contaminants. Real-time conditions were: 10 minutes at 95ºC, 40 cycles of denaturation at 95ºC for 15seconds, and annealing/extension at 60ºC for 1 minute. The Beta Actin RNA gene was used as a reference to normalize quantification of mRNA targets.

Table 1. GenBank accession numbers and primers used for Real-Time RT-PCR amplification of COL1A1, COL3A1, TGF-Beta 1 and Beta Actin genes.

Gene	GenBank accession no.	Sequence (5'-3')
COL1A1	NM_053304.1	Forward TCT GAC TGG AAG AGC GGA GAG T Reverse ACA CGA GTC TGA CCT GTC TCC AT
COL3A1	M21354	Forward CGC AAT TGC AGA GAC CTG AA Reverse AAC CCA GTA TTC TCC GCT CTT G
TGF-Beta 1	NM_021578	Forward GAG GTG ACC TGG GCA CCA T Reverse GGC CAT GAG GAG CAG GAA
Beta Actin	NM_031144.2	Forward TCA GGT CAT CAC TAT CGG CAA TG Reverse TTT CAT GGA TGC CAC AGG ATT C

RT-qPCRs for target and reference genes were run in the same RT reaction using two replicates of each sample and reference gene. An amplification plot graphically displayed the fluorescence detected over the number of cycles that were performed. Standard curves for both target genes and reference gene were obtained by using seven serial dilutions (1:10) of sample cDNA. Using the $2^{-\Delta\Delta Ct}$ method, data were recorded as the fold-change in gene expression normalized by the reference gene and relative to the calibrator sample [19]. All samples then were normalized to the ΔCt value of a calibrator sample to obtain a ΔΔCt value (ΔCttarget – Δctcalibrator). Dissociation-melting curves confirmed the specific amplification of the cDNA target and the absence of nonspecific products.

2.6 Statistical analysis

One-way analysis of variance (ANOVA) was performed to determine whether differences existed among all groups ($p < 0.05$), and then the Tukey–Kramer post-test was employed to determine the significance of the differences. A p-value of <0.05 was considered significant. The statistical tests were performed on Instat (version 3.0; Graph-Pad, Inc., San Diego, CA, USA).

3. Results

3.1 Ventral Prostate Morphology

The morphological analyses performed by transmission electron microscopy (TEM) showed control VP glandular area composed mainly by columnar epithelial clear cells (secretory cells) and by scattered dark cells (Figure 1A). The apical portion of the clear cell was composed by secretion vesicles and protein synthesis-related organelles (Figure 1B). The VP epithelium was surrounded by a thin fibromuscular stroma (Figure 1C). Smooth muscle cells detected by immunohistochemistry presented a thick layer composed by cells (Figure 1D).

Interactions between fibroblast and the epithelial basal membrane (Figures 2A,B) were promoted by DOX after 7 days od treatment. The treatment for 30 days promoted the

activation of fibroblasts (Figure 2C), composed by large nucleus, a great amount of organelles-related protein synthesis, absence of basal membrane and also characteristics similar to smooth muscle cells, like cytoskeleton fibers (Figure 2D). Smooth muscle layer showed apparently more compact, when compared with the same component in the control VP (Figure 2E). At day-30, DOX promoted apoptosis in the glandular epithelial cells and decreased the cells height (Figure 3A) and was common to find fibroblasts prolongations following the epithelial basal membrane folds (Figure 3B).

3.2 Type I and Type III Collagen Analyses

In the control, type I collagen was identified dispersed over the stroma, surrounding glandular acini and ducts (Figure 4A). DOX treatment promoted an increase of type I collagen density at day-7 (Figure 4D) and day-30 (Figure 4F). The gene expression analyze showed a transient increase of COL1A1 mRNA at day-7, which decreased significantly at day-30 of DOX treatment (Figure 6). On the other hand, type III collagen was found distributed in the interstitial stroma, filling epithelial-infoldings and strongly concentrated around blood vessels (Figure 4C) of the VP control stroma. The alpha 1 adrenergic blockade slightly increase the type III collagen distribution at day-7 (Figure 4E) and day-30 (Figure 4G) of treatment, while its mRNA gene expression was maintained at day-7 and decreased significantly at day-30 (Figure 6).

3.3 TGF-Beta 1 Expression

To evaluate the TGF-Beta 1 location, protein and mRNA quantification in the control VP and after DOX treatment, we used immunohistochemistry technique, western blotting and real time quantitative PCR, respectively. The immohistochemistry reaction for TGF-Beta 1 was weakly detected in both epithelial and stromal compartments from the control group (Figure 5A). DOX treatement increased TGF-Beta 1 immunostaining at day-7 (Figure 5B) and, while at day-30 the immunoreaction was similar than control (Figure 5C).

The figure 5D show a representative Western Blotting for TGF-Beta 1 in the VP of control and DOX-treated animals. The specific immunoreactive bands for TGF-Beta 1 (25

kDa) were more intense in those DOX-treated VPs for 7 days ($p<0.05$) (Figure 5E), comparing with the control ones.

The results of the q-RT-PCR for TGF-Beta 1 are shown in Figure 6. DOX treatment increased significantly TGF-Beta 1 mRNA expression at day-7 ($p<0.01$) and TGF-Beta mRNA expression was not different from control at day-30. Taken together, these results demonstrated that short-term DOX treatment increased both TGF-Beta 1 mRNA and protein.

4. Discussion

Benign prostatic hyperplasia (BPH) is a condition whose incidence is clearly age related and is characterized by a nodular enlargement of prostatic tissue resulting in obstruction of the urethra [20]. The relative degree of stromal and epithelial hyperplasia is highly variable [21]. Overall, approximately 80% and 20% of the hyperplastic volume is composed of stromal and epithelial elements, respectively [22]. Half of the stromal hyperplasia is composed of smooth-muscle elements [23].

The American Urological Association [7] recommends α1-adrenergic receptor blockers (A1Bs) as safe and efficacious pharmacologic treatment options for patients suffering from BPH [7]. A1Bs block the adrenergic receptors, which are abundant in the smooth muscle of the prostate and bladder, produces a reduction in smooth muscle tone [24].

An additional effect of inducing prostate cell apoptosis have also been demonstrated to be involved in long-term efficacious of quilinazole-based class of α-adrenoceptor blockers, such as doxazosin, in treating BPH [9, 10, 11, 12, 13]. The induction of apoptosis by DOX on prostate cells has been attributed to an increased expression of transforming growth factor (TGF)-beta 1 [13, 25, 26, 14]. However, Zao et al. [27], using a molecular approach, showed an involvement of TNF-alpha in the doxazosin molecular mechanism of action and deconstructed the participation of TGF-beta 1 pathway in the doxazosin-induced apoptosis, at least for stromal cells.

Beyond its possible involvement in the DOX-induced apoptosis, TGF-beta 1 is a multifunctional cytokine that regulates extracellular matrix production and degradation [28,

29, 30, 31]. In this sense, our group has been focusing the prostatic stromal changes induced by DOX treatment, with special attention to the extracellular matrix components. Previous works by our group demonstrated that DOX treatment increases both collagen system and elastic system fibers volume fraction in the stroma of rat prostatic complex [15, 32]. This pro-fibrotic effect was also observed in human prostates from patients orally treated with a1-blockers [16]. Although quantitative, those previous results were done using selective collagen fibers stains associated with morphometrical analysis.

In this study, using quantitative real time PCR, we showed that type I collagen gene expression is increased at 7 days of DOX treatment. Moreover, we demonstrated that DOX treatment for 7 days increases both mRNA and protein of TGF-beta1 in the rat ventral prostate. Together, these results confirmed the profibrotic effect of DOX treatment and strongly suggest the involvement of TGF-beta1 in collagen fiber deposition on prostate stroma from Dox-treated animals. Herein, we also show that type I and type III collagen fibers has a similar distribution around the acini and in the interstitial space of ventral prostate, and may have co-localization forming heterotypic fibrils as proposed by Cameron et al. [33]. Moreover, we also observed that tissue distribution of both collagen fibers increased after DOX treatment.

In contrast with collagen fibers deposition, we observed that smooth muscle cells layer appears to be reduced in DOX-treated prostates as showed by the reduced immunostaining for smooth muscle cell apha-actin. This result agrees with the study by Smith et al. (34) who found that contractility of prostatic smooth muscle cells in culture decreased following DOX treatment. These authors also showed that DOX treatment reduced the expression of actin and myosin proteins, suggesting that a1-blockers induce dedifferentiation of smooth muscle into fibroblasts and myofibroblasts. In this sense, our ultrastructural observation also found some stromal cells with typical phenotype of smooth muscle cells, that we called activated fibroblasts. The location of these cells, close to the epithelium, as the same of the preferential location of the fibroblasts and the absence of a continuous basement membrane suggest that these cells could be myofibroblasts. However, more studies are needed to show if those cells are derived from smooth muscle cells dedifferentiation or from fibroblast differentiation. We are most tempted to believe in the

second hypothesis due to another known effect of TGF-beta1 in inducing fibroblast-myofibroblast differentiation in vitro and in vivo, including prostate tissue [35-37]. Others typical fibroblasts from doxazosin-treated prostates appear to be involved in protein secretion and close associated with epithelium basement membrane rearrangement.

5. Conclusions

In conclusion, our data suggest that relaxation of smooth muscle cells by alpha-blockers treatment can exerts a profibrotic effect in the prostatic stroma via TGF-beta1 pathway signaling, leading to a marked prostate stroma cellular and extracellular elements remodeling. Our results contribute to a better understanding of the clinical data and also of the molecular mechanisms behind doxazosin treatment.

References

[1] Berry SJ, Coffey DS, Walsh PC et al. The development of human benign prostatic hyperplasia with age. J Urol 1984;132:474–9.

[2] Bartsch G, Muller HR, Oberholzer M, et al. Light microscopic stereological analysis of the normal human prostate and of benign prostatic hyperplasia. J Urol. 1979;122:487-9.

[3] Seftel AD, Rosen RC, Rosenberg MT, et al. Benign prostatic hyperplasia evaluation, treatment and association with sexual dysfunction: practice patterns according to physician specialty. Int J Clin Pract 2008;62:614-22.

[4] Baine WB, Yu W, Summe JP et al. Epidemiologic trends in the evaluation and treatment of lower urinary tract symptoms in elderly male Medicare patients from 1991 to 1995. J Urol 1998;160:816–20.

[5] Hieble JP, Ruffolo RR Jr. The use of α-adrenoceptor antagonists in the pharmacological management of benign prostatic hypertrophy: an overview. Pharmacol Res 1996;33:145-60.

[6] Forray C, Bard JA, Wetzel JM, et al. The alpha 1-adrenergic receptor that mediates smooth muscle contraction in human prostate has the pharmacological properties of the cloned human alpha 1c subtype. Mol Pharmacol 1994;45:703-8.

[7] AUA Practice Guidelines Committee. AUA guideline on management of benign prostatic hyperplasia. Chapter 1: Diagnosis and treatment recommendations. J Urol 2003;170:530–47.

[8] Tahmatzopoulos A, Kyprianou N. Apoptotic impact of alpha1-blockers on prostate cancer growth: a myth or an inviting reality? Prostate. 2004;59:91-100.

[9] Anglin IE, Glassman DT, Kyprianou N. Induction of prostate apoptosis by alpha1-adrenoceptor antagonists: mechanistic significance of the quinazoline component. Prostate Cancer Prostatic Dis 2002;5:88-95.

[10] Chiang CF, Son EL, Wu GJ. Oral treatment of the TRAMP mice with doxazosin suppresses prostate tumor growth and metastasis. Prostate. 2005 Sep 1;64(4):408-18.

[11] Kyprianou N. Doxazosin and terazosin suppress prostate growth by inducing apoptosis: clinical significance. J Urol. 2003;169:1520-5.

[12] Kyprianou N, Litvak JP, Borkowski A, et al. Induction of prostate apoptosis by doxazosin in benign prostatic hyperplasia. J Urol 1998;159:1810-5.

[13] Yang G, Timme TL, Park SH, et al. Transforming growth factor beta 1 transduced mouse prostate reconstitutions: II. Induction of apoptosis by doxazosin. Prostate 1997; 33:157-63.

[14] Partin JV, Anglin IE, Kyprianou N. Quinazoline-based alpha 1-adrenoceptor antagonists induce prostate cancer cell apoptosis via TGF-beta signalling and I kappa B alpha induction. Br J Cancer 2003;88:1615-21.

[15] Justulin LA Jr, Delella FK, Felisbino SL. Doxazosin reduces cell proliferation and increases collagen fibers in rat prostatic lobes. Cell Tissue Res 2008;332:171-83.

[16] Imamura T, Ishii K, Kanda H, et al. Structural changes in a1-adrenoceptor antagonist-treated human prostatic stroma. Clin Exp Med 2010;10:99-106.

[17] Yono M, Yamamoto Y, Yoshida M, et al. Effects of doxazosin on blood flow and mRNA expression of nitric oxide synthase in the spontaneously hypertensive rat genitourinary tract. Life Sci 2007;81:218–22.

[18] Cotta-Pereira G, Rodrigo FG, David-Ferreira JF. The use of tannic acid-glutaraldehyde in the study of elastic and elastic related fibers. Stain Technol 1976;51:7–11.

[19] Livak KJ, Schmittgen TD. Analysis of relative gene expression data using real-time quantitative PCR and the 2(-Delta Delta C(T)) Method. Methods 2001;25:402-8.

[20] Barry MJ. Epidemiology and natural history of benign prostatic hyperplasia. Urol Clin North Am 1990;17:495–07.

[21] Lepor H. Alpha Blockers for the Treatment of Benign Prostatic Hyperplasia. Reviews In Urology2007;9:181-90.

[22] Bartsch G, Muller HR, Oberholzer M, et al. Light microscopic stereological analysis of the normal human prostate and of benign prostate hyperplasia. J Urol 1979;122:487–91.

[23] Shapiro E, Becich MJ, Hartanto V, et al. The relative proportion of stromal and epithelial hyperplasia as related to the development of clinical BPH. J Urol. 1992;147:1293-97.

[24] Caine M. The present role of alpha-adrenergic blockers in the treatment of benign prostatic hypertrophy. J Urol 1986;136:1–4.

[25] Ilio KY, Park II, Pins MR, et al. Apoptotic activity of doxazosin on prostate stroma in vitro is mediated through an autocrine expression of TGF-beta1. Prostate. 2001;48:131-5.

[26] Glassman DT, Chon JK, Borkowski A, et al. Combined effect of terazosin and finasteride on apoptosis, cell proliferation, and transforming growth factor-beta expression in benign prostatic hyperplasia. Prostate 2001;46:45-51.

[27] Zhao H, Lai F, Nonn L, et al. Molecular targets of doxazosin in human prostatic stromal cells. Prostate 2005;62:400-10.

[28] Roberts AB, Heine UI, Flanders KC, et al. Transforming growth factor-b. Major role in regulation of extracellular matrix. Ann NYAcad Sci 1990;580:225–32.

[29] Fleisch MC, Maxwell CA, Barcellos-Hoff MH. The pleiotropic roles of transforming growth factor beta in homeostasis and carcinogenesis of endocrine organs. Endocr Relat Cancer 2006;13:379–400

[30] Mauviel A. Transforming growth factor-beta: a key mediator of fibrosis. Methods Mol Med 2005;117:69–80

[31] Hynes RO. The extracellular matrix: not just pretty fibrils. Science 2009;326:1216-9.

[32] Delella FK, Felisbino SL. Doxazosin treatment alters stromal cell behavior and increases elastic system fibers deposition in rat prostate. Microsc Res Tech 2010; In press.

[33] Cameron GJ, Alberts IL, Laing JH, et al. Structure of type I and type III heterotypic collagen fibrils: an X-ray diffraction study. J Struct Biol 2002;137:15-22.

[34] Smith P, Rhodes NP, Ke Y, et al. Influence of the a1-adrenergic antagonist, doxazosin, on noradrenalin-induced modulation of cytoskeletal proteins in cultured hyperplastic prostatic stromal cells. Prostate 1999;38:216–27.

[35] Vaughan MB, Howard EW, Tomasek JJ. Transforming growth factor beta1 promotes the morphological and functional differentiation of the myofibroblast. Exp. Cell Res 2000;257:180–9.

[36] Evans RA, Tian YC, Steadman R, et al. TGF-beta1-mediated fibroblast-myofibroblast terminal differentiation-the role of Smad proteins. Exp Cell Res 2003;282:90-100.

[37] Untergasser G, Gander R, Lilg C, et al. Profiling molecular targets of TGF-beta1 in prostate fibroblast-to-myofibroblast transdifferentiation. Mech Ageing Dev 2005;126:59-69.

LEGENDS OF FIGURES

Figure 1: A) Ultrastructure of control VP showing the glandular epithelium composed mainly by clear cells (cc) and few dark cells (dc). Basal cell (bc), Lumen (l), Stroma (s). Bar: 0,33 µm. **B)** Detail of the clear cell apical portion, composed by innumerous vesicles of secretion (arrow head), and organelles like mitochondria (*) and rough endoplasmic reticulum (rer). Lumem (l). Bar: 1 µm. **C)** Subepithelial stroma, collagen fibers (co) dispersed linearly and surrounding smooth muscle cells (smc) and fibroblasts (fb). Epithelium (ep). Bar: 0,33 µm. **D)** Immunohistochemical detecting alpha actin of the smooth muscle cells (arrow). Epithelium (ep), Stroma (s), Lumem (*). Bar: 20 µm.

Figure 1:

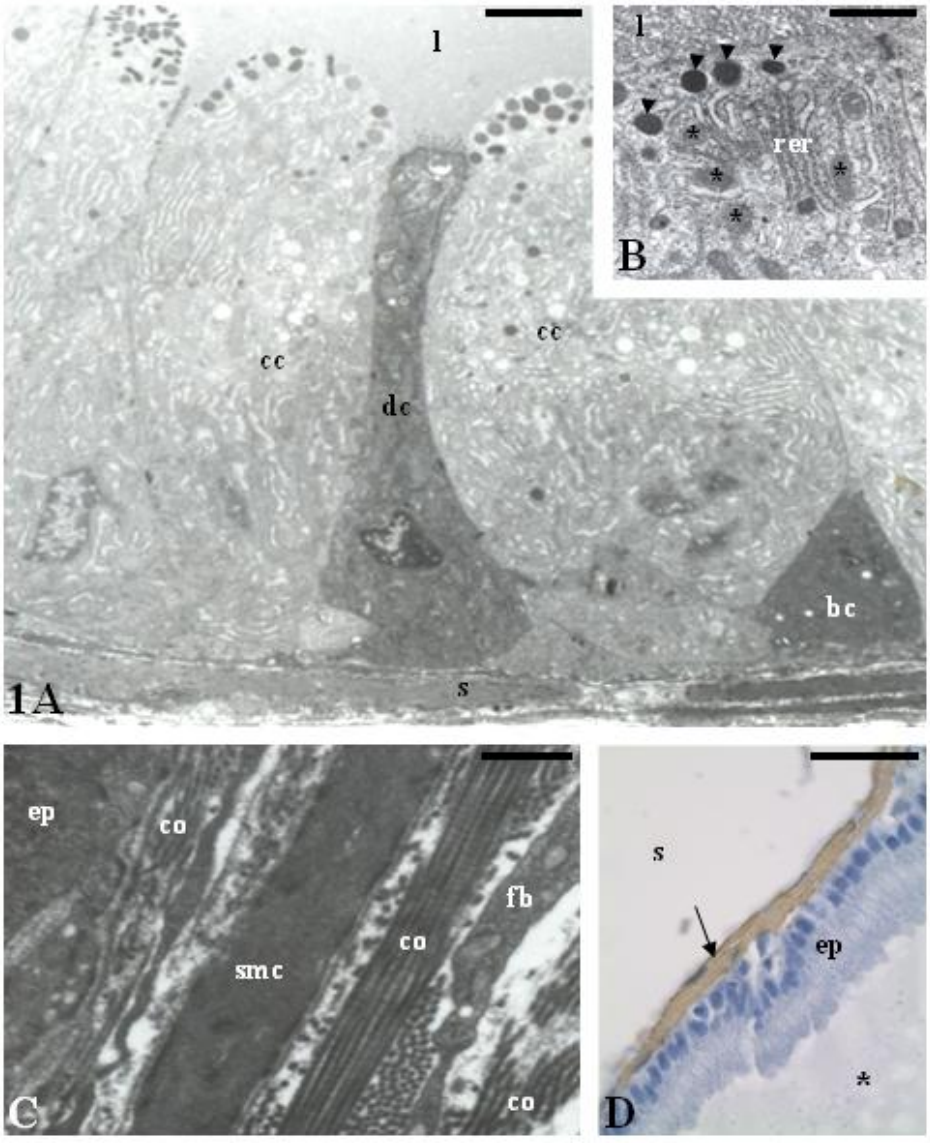

Figure 2: Ultrastructure of treated VP after 7 days (**A** and **B**) and after 30 days (**C, D** and **E**) **A)** Subepithelial stroma showing the interaction between a fibroblast (fb) and the epithelial basal membrane. Epithelium (ep), Nucleus (n), Smooth Muscle Cells (smc).Bar: 1 µm. **B)** Detail of the junction between a fibroblast and epithelial basal membrane showed in **A**. Bar: 0,5 µm. **C)** Subepithelial activated fibroblast (fbA) composed by large nucleus and a great amount of organelles-related protein synthesis, like Golgi complex (*), probably related with the collagen bundles (co) synthesis. Epithelial (ep), Nucleus (n), Smooth Muscle Cell (smc). Bar: 1 µm. **D)** Detail of activated fibroblast (fbA) showed in the anterior figure, presenting lack of basal membrane (arrows), and presence of Golgi complex (gc) and cytoskeleton fibers (*). Epitheliu (ep), collagen (co). Bar: 1 µm. **E)** Alpha actin immunolocation in VP at day 30 of Dox treatment. Smooth muscle layer showed apparently more compact than in control VP. Bar: 20 µm.

Figure 2:

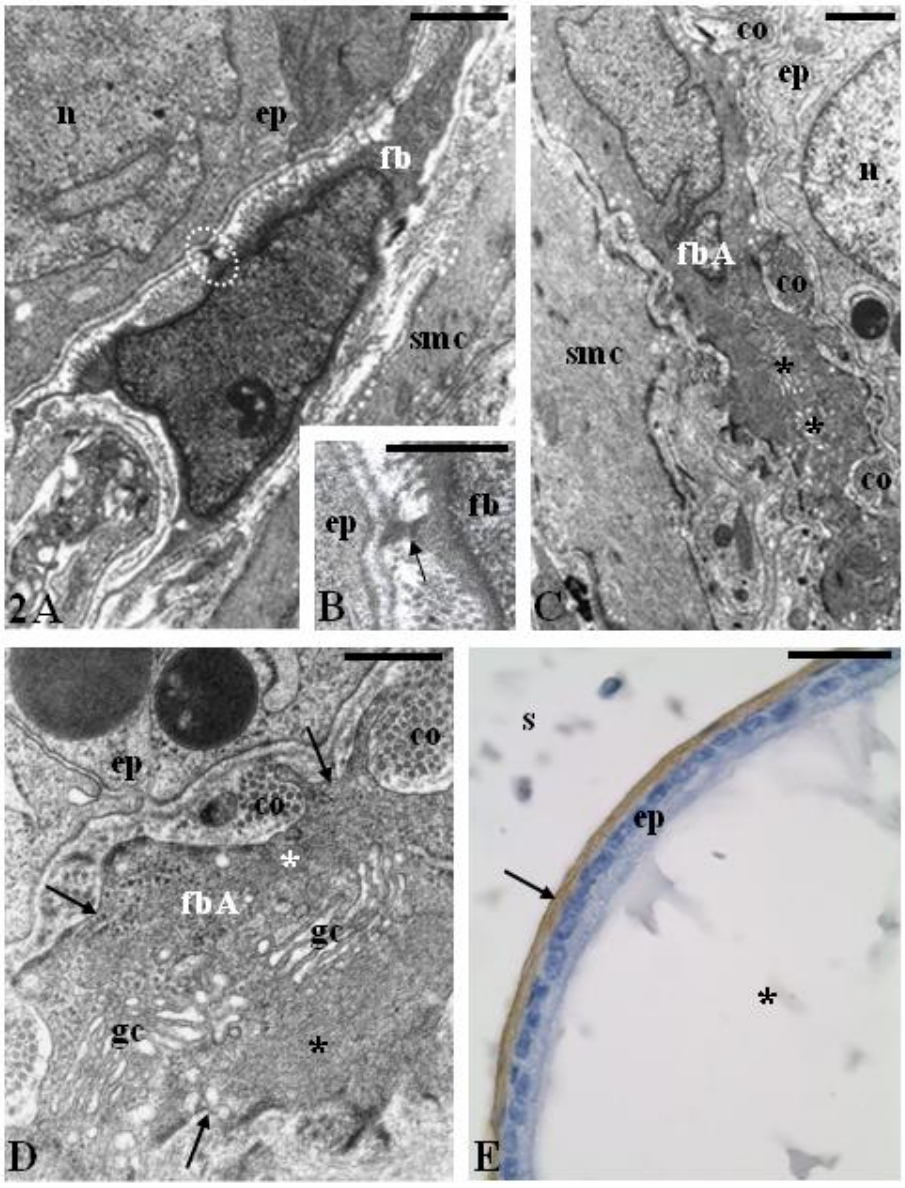

Figure 3: A) Ultrastructure of VP glandular epithelium after 30 days of doxazosin treatment. Cells in apoptosis process (black traced lines) were found, as well the decreased of the epithelial cells height. Epithelium (ep), Lumem (l), Nucleus (n), Rough Endoplasmic Reticulum (arrow head), Microvillous (arrows), Fibroblast (fb), Smooth Muscle Cell (smc). Bar: 2 µm. **B)** Detail of os subepithelial stroma, showing a fibroblast (fb) in a star format, with its prolongations (arrows head) following the epithelial basal membrane folds (arrows). Epithelium (ep). Bar: 0,5 µm.

Figure 3:

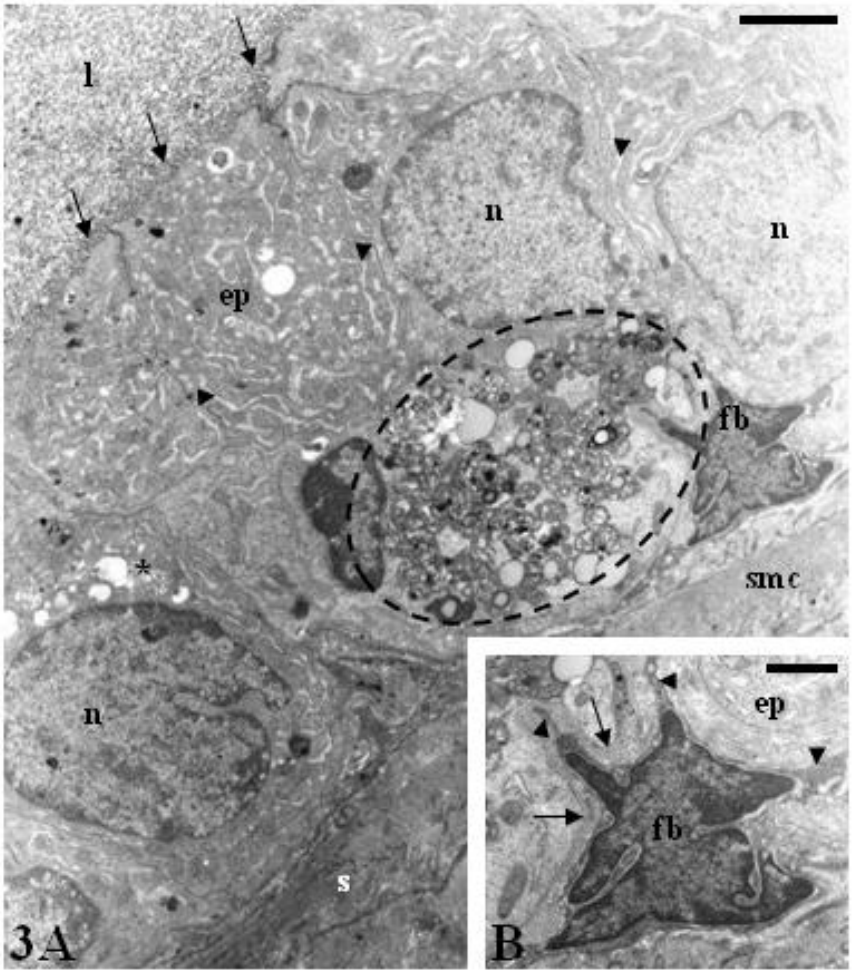

Figure 4: Dox effect on type I collagen and type III collagen immunohistochemical detection on ventral prostate (VP). **B:** negative control. Bar = 10 µm. **A**, **D** and **F:** type I collagen (**A:** control VP; **D:** Dox day 7; **F:** Dox day 30). **C**, **E** and **G:** type III collagen (**C:** control VP; **E:** Dox day 7; **G:** Dox day 30). Epithelium (ep), Blood Vessel (arrow head), Lumen (*). Bars = 20 µm.

Figure 4:

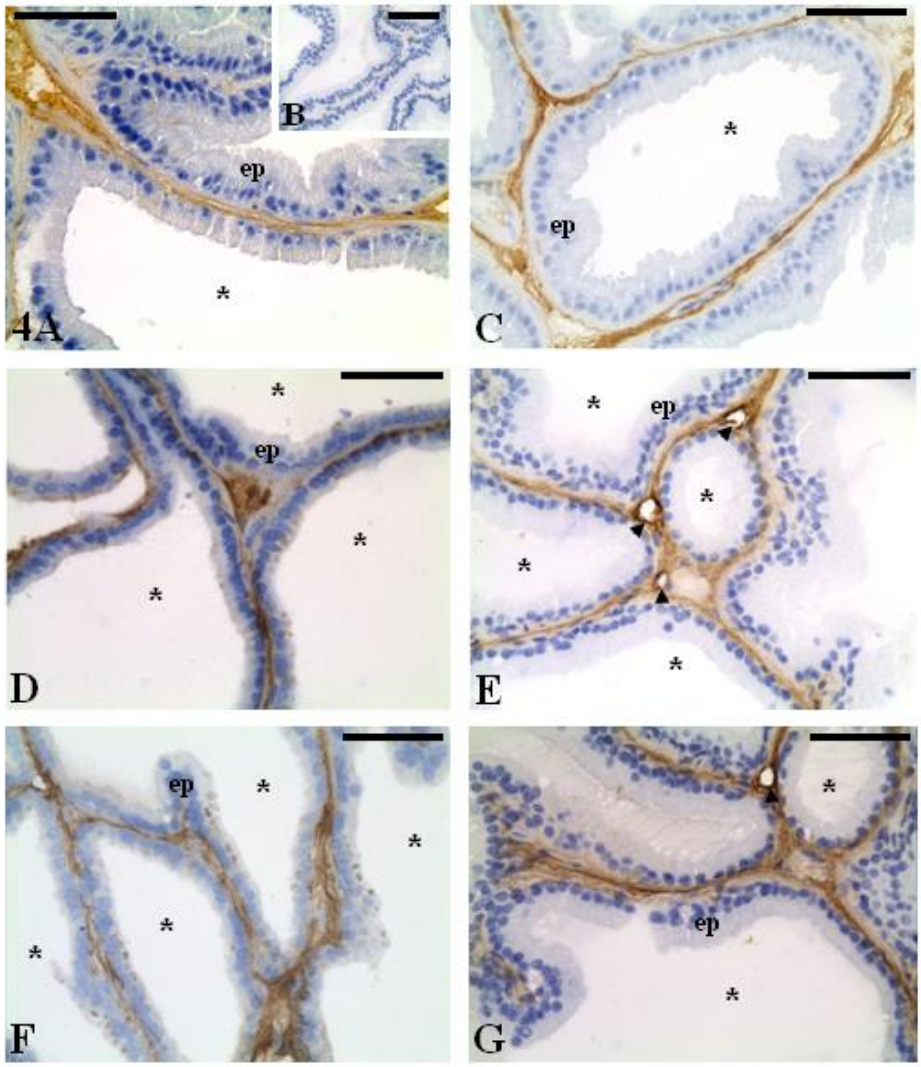

Figure 5: Expression of transforming growth factor beta 1 (TGF-Beta 1) protein in the rat ventral prostate (VP). Immunohistochemistry study: **A)** Control PV; **B)** Dox day 7; **C)** Dox day 30. Bars = 10 µm. **D)** Western blot analysis of Dox effects on TGF-Beta 1 and β-actin (Actin) in VP extracts (lane 1 control, lane 2 Dox day 7, lane 3 Dox day 30). Each lane represents a pool of 75 µg protein (15 µg from each of five individual extractions). **E)** Relative expression (IOD integrated optical density) of TGF-Beta 1 from ventral prostates in comparison with the constitutive control β-actin. Dox treatment altered the TGF-Beta 1 protein quantity at day 7. Data are significantly different from CT group at $p<0.01$. A-B superscript letters represent statistically significant differences between the experimental groups; values with the same letter are not statistically different.

Figure 5:

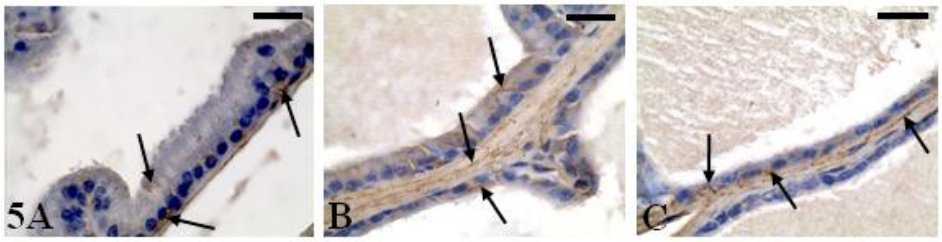
5A
B
C

D

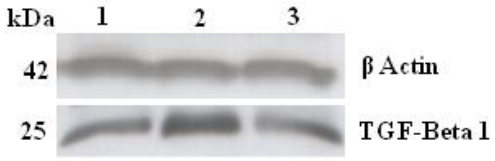
kDa
1
2
3
42
β Actin
25
TGF-Beta 1

E

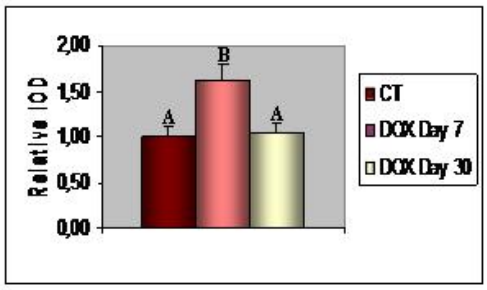
2,00
1,50
1,00
0,50
0,00
Relative IOD
A
B
A
CT
DOX Day 7
DOX Day 30

Figure 6: Quantification of type I and III Collagen and TGF Beta-1 mRNA expression by q-RT-PCR after 7 and 30 days of Dox treatment in the ventral rat prostate. Both Collagen I and TGF-Beta 1 mRNA expression were significantly up regulated after at day-7 of treatment and down regulated at day-30. Type III collagen mRNA was down regulated after both periods of Dox administration. Data are significantly different from CT group at $p < 0.01$. A-C superscript letters represent statistically significant differences between the experimental groups; values with the same letter are not statistically different.

Figure 6:

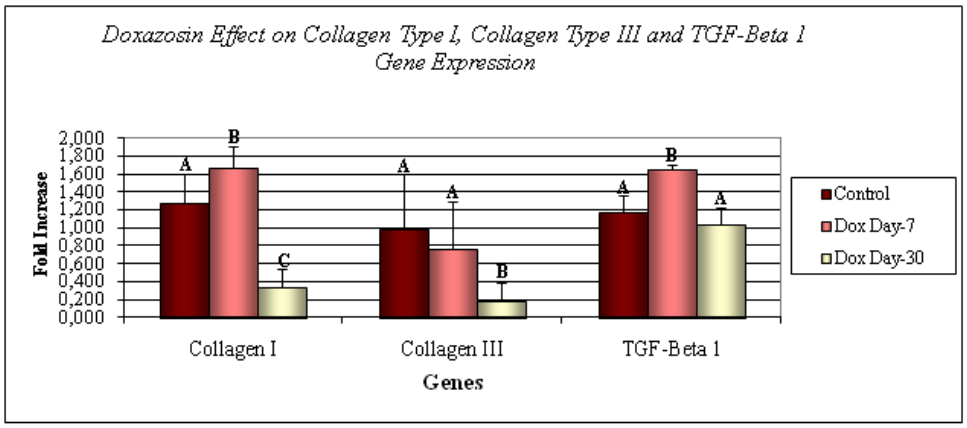
Doxazosin Effect on Collagen Type I, Collagen Type III and TGF-Beta 1 Gene Expression
Fold Increase
2,000
1,800
1,600
1,400
1,200
1,000
0,800
0,600
0,400
0,200
0,000
A
B
C
A
A
B
A
B
A
Collagen I
Collagen III
TGF-Beta 1
Genes
Control
Dox Day-7
Dox Day-30

4. Conclusões Finais

1. *A finasterida e a doxazosina são compostos que alteram a dinâmica dos elementos estromais celulares (células musculares lisas e fibroblastos) e fibrilares (fibras de colágeno e fibras do sistema elástico);*

2. *A doxazosina aumenta a deposição de fibras dos sistemas colágeno e elástico no estroma da próstata do rato Wistar;*

3. *A deposição de fibras de colágeno não é alterada pelo tratamento com finasterida, sugerindo que as fibras de colágeno já existentes sofrem rearranjo e distribuem-se em uma área estromal maior que aquela encontrada nos animais controle.*

4. *O fator de crescimento TGF-Beta 1, super expresso na próstata ventral de ratos Wistar após o tratamento com finasterida e com doxazosina, está relacionado com a apoptose promovida por ambos os tratamentos, mas também com o processo de fibrose promovido pelo segundo tratamento.*

5. *Estas alterações podem, a longo prazo, afetar a eficiência destes tratamentos para a hiperplasia prostática benigna e para a prevenção do câncer de próstata.*

5. Referências da Introdução

Ao M, Franco OE, Park D, Raman D, Williams K, Hayward SW. Cross-talk between paracrine-acting cytokine and chemokine pathways promotes malignancy in benign human prostatic epithelium. *Cancer Res* 2007; **67**: 4244-4253.

Bartsch G, Müller HR, Oberholzer M, Rohr HP. Light microscopic stereological analysis of the normal human prostate and of benign prostatic hyperplasia. *J Urol* 1979; **122**: 487-491.

Benning CM, Kyprianou N. Quinazoline-derived alpha1-adrenoceptor antagonists induce prostate cancer cell apoptosis via an alpha1-adrenoceptor-independent action. *Cancer Res* 2002; **62**: 597-602.

Berry PA, Maitland NJ, Collins AT. Androgen receptor signalling in prostate: effects of stromal factors on normal and cancer stem cells. *Mol Cell Endocrinol* 2008; **288**: 30–37.

Berry SJ, Coffey DS, Walsh PC, Ewing LL. The development of human benign prostatic hyperplasia with age. *J Urol* 1984; **132**: 474-479.

Bostwick DG, Burke HB, Djakiew D, Euling S, Ho SM, Landolph J, *et al*. Human prostate cancer risk factors. *Cancer* 2004; **101**: 2371-2490.

Bostwick DG, Cooner WH, Denis L, Jones GW, Scardino PT, Murphy GP. The association of benign prostatic hyperplasia and cancer of the prostate. *Cancer* 1992; **70**: 291-301.

Boyle P, Napalkov P. The epidemiology of benign prostatic hyperplasia and observations on concomitant hypertension. *Scand J Urol Nephrol Suppl* 1995; **168**: 7-12.

Collins AT, Robinson EJ, Neal DE. Benign prostatic stromal cells are regulated by basic fibroblast growth factor and transforming growth factor-β1. *J Endocrinol* 1996; **151**: 315–322.

Corradi LS, Góes RM, Carvalho HF, Taboga SR. Inhibition of 5a-reductase activity induces stromal remodeling and smooth muscle de-differentiation in adult gerbil ventral prostate. *Differentiation* 2004; **72**: 198-208.

Cunha G, Donjacour A, Cooke P, Bigsby R, Mee S, Higgins S, *et al*. The endocrinology and developmental biology of the prostate. *Endocr* 1987; **8**: 338-362.

Cunha GR, Chung LW. Stromal-epithelial interactions--I. Induction of prostatic phenotype in urothelium of testicular feminized (Tfm/y) mice. *J Steroid Biochem* 1981; **14**: 1317-1324.

Cunha GR, Fujii H, Neubauer BL, Shannon JM, Sawyer L, Reese BA. Epithelial-mesenchymal interactions in prostatic development. I. morphological observations of prostatic induction by urogenital sinus mesenchyme in epithelium of the adult rodent urinary bladder. *J Cell Biol* 1983; **96**: 1662-1670.

Cunha GR, Hayward SW, Dahiya R, Foster BA. Smooth muscle-epithelial interactions in normal and neoplastic prostatic development. *Acta Anat* 1996; **155**: 63-72.

Cunha GR, Ricke W, Thomson A, Marker PC, Risbridger G, Hayward SW, *et al.* Hormonal, cellular, and molecular regulation of normal and neoplastic prostatic development. *J Steroid Biochem Mol Biol* 2004; **92**: 221–236.

de Carvalho HF, Vilamaior PS, Taboga SR. Elastic system of the rat ventral prostate and its modifications following orchiectomy. *Prostate* 1997; **32**: 27-34.

Delella FK, Justulin Jr LA, Felisbino SL. Finasteride treatment alters MMP-2 and -9 gene expression and activity in the rat ventral prostate. *Int J Androl* 2009; 33: E114-E122.

De Marzo AM, Platz EA, Sutcliffe S, Xu J, Grönberg H, Drake CG, *et al*. Inflammation in prostate carcinogenesis. *Nat Rev Cancer* 2007; **7**: 256-269.

Deering RE, Bigler SA, King J, Choongkittaworn M, Aramburu E, Brawer MK. Morphometric quantitation of stroma in human benign prostatic hyperplasia. *Urology* 1994; **44**: 64-70.

Devlin H, Mudryj M. Progression of prostate cancer: Multiple pathways to androgen independence. *Cancer Letters* 2009; **274**: 177–186.

Donjacour AA, Cunha GR. The effect of androgen deprivation on branching morfogenesis in the mouse prostate. *Dev Biol* 1988; **128**: 1-14.

Feldman BJ, Feldman D. The development of androgen-independent prostate cancer. *Nat Rev Cancer* 2001; **1**: 34-45.

Fleisch MC, Maxwell CA, Barcellos-Hoff MH. The pleiotropic roles of transforming growth factor beta in homeostasis and carcinogenesis of endocrine organs. *Endocr Relat Cancer* 2006; **13**: 379-400.

Forray C, Bard JA, Wetzel JM. The alpha 1-adrenergic receptor that mediates smooth muscle contraction in human prostate has the pharmacological properties of the cloned human alpha 1c subtype. *Mol Pharmacol* 1994; **45**: 703-708.

Ghahary A, Shen YJ, Scott PG, Tredget EE. Expression of fibronectin messenger RNA in hypertrophic and normal dermal tissues and in vitro regulation by interferon alfa-2b. *Wound Repair Regen* 1993; **1**: 166-174.

Gerdes MJ, Larsen M, Dang TD, Ressler SJ, Tuxhorn JA, Rowley DR. Regulation of rat prostate stromal cell myodifferentiation by androgen and TGF-beta1. *Prostate* 2004; **58**: 299-307.

Griffiths K, Morton MS, Nicholson RI. Androgens, androgens receptors, antiandrogens and treatment of prostate cancer. *Eur Urol* 1997; **32**: 24-40.

Golbano JM, López-Aparicio P, Recio MN, Pérez-Albarsanz MA. Finasteride induces apoptosis via bcl-2, bcl-xl, bax and caspase-3 proteins in LNCaP human prostate cancer cell line. *Int J Oncol* 2008; **32**: 919-924.

Hall BR. *Developmental Biology and Cellular Skeletal Biology*. Academic, New York, USA, 1978.

Hay ED. *Cell Biology of the Extracellular Matrix*. Plenum, New York, USA 1981.

Hayward SW, Baskin LS, Haughney PC, Foster BA, Cunha AR, Dahiya R, *et al*. Stromal development in the ventral prostate, anterior prostate and seminal vesicle of the rat. *Acta Anat* 1996; **155**: 94-103.

Hayward SW, Cunha GR. The prostate: development and physiology. *Radiol Clin North Am* 2000; **38**: 1-14.

Hayward SW, Rosen MA, Cunha GR. Stromal-epithelial interactions in the normal and neoplastic prostate. *Br J Urol* 1997; **79**: 18-26.

Hieble JP, Ruffolo RR Jr. The use of alpha-adrenoceptor antagonists in the pharmacological management of benign prostatic hypertrophy: an overview. *Pharmacol Res* 1996; **33**: 145-160.

Huang X, Lee C. Regulation of stromal proliferation, growth arrest, differentiation and apoptosis in benign prostatic hyperplasia by TGF-beta. *Front Biosci* 2003; **8**: 740-749.

http://www.inca.gov.br/estimativa/2010/index.asp?link=conteudo_view.asp&ID=5

Imperato-McGinley J, Zhu YS. Androgens and male physiology the syndrome of 5alpha-reductase-2 deficiency. *Mol Cell Endocrinol* 2002; **198**: 51–59.

Isaacs JT. Antagonistic effect of androgen on prostatic cell death. *Prostate* 1984; **5**: 545-557.

Isaacs JT. Etiology of benign prostatic hyperplasia. *Eur Urol* 1994; **1**: 6-9.

Jemal A, Kulldorff M, Devesa SS, Hayes RB, Fraumeni JF Jr. A geographic analysis of prostate cancer mortality in the United States, 1970-89. *Int J Cancer* 2002; **101**: 168-174.

Justulin LA Jr, Delella FK, Felisbino SL. Doxazosin reduces cell proliferation and increases collagen fibers in rat prostatic lobes. *Cell Tissue Res* 2008; **332**: 171-183.

Keledjian K, Kyprianou N. Anoikis induction by quinazoline based alpha 1-adrenoceptor antagonists in prostate cancer cells: antagonistic effect of bcl-2. *J Urol* 2003; **169**: 1150–1156.

Koltz L, Clarke N. Open to debate. The Motion: all men over the age of 50 should be encouraged to take a 5alpha-reductase inhibitor to prevent prostate cancer. *Eur Urol* 2008; **53**: 1079–1083.

Kramer BS, Hagerty KL, Justman S. Use of 5alpha-reductase inhibitors for prostate cancer chemoprevention: American Society of Clinical Oncology/American Urological Association 2008 Clinical Practice Guideline. *J Urol* 2009; **181**: 1642-1657.

Kyprianou N, Benning CM. Suppression of human prostate cancer cell growth by alpha1-adrenoceptor antagonists doxazosin and terazosin via induction of apoptosis. *Cancer Res* 2000; **60**: 4550-4555.

Kyprianou N, Litvak JP, Borkowski A, Alexander R, Jacobs SC. Induction of prostate apoptosis by doxazosin in benign prostatic hyperplasia. *J Urol* 1998; **159**: 1810-1815.

Kyprianou N, Vaughan TB, Michel MC. Apoptosis induction by doxazosin and other quinazoline α1-adrenoceptor antagonists: a new mechanism for cancer treatment? *Naunyn-Schmied Arch Pharmacol* 2009; **380**: 473–477.

Kyprianou N. Apoptosis: therapeutic significance in the treatment of androgen-dependent and androgen-independent prostate cancer. *World J Urol* 1994; **12**: 299–303.

Lejeune B, Van Hoeck J, Leroy F. Transmitter role of the luminal uterine epithelium in the induction of decidualization in rats. *J Reprod Fertil* 1981; **61**: 235-240.

Lin CQ, Bissell MJ. Multi-faceted regulation of cell differentiation by extracellular matrix. *FASEB J* 1993; **7**: 737-743.

Marker PC, Donjacour AA, Dahiya R, Cunha GR. Hormonal, cellular, and molecular control of prostatic development. *Dev Biol* 2003; **253**: 165-74.

Marks LS, Partin AW, Glenn JG, Dorey FJ, Shery ED, Garris JB, *et al*. Prostate tissue composition and response to Finasterida in men with symptomatic benign prostatic hyperplasia. *J Urol* 1997; **157**: 2171- 2178.

Marshall S, Narayan P. Treatment of prostatic bleeding: suppression of angiogenesis by androgen deprivation. *J Urol* 1993; **149**: 1553-1554.

McAlhany SJ, Ressler SJ, Larsen M, Tuxhorn JA, Yang F, Dang TD, *et al*. Promotion of angiogenesis by ps20 in the differential reactive stroma prostate cancer xenograft model. *Cancer Res* 2003; **63**: 5859-5865.

McNeal J. Pathology of benign prostatic hyperplasia. Insight into etiology. *Urol Clin North Am* 1990; **17**: 477-486.

McNeal JE. Anatomy of the prostate and morphogenesis of BPH. *Prog Clin Biol Res* 1984; **145**: 27-53.

McNeal JE. Origin and development of carcinoma in the prostate. *Cancer* 1969; **23**: 24–34.

McNeal JE.The zonal anatomy of the prostate. *Prostate* 1981; **2**: 35-49.

Meinbach DS, Lokeshwar BL. Insulin-like growth factors and their binding proteins in prostate cancer: cause or consequence? *Urol Oncol* 2006; **24**: 294-306.

Nazian SJ. Concentrations of free testosterone, total testosterone and androgens binding protein in the peripheral serum of male rats during sexual maturation. *J Androl* 1986; **7**: 49-54.

Nemeth JA, Lee C. Prostatic ductal system in rats: regional variation in stromal organization. *Prostate* 1996; **28**: 124-128.

Olumi AF, Grossfeld GD, Hayward SW, Carroll PR, Tlsty TD, Cunha GR. Carcinoma-associated fibroblasts direct tumor progression of initiated human prostatic epithelium. *Cancer Res* 1999; **59**: 5002-5011.

Pareek G, Shevchuk M, Armenakas NA, Vasjovic L, Hochberg DA, Basillote JB, *et al*: The effect of finasteride on the expression of vascular endothelial growth factor and microvessel density: a possible mechanism for decreased prostatic bleeding in treated patients. *J Urol* 2003; **169**: 20 –23.

Parrinello S, Coppe JP, Krtolica A, Campisi J. Stromal-epithelial interactions in aging and cancer: senescent fibroblasts alter epithelial cell differentiation. *J Cell Sci* 2005; **11**: 485-496.

Peehl DM. Primary cell cultures as models of prostate cancer development. *Endocri Relat Cancer* 2005; **12**: 19–47.

Péterszegi G, Andrès E, Molinari J, Ravelojaona V, Robert L. Effect of cellular aging on collagen biosynthesis I. Methodological considerations and pharmacological applications. *Arch Gerontol Geriatr* 2008; **47**: 356-367.

Prahalada SR, Keenan KP, Hertzog PR, Gordon LR, Peter CP, Soper KA, *et al*. Qualitative and quantitative evaluation of prostatic histomophology in rats following chronic treatment with Finasterida, a 5-alpha reductase inhibitor. *Urol* 1994; **43**: 680-685.

Prahalada SR, Rhodes L, Grossman SJ, Heggan D, Keenan KP, Cukierski MA, *et al*. Morphological and hormonal changes in the ventrtal and dorsolateral prostatic lobes of rats treated with Finasterida, a 5-alpha reductase inhibitor. *Prostate* 1998; **35**: 157-164.

Reddy GK. Finasteride, a selective 5-alpha-reductase inhibitor in the prevention and treatment of human prostate cancer. *Clin Prostate Cancer* 2004; **2**: 206-208.

Rittmaster RS, Fleshner EN, Thompson IM. Pharmacological Approaches to Reducing the Risk of Prostate Cancer. *Eur Urol* 2009; **55**: 1064–1074.

Rittmaster RS, Manning AP, Wright AS, Thomas LN, Whitefield S, Norman RW, *et al*. Evidence for atrophy and apoptosis in the ventral prostate of rats given the 5-reductase inhibitor finasteride. *Endocrinology* 1995; **136**: 741-748.

Rittmaster RS. 5α-Reductase inhibitors in benign prostatic hyperplasiavand prostate cancer risk reduction. *Best Pract Res Clin Endocrinol Metab* 2008; **22**: 389-402.

Rittmaster RS. Finasteride. *N Engl J Med* 1994; **330**: 120-125.

Roy-Burman P, Wu H, Powell WC, Hagenkord J, Cohen MB. Genetically defined mouse models that mimic natural aspects of human prostate cancer development. *Endocr Relat*

Cancer 2004; **11**: 225-254.

Ruizeveld de Winter JA, Trapman J, Vermey M, Mulder E, Zegers ND, van der Kwast TH. Androgen receptor expression in human tissues: an immunohistochemical study. *J Histochem Cytochem* 1991; **39**: 927–936.

Russell PJ, Bennet S, Stricker P. Growth factor involvement in progression of prostate cancer. *Clin Chem* 1998; **44**: 705–723.

Sakr WA, Grignon DJ, Crissman JD, Heilbrun LK, Cassin BJ, Pontes JJ, *et al*. High grade prostatic intraepithelial neoplasia (HGPIN) and prostatic adenocarcinoma between the ages of 20–69: an autopsy study of 249 cases. *In Vivo* 1994; **8**: 439–443.

Seftel AD, Rosen RC, Rosenberg MT, Sadovsky R. Benign prostatic hyperplasia evaluation, treatment and association with sexual dysfunction: practice patterns according to physician specialty. *Int J Clin Pract* 2008; **62**: 614-622.

Shapiro E, Becich MJ, Hartanto V, Lepor H. The relative proportion of stromal and epithelial hyperplasia is related to the development of symptomatic benign prostate hyperplasia. *J Urol* 1992; **147**: 1293-1297.

Stoner E. The clinical development of a 5 alpha-reductase inhibitor, finasteride. J *Steroid Biochem Mol Biol* 1990; **37**: 375-378.

Strohmeyer D, Rossing C, Bauerfeind A, et al. Vascular endothelial growth factor and its correlation with angiogenesis and p53 expression in prostate cancer. *Prostate* 2000; **45**: 216–224.

Tahmatzopoulos A, Kyprianou N. Apoptotic impact of alpha1-blockers on prostate cancer growth: a myth or an inviting reality? *Prostate* 2004; **59**: 91-100.

Taylor RA, Risbridger GP. Prostatic Tumor Stroma: A Key Player in Cancer Progression. *Curr Cancer Drug Targets* 2008; **8**: 490-497.

Thomas LN, Douglas RC, Lazier CB, Gupta R, Norman RW, Murphy PR, *et al.* Levels of 5α-reductase type 1 and type 2 are increased in localized high grade compared to low grade prostate cancer. *J Urol* 2008; **179**: 147-151.

Thompson IM, Coltman CA Jr, Crowley J. Chemoprevention of prostate cancer: the Prostate Cancer Prevention Trial. *Prostate* 1997; **33**: 217-221.

Thompson IM, Klein EA, Lippman SM, Coltman CA, Djavan B. Prevention of prostate cancer with finasteride: US/European perspective. *Eur Urol* 2003; **44**: 650-655.

Thompson IM, Tangen CM, Goodman PJ, Scott Lucia M, Klein EA. Chemoprevention of Prostate Cancer. *J Urol* 2009; **182**: 499-508.

Tindall DJ, Rittmaster RS. The rationale for inhibiting 5-reductase isoenzymes in the prevention and treatment of prostate cancer. *J Urol* 2008; **179**: 1235-1242.

Tuxhorn JA, Ayala GE, Smith MJ, Smith VC, Dang TD, Rowley DR. Reactive stroma in human prostate cancer: induction of myofibroblast phenotype and extracellular matrix remodeling. *Clin Cancer Res* 2002; **8**: 2912-2923.

Untergasser G, Madersbacher S, Berger P. Benign prostatic hyperplasia: age-related tissueremodeling. *Exp Gerontol* 2005; 40: 121-128.

Verrecchia F, Mauviel A. Transforming growth factor-β and fibrosis. *World J Gastroenterol* 2007; **13**: 3056-3062.

Vilamaior PSL, Felisbino SL, Taboga SR, Carvalho HF. Collagen fiber reorganization in the rat ventral prostate following androgen deprivation: A possible role for the smooth muscle cells. *Prostate* 2000; **45**: 253-258.

Wikström P, Damber J, Bergh A. Role of transforming growth factor-beta1 in prostate cancer. *Microsc Res Tech* 2001; **52**: 411-419.

Wu JD, Haugk K, Woodke L, Nelson P, Coleman I, Plymate SR. Interaction of IGF signaling and the androgen receptor in prostate cancer progression. *J Cell Biochem* 2006; **99**: 392-401.

Yang G, Timme TL, Park SH, Wu X, Wyllie MG, Thompson TC.Transforming growth factor beta 1 transduced mouse prostate reconstitutions: II. Induction of apoptosis by doxazosin. *Prostate* 1997; **33**: 157-163.

Zhu B, Kyprianou N. Transforming growth factor beta and prostate cancer. *Cancer Treat Res* 2005; **126**: 157-173.

ANEXO

Estágio de Doutorado Realizado na Universidade de Michigan - EUA, *Comprehensive Cancer Center*, Departamento de Urologia.

1. A Universidade de Michigan:

A Universidade de Michigan (UM) foi fundada em 1817, na cidade de Detroit, como uma das primeiras universidades públicas dos Estados Unidos. Em 1837, foi transferida para a cidade de Ann Arbor, a aproximadamente 70 Km de Detroit. A reputação da universidade na elite estadunidense começou a crescer cada vez mais. A universidade passou a ser a principal opção de escolha para os estudantes judeus que vinham de Nova Iorque nos anos de 1920 a 1930, pois as escolas Ivy League começaram a restringir o número máximo de judeus a serem aceitos. Como resultado, a UM ganhou o apelido de "Harvard do Oeste", que se tornou comum depois da brincadeira que o ex-presidente dos Estados Unidos, John F. Kennedy, disse: "eu me graduei na Michigan do leste, a Universidade Harvard".

Hoje, existem treze cursos de graduação na universidade. Há dezoito escolas e colégios de graduação na universidade, sendo os maiores deles o Colégio de Literatura, Ciência e Artes, o Colégio de Engenharia, Escola de Direito e a Ross School de Negócios. A Escola de Medicina é parceira do Sistema de Saúde da Universidade de Michigan, que engloba os três hospitais universitários, dezenas de ambulatórios, e diversos centros de assistência médica, reservas e educação. A universidade tem 26.083 matriculados e 14.959 graduados, em 600 programas acadêmicos, e em cada ano cerca de 5400 novos estudantes se matriculam. Os alunos vêm de todos os estados dos Estados Unidos e de mais de 100 países ao redor do mundo.

A UM administra um dos maiores orçamentos anuais de universidades nos Estados Unidos, totalizando cerca de 775 milhões de dólares por ano, entre 2004 e 2005, 797 milhões de dólares em 2006, e 823 milhões de dólares no final do ano 2007.

O *Comprehensive Cancer Center* da UM oferece atendimento, orientação para prevenção e terapia aos pacientes, além de extensos e inovadores laboratórios de pesquisa que estudam o comportamento dos mais variados tipos de câncer mediante o tratamento com drogas e terapias.

2. Dra Jill Macoska:

A Dra Jill Macoska é professora associada do Departamento de Urologia da UM, vice coordenadora do Centro O'Brien para pesquisas urológicas da UM e diretora do Centro de Affymetrix e Microarray também da universidade.

A pesquisa no laboratório da Dra Macoska busca elucidar o papel das interações parácrinas entre o epitélio e as células estromais na etiologia das afecções benignas e malignas da próstata. Os projetos visam definir quais mecanismos de sinalização específicos das células epiteliais são ativados ou inativados por proteínas secretadas pelo estroma; além de determinar como os fatores de crescimento secretados por fibroblastos estromais senescentes estimulam a proliferação e motilidade das células epiteliais.

Alguns estudos em andamento e outros já publicados pelo grupo da Dra Macoska demonstram que as quimiocinas do tipo CXC, secretadas como consequência da idade avançada, promovem proliferação de células epiteliais e de fibroblastos próstaticos, servindo como quimioatratores de leucócitos capazes de promover processo inflamatório na próstata. Esses estudos empregam pararelamente cultura de células humanas e modelos de roedores para entender o desenvolvimento natural do processo de fibrose prostática e testar novas terapias anti-fibróticas.

Para o grupo, apesar do sucesso das terapias de ablação hormonal no tratamento do CaP em alguns pacientes, estudos recentes mostram que além dos hormônios esteróides, alguns fatores de crescimento promovem papéis importantes no desenvolvimento e progressão do CaP (Begley et al., 2008). Entre esses fatores encontra-se uma ampla classe de proteínas imunomodeladoras denominadas citocinas, que são mediadores solúveis envolvidos na angiogênese, controle do crescimento celular, mobilidade celular e respostas inflamatórias (Koch, 2005).

Recentemente, a citocina CXCL-5 tornou-se o foco de estudos que examinam os papéis das citocinas na tumorigênese. Assim como outras citocinas que reconhecem e se ligam ao receptor CXCR2 (uma proteína do tipo G), a CXCL-5 é pró-angiogênica e atrai células imunes granulocíticas. É secretada por muitos tipos celulares, tais como células epiteliais, células endoteliais, fibroblastos, neutrófilos, monócitos e macrófagos (Walz et al., 1997; Koch, 2005). Estudos examinando a expressão da CXCL-5 em tumores humanos e em células tumorais in vitro descrevem que os transcritos desta citocina são significativamente mais expressos em adenocarcinoma endometrial, quando comparado ao endométrio normal (Wong et al., 2007). Park e colaboradores (2007) demonstraram que a super expressão da proteína CXCL-5 estava associada com o estágio avançado do câncer gástrico, sugerindo um papel da CXCL-5 na progressão desse tipo de câncer.

3. Estágio de Doutorado

O estágio de doutorado realizado no laboratório da Dra Macoska teve início em Agosto de 2008 e término em Dezembro de 2008. O responsável pela orientação em laboratório foi o Dr Satish Kasina, pós doutorando do laboratório e cujo projeto em desenvolvimento tem como objetivo elucidar o papel da quimiocina CXCL-12 no desenvolvimento de afecções proliferativas benignas e malignas na próstata.

Abaixo segue, resumidamente, os principais protocolos desenvolvidos durante o estágio.

A. Proposta do projeto de estágio

O objetivo do projeto proposto pela Dra Macoska foi revelar se a resposta transcricional mediada por CXCL-5 nas linhagens de células epiteliais prostáticas dependentes de andrógeno (N15C6) e independentes de andrógeno (LNCaP). é substancialmente similar ou diferente da resposta mediada por CXCL-12 (como descrito por Begley e colaboradores, JBC 282: 26767-26774, 2007) e se a resposta transcricional mediada por CXCL-5 é promovida através das vias de sinalização MEK/ERK ou PI3K/NFkappaB, ou ambas (como sugerido por Begley, Kasina e colaboradores, Neoplasia 10: 244-254, 2008). Para tal finalidade, as células foram tratadas com 10pM CXCL-5 +

0,05% DMSO ou com apenas o veículo (0,05% DMSO) e durante 0, 30 e 60 minutos. Posteriormente o RNA destas células tratadas foi extraído para as análises descritas abaixo.

B. Material e Métodos

Cultura Celular:

1. *Divisão das Células*

Todas as operações envolvidas no manuseamento das células e respectivos meios foram efectuadas em condições de assepsia, com material estéril e em câmara de fluxo laminar. O pH do meio foi mantido numa atmosfera com CO2 a 5% (obtida pela colocação das placas de cultura em estufa de CO2 com atmosfera úmida).

As duas linhagens celulares utilizadas (N15C6 e LNCaP) crescem em monocamada, aderentes à superfície do frasco ou da placa de cultura.

As novas passagens das células em crescimento foram feitas habitualmente a partir de culturas celulares com confluência entre 70 e 80%. As células foram subcultivadas, a partir de suspensões celulares obtidas por tripsinização das células da monocamada. Para a obtenção de uma nova passagem celular, o meio de cultura foi aspirado e em seguida o frasco foi lavado delicadamente com PBS. Após aspirar o PBS, os frascos receberam 1X tripsina/EDTA e foram colocados na estufa para as células entrarem em suspensão (10 minutos para a linhagem N15C6 e 2 minutos para a linhagem LNCaP). Após esse tempo, as células receberam aproximadamente 5 mL do meio de cultura, que foi delicadamente misturado às células em suspensão na tripsina. Esse material foi centrifugado durante 5 minutos, a 4ºC e na rotação de 1000 rpm. Em seguida o sobrenadante foi aspirado, as células lavadas com 5mL de meio, resuspendidas e novamente centrifugadas. Após essa segunda centrifugação, o sobrenadante foi aspirado e, de acordo com o tamanho do pellet de células obtido, foi calculado o volume do meio de cultura a ser adicionado. Essas células foram divididas em duas novas placas para a manutenção do estoque da linhagem ou divididas nas placas para receberem os tratamentos e armazenadas na estufa.

Meios de Cultura

- HIEC 5%

O meio de cultura HIEC 5% foi usado especificamente para as células N15C6. A um frasco de 500 mL de HIEC 5%, foram adicionados 25 mL de FBS (Fetal Bovine Serum), 1 mL de Fungizona, 500 uL de Gentamicina e 2,5 mL de Insulina. Após misturar bem e filtrar o conteúdo usando vácuo, foram acrescidos 104 uL de Plasmocin, 500 uL de Toxina Colérica, 500 uL de Hidrocortisona e 50 uL de EGF (Fator de Crescimento Endotelial). O meio de cultura foi armazenado em câmera fria e, antes do uso, colocado em banho-maria a 37ºC.

- RPMI 10%

O meio de cultura HIEC 5% foi usado especificamente para as células LNCaP. A um frasco de 500 mLs de RPMI 10%, foram adicionados 50 mL de FBS (Fetal Bovine Serum), 1 mL de Fungizona, 500 uL de Gentamicina e 104 uL de Plasmocin. Após adicionados os reagentes, o meio de cultura era armazenado em câmera fria e, antes do uso, colocado em banho-maria a 37ºC.

Protocolo de descongelamento das células

O estoque das células N15C6 e LNCaP do laboratório da Dra Jill Macoska é criopreservado em nitrogênio líquido, armazenados em criotubos de 1,5mL identificados com o nome da linhagem, número da passagem celular e data de estocagem. Quando necessária a utilização de novas células para os experimentos, um tubo da linhagem a ser utilizada era retirado do nitrogênio líquido e descongelado em banho-maria. Após a adição de 1mL do meio de cultura às células do criotubo e transferido para um tubo falcon de 15 mL, esse material era centrifugado a 4ºC, durante 5 minutos e o sobrenadante descartado. Na sequência, 10 mL do meio de cultura eram adicionados, homogeneizados às células com a ajuda de uma pipeta e o meio contendo as células eram colocados em uma placa. As células eram então armazenadas em estufa até a obtenção de, pelo menos, 80% de confluência na placa de cultura. O meio de cultura era trocado de 2 em 2 dias para a renovação de nutrientes.

Protocolo de congelamento das células

Quando não havia a necessidade da utilização de células para experimento, seguia-se o protocolo de congelamento. O procedimento para o congelamento iniciou-se com a tripsinização e posterior suspensão dessas células em tripsina + o meio de congelamento. Após serem transferidas para um tubo falcon de 15 ml, as células foram centrifugadas em 1000 rpm durante 5 minutos. Após o liquído ser aspirado, adicionou-se às células 5 ml de meio de congelamento (25% FBS, 10% DMSO, 65% meio de congelamento). Alíquotas de 1 ml foram transferidas para criotubo identificado, congelados em freezer -80ºC por 24 horas e, no dia seguinte, transferidos para o botijão de nitrogênio líquido para estocagem.

Tratamento das células

As células foram tratadas em triplicata, em placas de 6 poços. O volume estabelecido para cada poço foi de 2 mL, sendo 1,7 mL de meio de cultura e 0,3 mL de meio contendo as células recém tripsinizadas. As células foram mantidas por um dia no meio de cultura para a adaptação à placa. No dia anterior ao tratamento, foi feita a privação das células aos nutrientes, aspirando o meio de cultura e adicionando aos pocinhos o soro sem o meio de cultura.

Alguns testes foram feitos com e sem o veículo DMSO para a averiguação da existência ou não de interferência desse composto na resposta ao tratamento com CXCL-5. A Figura 1 mostra em detalhes as condições dos tratamentos realizados.

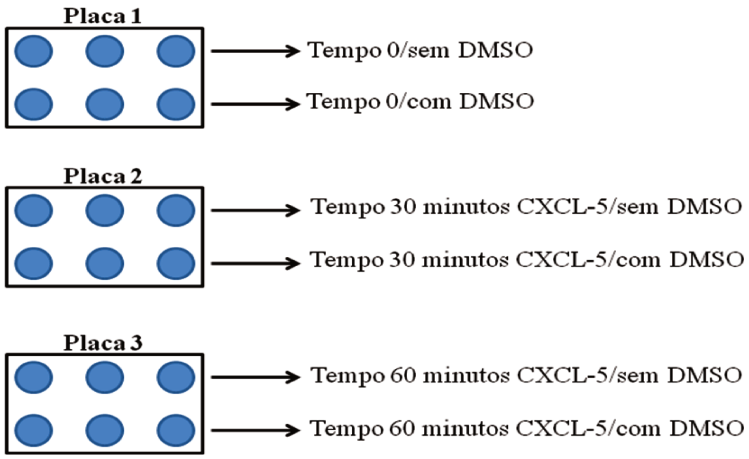

Figura 1: Esquema das placas de tratamento com 6 poços. Placa 1: controle das células, sem adição da citocina CXCL-5. Linha 1: sem adição de DMSO. Linha 2: com adiçao de DMSO. Placa 2: células tratadas durante 30 minutos com a citocina CXCL-5. Linha 1: sem adição de DMSO. Linha 2: com adição de DMSO. Placa 3: células tratadas durante 60 minutos com a citocina CXCL-5. Linha 1: sem adição de DMSO. Linha 2: com adição de DMSO.

C. PCR Quantitativo em Tempo Real

As análises quantitativas em tempo real foram realizadas utilizando o sistema 7900 HT da Applied Biosystems (Foster City, CA) e reagents da mesma empresa. Após o tratamento das células, foi feita a extração de RNA utilizando o reagent Trizol (Invitrogen Life Technologies). Para todos os experimentos, 1 µg de RNA foi transcrito reversamente, usando o kit *Superscript III Reverse Transcriptase* (Invitrogen). O c-DNA resultante foi diluído na proporção de 1:10 com água ultra pura. As reações foram aplicadas em triplicata em placa de 384 poços, incluindo os controles negativos (adição de água no lugar de c-DNA) e o controle endógeno RPLPO (proteina ribosomal). O número de ciclos do threshold foi calculado subtraindo os valores das médias dos controles das médias dos grupos experimentais em cada ponto, e as diferenças na expressão gênica foram calculadas elevando esses valores exponenciais à base 2. Os valores das diferenças dos transcritos obtidos no tempo 0 foram estabelecidos e normalizados igual a 1 para permitir a comparação com o tempos subsequentes de tratamento.

D. Resultados Parciais

O aprimoramento das técnicas utilizadas no tratamento das culturas celulares, o processo de padronização do tratamento quanto à dose específica da citocina CXCL-5 a ser usada (10 ou 100 pM), o uso ou não do veículo DMSO e a técnica de PCR em Tempo Real dispensaram grande parte do período do estágio e assim apenas alguns resultados foram obtidos com precissão, os quais serão descritos a seguir.

Após a extração de RNA das células tratadas, alicotas de 2 µL foram colocadas em eppendorfs estéreis, identificados com a data da estração e levados ao laboratório

University of Michigan Affymetrix and cDNA Microarray Core para a análise da qualidade do RNA total e quantificação no *Agilant 2100 Bioanalyzer*. Os resultados foram apresentados como mostra o exemplo da figura 2. Aconcentração de RNA de cada amostra foi dada em ng/µL.

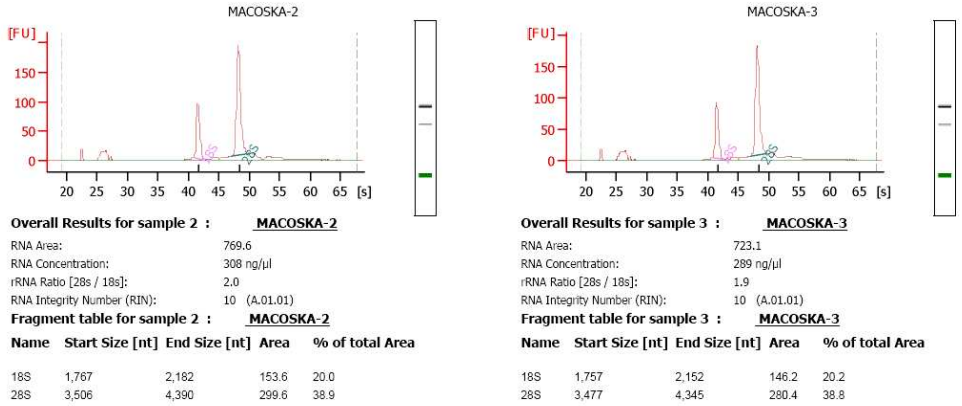

Figura 2: Resultado da análise das amostras de RNA, mostrando a qualidade e a concentração do RNA total de cada amostra em ng/µL.

Os valores das concentrações das amostras de RNA dadas em ng/µL foram plotadas em tabela do excel e transformados em µg/µL. Foram calculadas também a quantidade de RNA para a obtenção de 1µg/µL para cada amostra, assim como a quantidade de água ultra a ser adicionada para um volume final de 8 µL (tabela 1).

Samples 11/19/08 - Cells LNCaPs (P31) treated with 100pM CXCL5 (1st time - triplicate) cDNA ready

Samples	[RNA] - ng/µL	[RNA] - µg/µL	[RNA] - 1µg/µL	Water	
1	834	0,834	1,20	6,80	control I: 0,05% DMSO 60'
2	483	0,483	2,07	5,93	control II: 0,05% DMSO 60'
3	360	0,36	2,78	5,22	control III: 0,05% DMSO 60'
4	281	0,281	3,56	4,44	control I: without DMSO 60'
5	246	0,246	4,07	3,93	control II: without DMSO 60'
6	201	0,201	4,98	3,02	control III: without DMSO 60'
7	329	0,329	3,04	4,96	0,05% DMSO + 100pM CXCL-5 30' I
8	215	0,215	4,65	3,35	0,05% DMSO + 100pM CXCL-5 30' II
9	235	0,235	4,26	3,74	0,05% DMSO + 100pM CXCL-5 30' III
10	262	0,262	3,82	4,18	100pM CXCL-5 (without DMSO) 30' I
11	305	0,305	3,28	4,72	100pM CXCL-5 (without DMSO) 30' II
12	196	0,196	5,10	2,90	100pM CXCL-5 (without DMSO) 30' III
13	296	0,296	3,38	4,62	0,05% DMSO + 100pM CXCL-5 60' I
14	313	0,313	3,19	4,81	0,05% DMSO + 100pM CXCL-5 60' II
15	181	0,181	5,52	2,48	0,05% DMSO + 100pM CXCL-5 60' III
16	173	0,173	5,78	2,22	100pM CXCL-5 (without DMSO) 60' I
18	168	0,168	5,95	2,05	100pM CXCL-5 (without DMSO) 60' III

Tabela 1: Exemplo do cálculo da concentração do RNA de cada amostra (em triplicata) para a obtenção da concentração final de 1µg/µL.

Após a análise das placas de PCR em Tempo Real no sistema HT da Applied Biosystems (Foster City, CA), os valores foram analisados segundo o método de validação ΔΔCT. As análises mostraram melhores resultados com as amostras tratadas com o veículo DMSO, tanto para as células LNCaP (resultados não mostrados), como para as células N15C6 (figura 3) e optou-se pelo seu uso nos demais tratamentos.

Após o tratamento com a citocina CXCL-5, houve aumento na expressão do gene EGR-1 de aproximadamente 1,7 vezes após 30 minutos (figura 3).

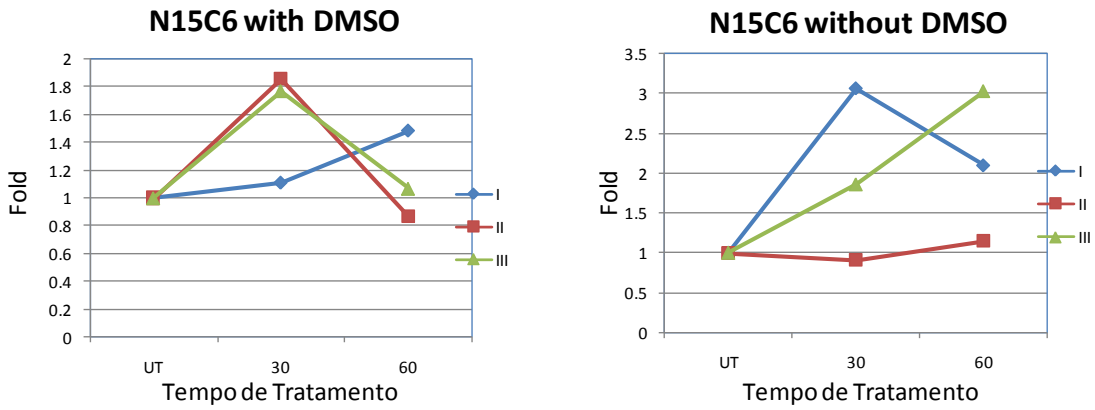

Figura 3: Gráfico dos resultados do PCR em Tempo Real, ilustrando os efeitos da citocina CXCL-5 nas células N15C6 com (primeiro gráfico) e sem (segundo gráfico) o veículo DMSO.

O projeto continua em desenvolvimento pela pós-graduanda Gwyneth Halstead-Nussloch e novos resultados são esperados para a conclusão e publicação do trabalho.

E. Conclusões sobre o estágio

O estágio de doutorado realizado no laboratório da Dra. Jill Macoska me proporcionou importante experiência com cultura celular, no qual tive grande êxito, o aprimoramento da técnica de PCR em Tempo Real para o termociclador modelo 7900 (Applied Biosystems), além da participação em uma futura publicação referente aos

resultados do projeto de estágio. A experiência com cultura de células epiteliais prostáticas será de extrema importância no desenvolvimento do projeto de pós doutorado, cujo título é "Expressão de Micro-RNAs em Células Epiteliais Prostáticas Normais e Tumorais Tratadas com Finasterida", que terá início em Agosto de 2010. Além disso, trabalhar com a Dra Jill Macoska e sua equipe ensinou-me que o sucesso e o diferencial das pesquisas em um país de primeiro mundo não se resumem apenas às facilidades financeiras, mas deve-se também à determinação e à organização de todo um grupo. Foi a realização de um sonho!

F. Referências

Begley LA, Kasina S, Mehra R, Adsule S, Admon AJ, Lonigro RJ, Chinnaiyan AM, Macoska JA (2008) CXCL5 promotes prostate cancer progression Neoplasia, Mar;10(3):244-54.

Koch AE (2005). Chemokines and their receptors in rheumatoid arthritis: future targets? Arthritis Rheum 52, 710–721.

Park JY, Park KH, Bang S, Kim MH, Lee JE, Gang J, Koh SS, and Song SY (2007). CXCL5 overexpression is associated with late stage gastric cancer. J Cancer Res Clin Oncol 133(11), 835–840.

Walz A, Schmutz P, Mueller C, and Schnyder-Candrian S (1997). Regulation and function of the CXC chemokine ENA-78 in monocytes and its role in disease. J Leukoc Biol 62(5), 604–611.

Wong YF, Cheung TH, Lo KW, Yim SF, Siu NS, Chan SC, Ho TW, Wong KW, Yu MY, Wang VW, et al. (2007). Identification of molecular markers and signaling pathway in endometrial cancer in Hong Kong Chinese women by genome-wide gene expression profiling. Oncogene 26, 1971–1982.

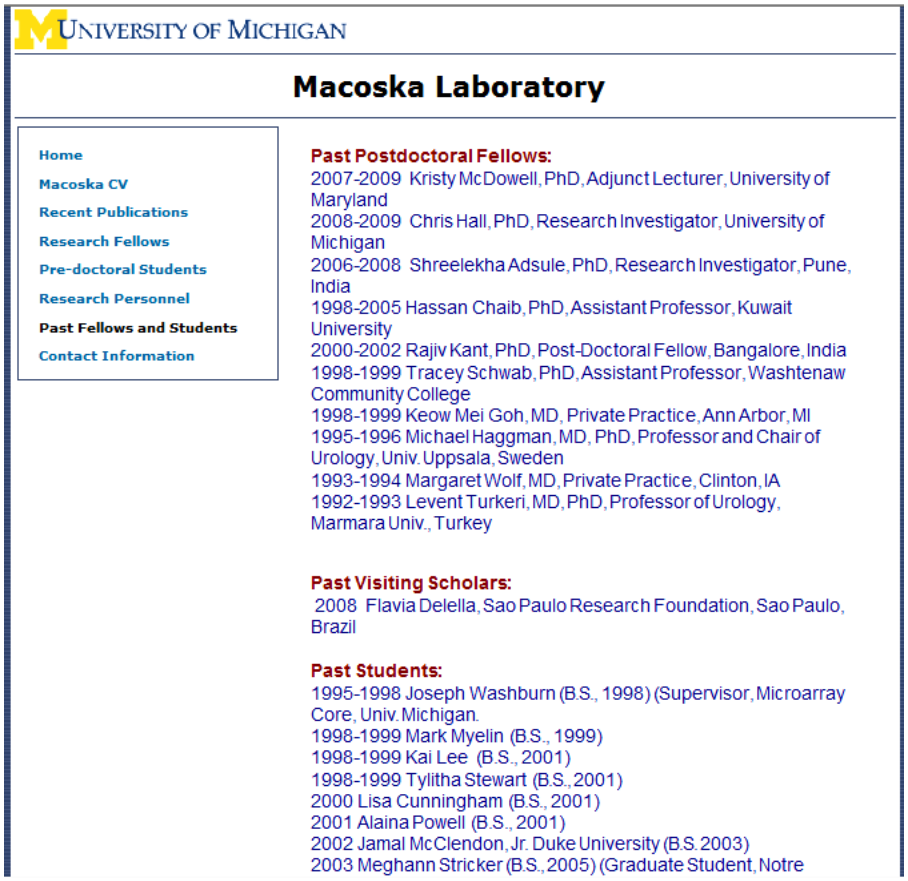

UNIVERSITY OF MICHIGAN

Macoska Laboratory

Home
Macoska CV
Recent Publications
Research Fellows
Pre-doctoral Students
Research Personnel
Past Fellows and Students
Contact Information

Past Postdoctoral Fellows:
2007-2009 Kristy McDowell, PhD, Adjunct Lecturer, University of Maryland
2008-2009 Chris Hall, PhD, Research Investigator, University of Michigan
2006-2008 Shreelekha Adsule, PhD, Research Investigator, Pune, India
1998-2005 Hassan Chaib, PhD, Assistant Professor, Kuwait University
2000-2002 Rajiv Kant, PhD, Post-Doctoral Fellow, Bangalore, India
1998-1999 Tracey Schwab, PhD, Assistant Professor, Washtenaw Community College
1998-1999 Keow Mei Goh, MD, Private Practice, Ann Arbor, MI
1995-1996 Michael Haggman, MD, PhD, Professor and Chair of Urology, Univ. Uppsala, Sweden
1993-1994 Margaret Wolf, MD, Private Practice, Clinton, IA
1992-1993 Levent Turkeri, MD, PhD, Professor of Urology, Marmara Univ., Turkey

Past Visiting Scholars:
2008 Flavia Delella, Sao Paulo Research Foundation, Sao Paulo, Brazil

Past Students:
1995-1998 Joseph Washburn (B.S., 1998) (Supervisor, Microarray Core, Univ. Michigan.
1998-1999 Mark Myelin (B.S., 1999)
1998-1999 Kai Lee (B.S., 2001)
1998-1999 Tylitha Stewart (B.S., 2001)
2000 Lisa Cunningham (B.S., 2001)
2001 Alaina Powell (B.S., 2001)
2002 Jamal McClendon, Jr. Duke University (B.S. 2003)
2003 Meghann Stricker (B.S., 2005) (Graduate Student, Notre

Quadro de pesquisadores e alunos que passaram pelo laboratório da Dra Jill Macoska -

http://sitemaker.umich.edu/macoskalaboratory/past_fellows_and_students

Algumas imagens do meu arquivo pessoal de fotos do período do estágio na Universidade de Michigan. Primeira foto canto esquerdo acima: Dr Satish Kasina, Dr Chris Hall, Jan Evangelista (Secretária); Dra Jill Macoska, Eu, Dra Kristy McDowell.

University of Michigan
Medical School

Jill A. Macoska, PhD
Associate Professor
Director, UMCCC
Affymetrix and cDNA
Microarray Core

Department of Urology
6217 Comprehensive
Cancer Center
1500 E. Medical Center Drive
Ann Arbor, MI 48109-5944
(734) 647-8121
(734) 647-9271 fax
jcoska@umich.edu

February 16, 2009

Dear Sir/Madam,

Ms. Flavia Delella pursued a research project in my laboratory as a visiting scholar during the period August 15, 2008 – December 15, 2008. Ms. Delellea's project focused on the role of CXC-type chemokines in the development of benign hyperplastic and malignant prostate disease, with an emphasis on chemokine-mediated proliferative, migratory/invasive, and gene transcriptional responses. In order to pursue this project, Ms. Delella learned several laboratory techniques, including mammalian cell culture (and, in particular, the culture of several human prostate epithelial cell lines), the experimental maniupulation of human cells, purification of mRNA from human cells, and quantitative real-time polymerase chain reaction (qRT-PCR) methodologies. Ms. Delella successfully learned and applied these techniques towards understanding how the CXC-type chemokine, CXCL5, stimulates gene transcription in both non-transformed and transformed prostate epithelial cells. Ms. Delella also became knowledgeable on this topic of gene expression profiling techniques, such as microarray technology, as these techniques will be used as part of a larger parent project directly related to her brief project in my laboratory

We were very pleased to have Ms. Delella with us as a visiting scholar, and she proved to be a very industrious and productive student. Ms. Delella successfully accomplished much of an ambitious project that we continue to pursue in the laboratory. Her work will certainly be recognized in the form of a co-authorship on any publications that result from completion of the larger project on which she participated.

Regards,

Jill A Macoska

Jill A. Macoska, PhD
Associate Professor
Associate Chair for Laboratory Research, Department of Urology
Director, University of Michigan Affymetrix and cDNA Microarray Core
Faculty, Programs in Cellular and Molecular Biology and Bioinformatics

DECLARAÇÃO

Declaro para os devidos fins que o conteúdo de minha **Tese de Doutorado** intitulada **"Efeito da finasterida e da doxazosina sobre a próstata de rato: análise ultra-estrutural e da expressão dos colágenos tipo I e tipo III e do TGF-β 1"**:

( ) não se enquadra no § 3º do Artigo 1º da Informação CCPG 01/08, referente a bioética e biossegurança.

(X) tem autorização da(s) seguinte(s) Comissão(ões) de Bioética ou Biossegurança*: Comissão de Ética na Experimentação Animal (CEEA), sob Protocolo(s) nº 44/07-CEEA.

** Caso a Comissão seja externa à UNICAMP, anexar o comprovante de autorização dada ao trabalho. Se a autorização não tiver sido dada diretamente ao trabalho de tese ou dissertação, deverá ser anexado também um comprovante do vínculo do trabalho do aluno com o que constar no documento de autorização apresentado.*

Aluna: Flávia Karina Delella

Orientador: Sérgio luis Felisbino

Para uso da Comissão ou Comitê pertinente:
(X) Deferido ( ) Indeferido

Nome:
Função:

Profa. Dra. ANA MARIA APARECIDA GUARALDO
Presidente da CEEA/UNICAMP